Pendulum Testing of an FRP Composite Guardrail: FOIL Test Numbers 96P019 Through 96P023, 97P001, and 97P002

PUBLICATION NO. FHWA-RD-98-017

MARCH 1998

U.S. Department of Transportation
Federal Highway Administration

Research and Development
Turner-Fairbank Highway Research Center
6300 Georgetown Pike
McLean, VA 22101-2296

FOREWORD

This report contains the test procedures used and the test results from seven pendulum crash tests performed at the Federal Outdoor Impact Laboratory (FOIL) located at the Turner-Fairbank Highway Research Center (TFHRC). The Federal Highway Administration (FHWA), together with the Catholic University of America (CUA), have been investigating the use of a fiber-reinforced plastic (FRP) material in guardrail applications. The FRP material would be used in the design of a rail element as opposed to the conventional steel w-beam in use today. The FHWA's FOIL 820-kg pendulum facility was used to conduct the seven dynamic impact tests on FRP rails designed and fabricated by CUA. Three 2440-mm-long and four 3660-mm-long FRP composite rail specimens were delivered to the FOIL. The nominal weight of the FOIL pendulum with a rigid nose assembly was 912 kg.

This report (FHWA-RD-98-017) contains test data, photographs taken with high-speed film, and a summary of the test results. The tests were conducted at nominal speeds ranging from 20 km/h to 35 km/h.

This report will be of interest to all State departments of transportation, FHWA headquarters, region and division personnel, and highway safety researchers interested in the crashworthiness of roadside safety hardware.

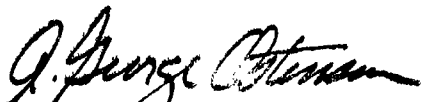

A. George Ostensen, Director
Office of Safety and Traffic
Operations Research and Development

NOTICE

Technical Report Documentation Page

1. Report No.	2. Government Accession No.	3. Recipient's Catalog No.
FHWA-RD-98-017		

4. Title and Subtitle	5. Report Date
PENDULUM TESTING OF AN FRP COMPOSITE GUARDRAIL: FOIL TEST NUMBERS 96P019 THROUGH 96P023, 97P001, and 97P002	March 1998
	6. Performing Organization Code

7. Author(s)	8. Performing Organization Report No.
Christopher M. Brown	

9. Performing Organization Name and Address	10. Work Unit No. (TRAIS)
MiTech Incorporated 9430 Key West Avenue Suite 100 Rockville, MD 20850	3A5F3142
	11. Contract or Grant No. DTFH61-94-C-00008

12. Sponsoring Agency Name and Address	13. Type of Report and Period Covered
Office of Safety and Traffic Operations R&D Federal Highway Administration 6300 Georgetown Pike McLean, VA 22101-2296	Test Report, August 1996 and January 1997
	14. Sponsoring Agency Code

15. Supplementary Notes
Contracting Officer's Technical Representative (COTR)- Richard King, HSR-20

16. Abstract

This report contains the test setup and results from seven pendulum crash tests conducted at the Federal Outdoor Impact Laboratory (FOIL) located at the Turner-Fairbank Highway Research Center (TFHRC) in McLean, Virginia. The tests were conducted on fiber-reinforced plastic (FRP) composite guardrail elements. Three 2440-mm-long and four 3660-mm-long FRP specimens were tested. The shorter specimens were tested in a two-post, no end-anchorage configuration and the longer specimens were tested in a four-post, fixed-end configuration. The tests were conducted as part of an ongoing research effort to compare the dynamic response from standard w-beam guardrail with the dynamic response of an FRP composite rail. The data establishes that the energy from a pendulum with a mass of 912 kg and a velocity of 35 km/h is not enough to produce the forces necessary to load the FRP rail element to failure. A heavier, faster pendulum is needed to generate sufficient forces to fail the FRP composite rail. Results from the tests are presented as test summaries of data; graphs of data; and photographs taken before, during, and after the tests.

17. Key Words	18. Distribution Statement
Fiberglass reinforced plastic, FRP, composite, rail, pendulum, box-section, end-anchorage, fixed-end	No restrictions. This document is available to the public through the National Technical Information Service, Springfield, VA 22161.

19. Security Classif. (of this report)	20. Security Classif. (of this page)	21. No. of Pages	22. Price
Unclassified	Unclassified	97	

Form DOT F 1700.7 (8-72) Reproduction of completed page authorized

SI* (MODERN METRIC) CONVERSION FACTORS

APPROXIMATE CONVERSIONS TO SI UNITS

Symbol	When You Know	Multiply By	To Find	Symbol
	LENGTH			
in	inches	25.4	millimeters	mm
ft	feet	0.305	meters	m
yd	yards	0.914	meters	m
mi	miles	1.61	kilometers	km
	AREA			
in^2	square inches	645.2	square millimeters	mm^2
ft^2	square feet	0.093	square meters	m^2
yd^2	square yards	0.836	square meters	m^2
ac	acres	0.405	hectares	ha
mi^2	square miles	2.59	square kilometers	km^2
	VOLUME			
fl oz	fluid ounces	29.57	milliliters	mL
gal	gallons	3.785	liters	L
ft^3	cubic feet	0.028	cubic meters	m^3
yd^3	cubic yards	0.765	cubic meters	m^3
NOTE: Volumes greater than 1000 l shall be shown in m^3.				
	MASS			
oz	ounces	28.35	grams	g
lb	pounds	0.454	kilograms	kg
T	short tons (2000 lb)	0.907	megagrams (or "metric ton")	Mg (or "t")
	TEMPERATURE (exact)			
°F	Fahrenheit temperature	5(F-32)/9 or (F-32)/1.8	Celcius temperature	°C
	ILLUMINATION			
fc	foot-candles	10.76	lux	lx
fl	foot-Lamberts	3.426	candela/m^2	cd/m^2
	FORCE and PRESSURE or STRESS			
lbf	poundforce	4.45	newtons	N
lbf/in^2	poundforce per square inch	6.89	kilopascals	kPa

APPROXIMATE CONVERSIONS FROM SI UNITS

Symbol	When You Know	Multiply By	To Find	Symbol
	LENGTH			
mm	millimeters	0.039	inches	in
m	meters	3.28	feet	ft
m	meters	1.09	yards	yd
km	kilometers	0.621	miles	mi
	AREA			
mm^2	square millimeters	0.0016	square inches	in^2
m^2	square meters	10.764	square feet	ft^2
m^2	square meters	1.195	square yards	yd^2
ha	hectares	2.47	acres	ac
km^2	square kilometers	0.386	square miles	mi^2
	VOLUME			
mL	milliliters	0.034	fluid ounces	fl oz
L	liters	0.264	gallons	gal
m^3	cubic meters	35.71	cubic feet	ft^3
m^3	cubic meters	1.307	cubic yards	yd^3
	MASS			
g	grams	0.035	ounces	oz
kg	kilograms	2.202	pounds	lb
Mg (or "t")	megagrams (or "metric ton")	1.103	short tons (2000 lb)	T
	TEMPERATURE (exact)			
°C	Celcius temperature	1.8C + 32	Fahrenheit temperature	°F
	ILLUMINATION			
lx	lux	0.0929	foot-candles	fc
cd/m^2	candela/m^2	0.2919	foot-Lamberts	fl
	FORCE and PRESSURE or STRESS			
N	newtons	0.225	poundforce	lbf
kPa	kilopascals	0.145	poundforce per square inch	lbf/in^2

* SI is the symbol for the International System of Units. Appropriate rounding should be made to comply with Section 4 of ASTM E380.

(Revised September 1993)

TABLE OF CONTENTS

LIST OF FIGURES

LIST OF FIGURES (continued)

LIST OF TABLES

BACKGROUND

The Federal Highway Administration (FHWA) has been evaluating the use of advanced composite materials in lieu of conventional materials used in the construction of roadside safety hardware. FHWA and the Catholic University of America (CUA) have been investigating the use of a fiber-reinforced plastic (FRP) material in guardrail applications. The FRP material would be used in the design of a rail element as opposed to the conventional steel w-beam in use today. Baseline data on the dynamic properties of standard steel w-beam were previously obtained to develop a design envelope for an FRP rail element. FHWA's Federal Outdoor Impact Laboratory (FOIL) 820-kg pendulum facility was used to conduct seven dynamic impact tests on 1.9-m-long steel w-beam rail elements attached to two standard steel I-section guardrail posts (a two-post configuration) and six dynamic impact tests on w-beam rail elements semi-rigidly fixed at each end (a four-post configuration). The pendulum was fitted with a rigid nose to allow for complete energy absorption by the w-beam rail. The results from these pendulum tests are presented in the reports *Pendulum Testing of Fixed-End W-Beam Guardrail: FOIL Test Numbers 96P001-96P006*, Report Number FHWA-RD-97-078,[1] and *Pendulum Impact Testing of Steel W-Beam Guardrail: FOIL Test Numbers 94P023-94P027, 94P030, and 94P031* (pending report).[2] The data from these 13 pendulum tests served as a design envelope for the development of an FRP composite guardrail element. An FRP rail was designed and fabricated by CUA and delivered to the FOIL for testing. Three 2440-mm-long and four 3660-mm-long FRP composite rail specimens were delivered.

SCOPE

This document contains the test setup and results from seven pendulum crash tests conducted at FHWA's FOIL facility located at the Turner-Fairbank Highway Research Center (TFHRC) in McLean, Virginia. The tests were conducted on FRP composite guardrail elements. The shorter specimens were tested in a two-post, no end-anchorage configuration and the longer specimens were tested in a four-post, fixed-end configuration. The four-post, fixed-end configuration was developed to better restrain the rail element and to better approximate the longitudinal tension found in an installed "line run" of roadside guardrail. The composite rail element was semi-rigidly restrained in the longitudinal direction using a cable attachment at each end of the rail element.

The tests were conducted as part of an ongoing research effort to compare the dynamic response from standard w-beam guardrail with the dynamic response of an FRP composite rail. The nominal weight of the FOIL pendulum with a rigid nose assembly was 912 kg. The tests were conducted at nominal speeds ranging from 20 km/h

to 35 km/h. The 20-km/h tests were conducted to observe the performance of the FRP rail before conducting higher-speed tests.

It should be noted that the 35-km/h tests are roughly equivalent to the National Cooperative Highway Research Program (NCHRP) Report 350 test 3-10,[3] a small lightweight vehicle impacting a roadside rail system at a speed of 100 km/h and at an angle of 20°. This is because, for test 3-10, the speed component of the test vehicle, perpendicular to the rail, is approximately 35 km/h. This perpendicular speed component is the same as the higher speed (35 km/h) pendulum tests. Also, the pendulum weight (912 kg) is that of a small, lightweight passenger sedan. Thus, the 35-km/h pendulum test as described in this report roughly approximates NCHRP Report 350 test 3-10. As such, these higher speed pendulum tests are used to determine, in a preliminary manner, the structural adequacy of the prototype composite rail system.

TEST MATRIX

Seven pendulum tests were conducted on FRP composite rail elements. Four tests were conducted with the rail anchored at both ends (four-post configuration) and three tests were conducted without end-anchorage. The mass of the pendulum was 912 kg for all tests. Table 1 is the test matrix for the pendulum testing of the FRP composite rails.

Table 1. FRP composite rail pendulum testing matrix.

Test number	Test date	Test speed (km/h)	FRP length (mm)	Tension in rail (yes/no)	Impact location	CUA specimen no.
96P019	08-20-96	20	2440	no	center FRP rail	CUA-1
96P020	08-21-96	20	3660	yes	center FRP rail	CUA-4
96P021	08-22-96	35	3660	yes	center FRP rail	CUA-5
96P022	08-23-96	25	2440	no	center FRP rail	CUA-2
96P023	08-27-96	35	2440	no	center FRP rail	CUA-3
97P001	01-22-97	35	3660	yes	center FRP rail	None
97P002	01-24-97	35	3660	yes	center FRP rail	None

Shaded areas are the four cable-anchored tests.

PENDULUM

The test vehicle was the FOIL's 820-kg pendulum. The pendulum consisted of a reinforced concrete mass with steel end-plates suspended from a steel structure by four 25-mm steel cables. The usual pendulum setup has a crushable nose inserted inside the concrete/steel body or mass. This nose was replaced with a rigid, solid oak nose. This was done so that the FRP composite rail specimen would be subjected to all of the energy with no energy dissipation from deformation of the nose. Within the concrete mass were two aluminum guide sleeves and the wood nose was attached to two aluminum guide tubes that were inserted into the guide sleeves. Seven oak spacers (total length of 325 mm) were placed between the nose assembly and the pendulum mass. The spacers were necessary to allow for optimal contact between the w-beam specimen and the pendulum nose. This was determined during previous pendulum testing of the two-post w-beam setup. A thin rubber mat was attached to the pendulum nose to reduce the high-frequency ring and inertial spike associated with contact between two rigid objects. The rigid nose assembly and wood spacers increased the mass of the pendulum from 820 kg to 912 kg. The vertical center of the pendulum was set at 533 mm above ground. This height corresponds to the height of the center of the FRP specimens. Photographs of the pendulum mass and rigid nose assembly are seen in Figure 1. The pendulum was set up the same way for each test.

TEST ARTICLE

The FRP composite rail specimens were supplied by CUA. The specimens were delivered to the FOIL with strain gages and blockouts attached. The specimens to be tested with end-anchorage were delivered with a standard cable anchor bracket attached to the rail. The FRP rail was fabricated from several extruded FRP rectangular box-sections, bonded together and then bonded to a 6-mm-thick FRP sheet with an epoxy resin. In addition to the resin, small self-tapping screws were used to attach the FRP sheet to the FRP box-sections. The extruded box-sections varied in size to produce a specific geometry. The cross-section shape of the rail formed a "C" shape, with a depth of 125 mm. This shape would enhance the rail's ability to catch a vehicle's bumper in a real-world application. Three 2440-mm rails and four 3660-mm rails were produced. The shorter specimens were tested without anchoring each end. The longer specimens were tested with each end rigidly fixed using standard 25-mm-diameter cable anchors tightened to produce a predetermined tension in the FRP rail. Cable anchor brackets were attached to the backside of the FRP rail, one at each end. The anchor brackets were welded to a steel plate bolted to the FRP rail. Small wood blocks were inserted inside each end of each rectangular section to allow for the attachment of the cable anchor bracket and plate without collapsing the shape of the FRP

box-sections. The cables were passed between the rail anchor bracket and the anchor stanchions and were fastened with a 25-mm cable-nut and washer at each end. The blockouts affixed to the FRP rails were attached to two standard strong-posts (I-sections) using two standard blockout-to-post bolts. The post spacing between posts was 1,905 mm, which is standard for strong-post guardrail systems. The blockout-to-post connections were made using standard bolts in the same pattern used on the National Highway System (NHS). The standard post height of 710 mm was used for set up of the FRP systems. However, due to the geometry of the FRP rails, the rail protruded 25 mm higher than the strong posts, which is atypical of strong-post guardrail systems. Figure 2 shows a sketch of each type of FRP rail. An overhead view of each type of test setup is shown in figure 3, along with the placement of high-speed cameras. Photographs of a typical test installation for the two-post and four-post setup are shown in figures 4 and 5, respectively. Tension was applied to the four-post FRP systems prior to testing by tightening the anchor cables. For tests 96P020 and 96P021, CUA decided that 500 $\mu\varepsilon$ was a reasonable amount of pre-tension in the FRP rail. Pre-tension was determined by monitoring output from strain gages bonded to the FRP rail with a strain indicator. For tests 97P001 and 97P002, the voltage output from the rail gages was monitored during installation and the voltages were recorded when tension in the cable reached an arbitrary tightness believed to be close to real-world tension.

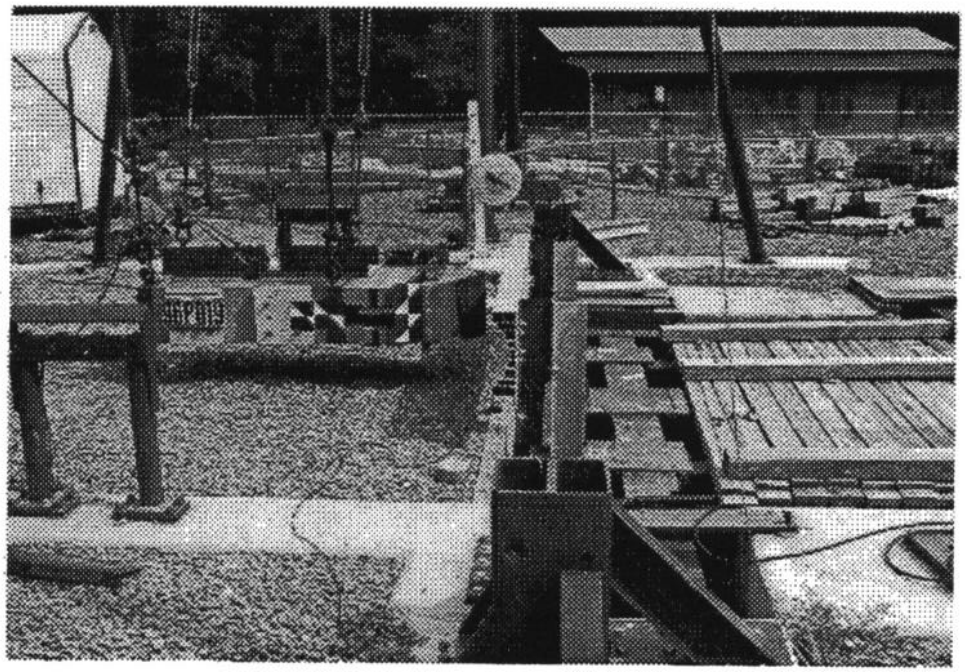

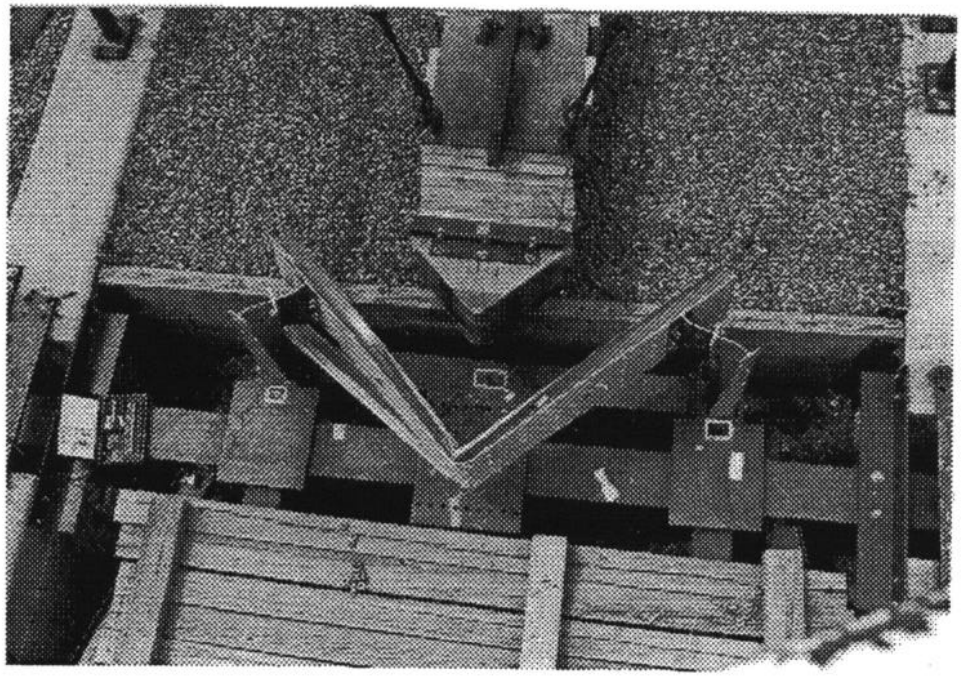

Figure 1. Photographs of the pendulum mass and rigid nose assembly.

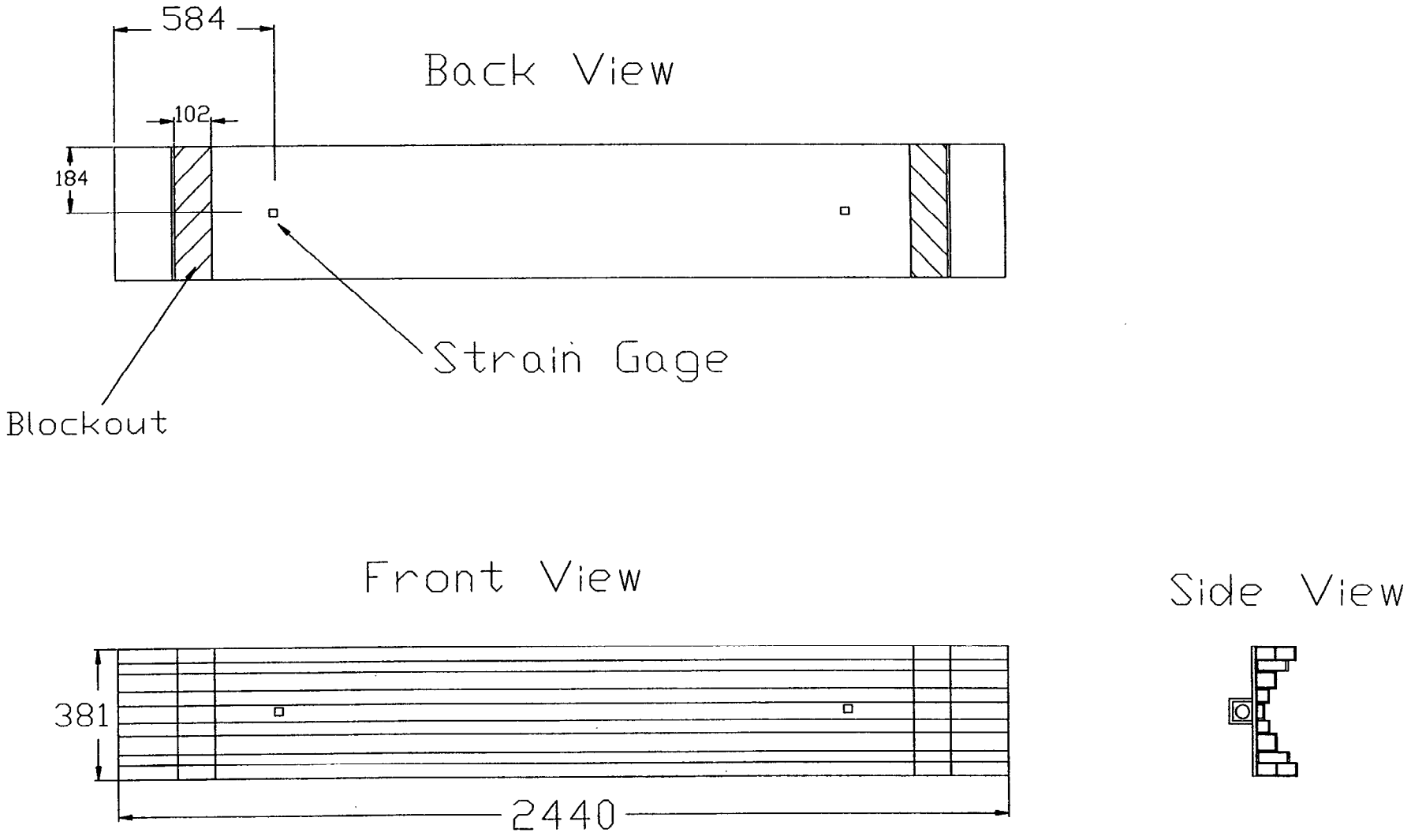

Measurements are in millimeters.

Figure 2. Sketch of FRP rails.

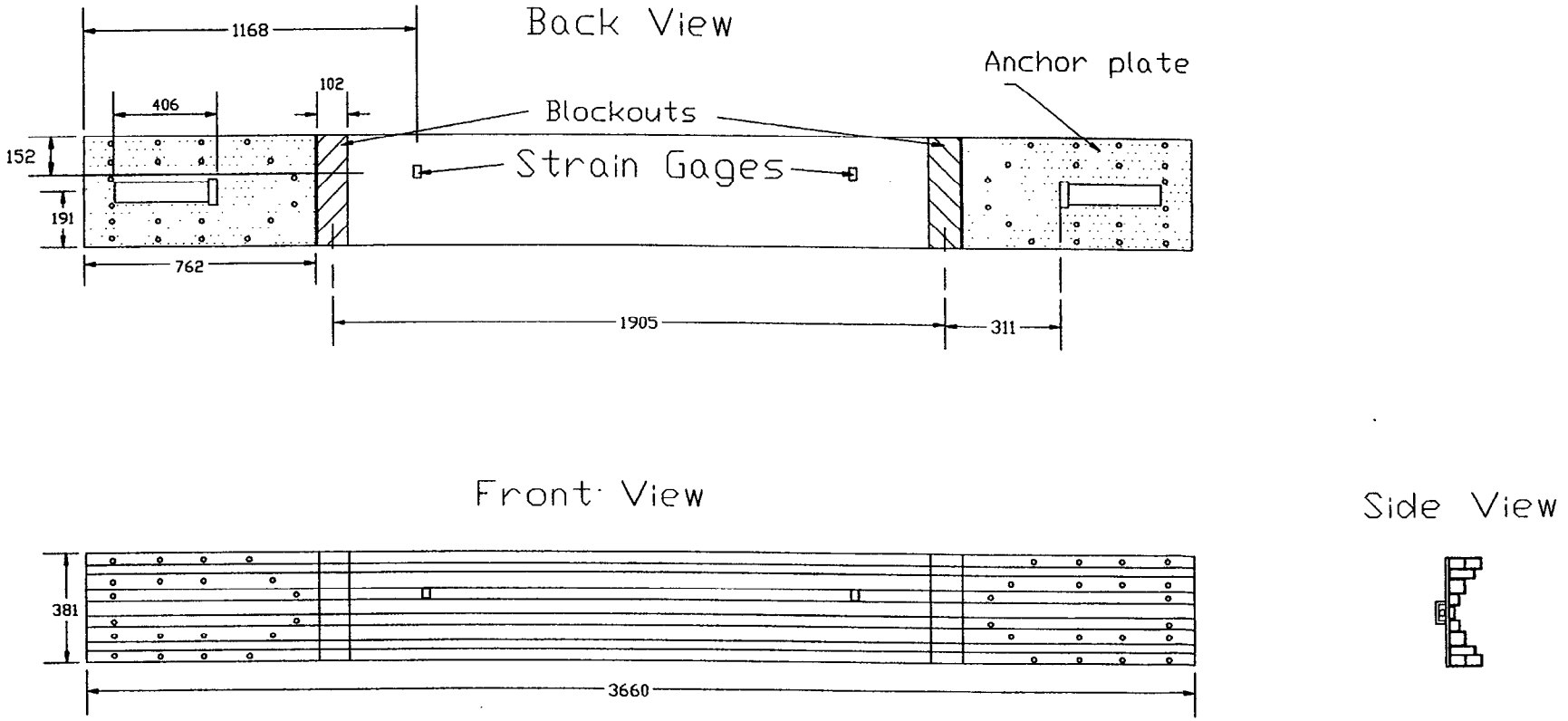

Measurements are in millimeters.

Figure 2. Sketch of FRP rails (continued).

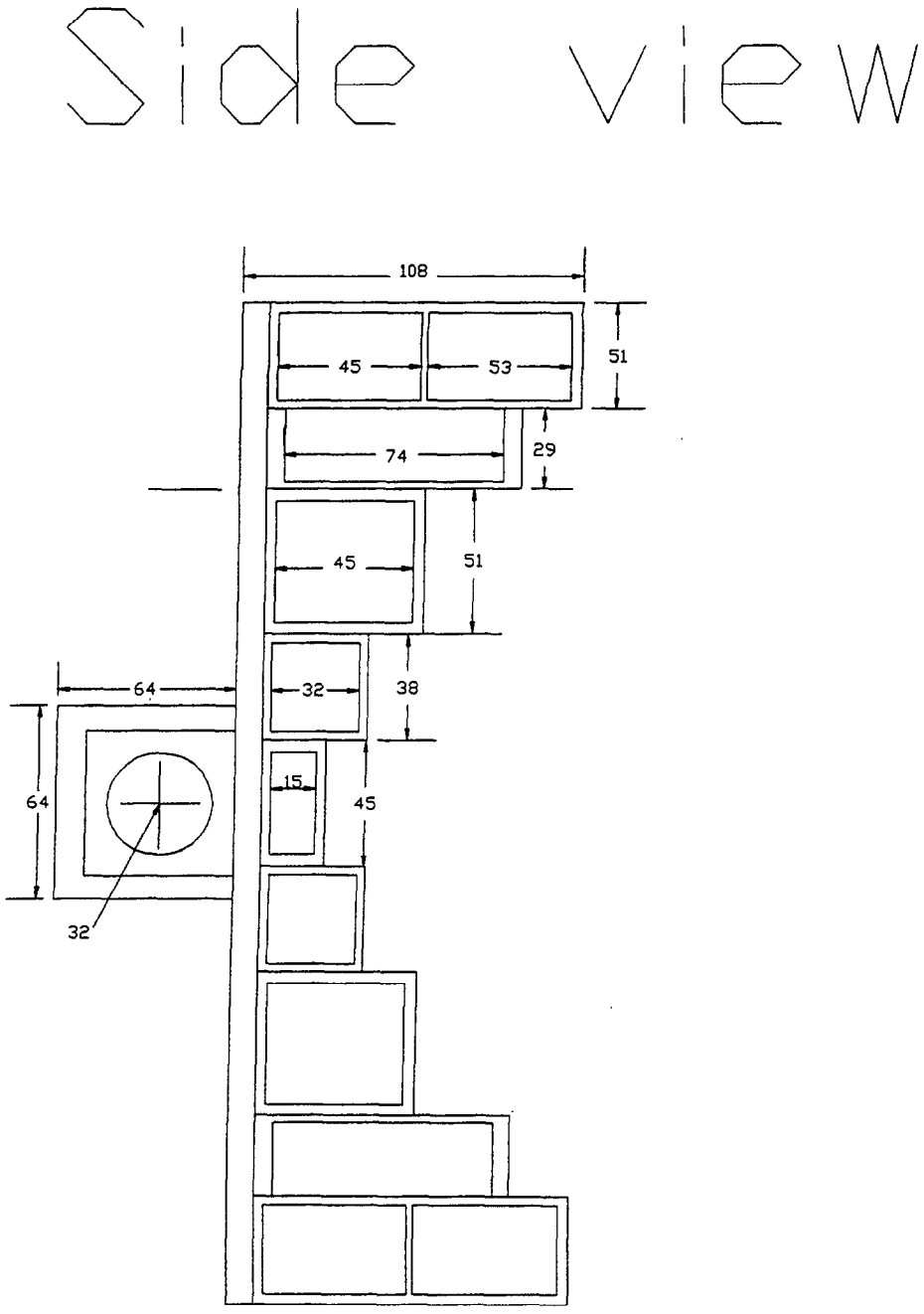

Measurements are in millimeters.

Figure 2. Sketch of FRP rails (continued).

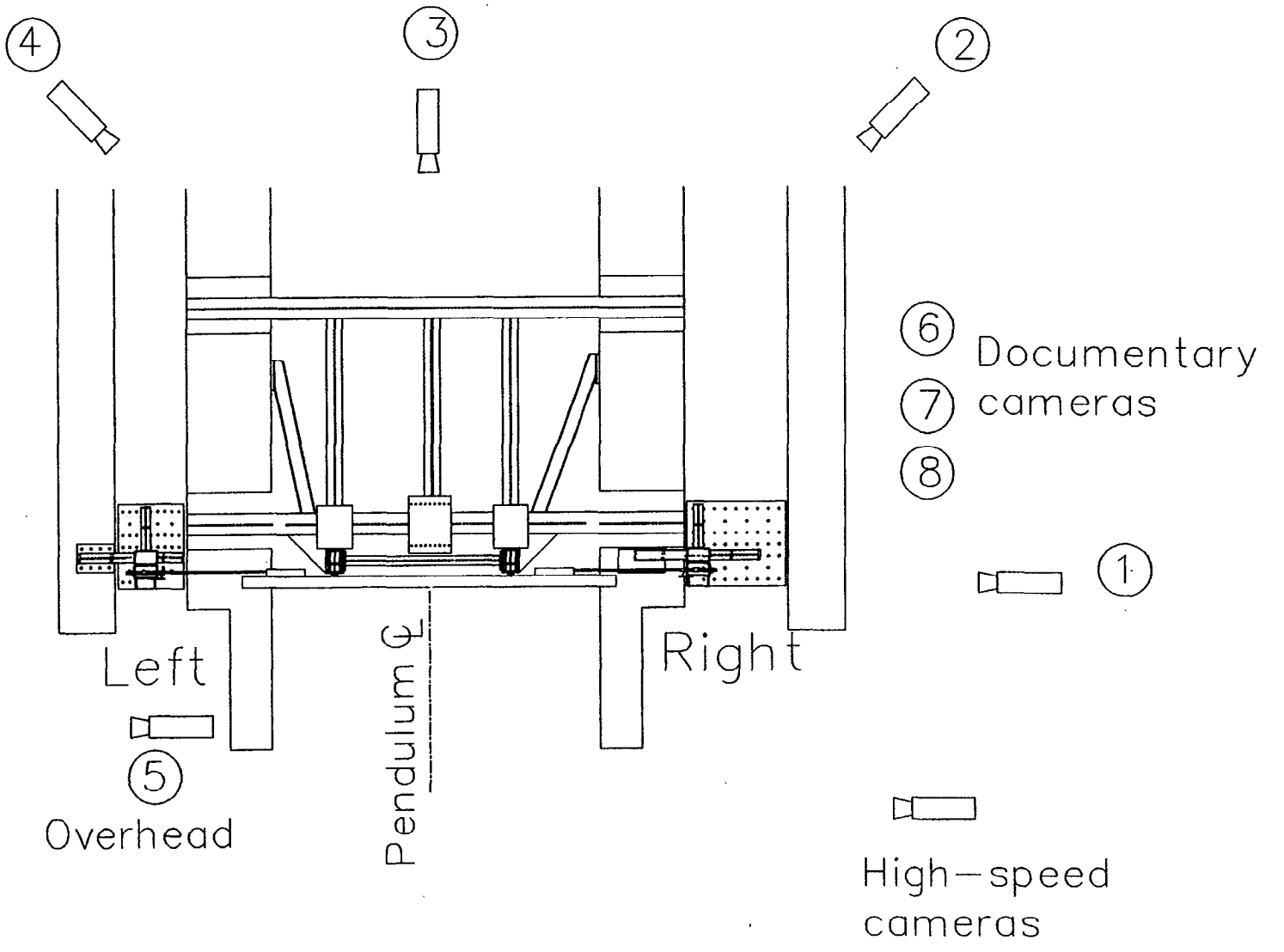

Figure 3. Overhead view of test setup and placement of high-speed cameras.

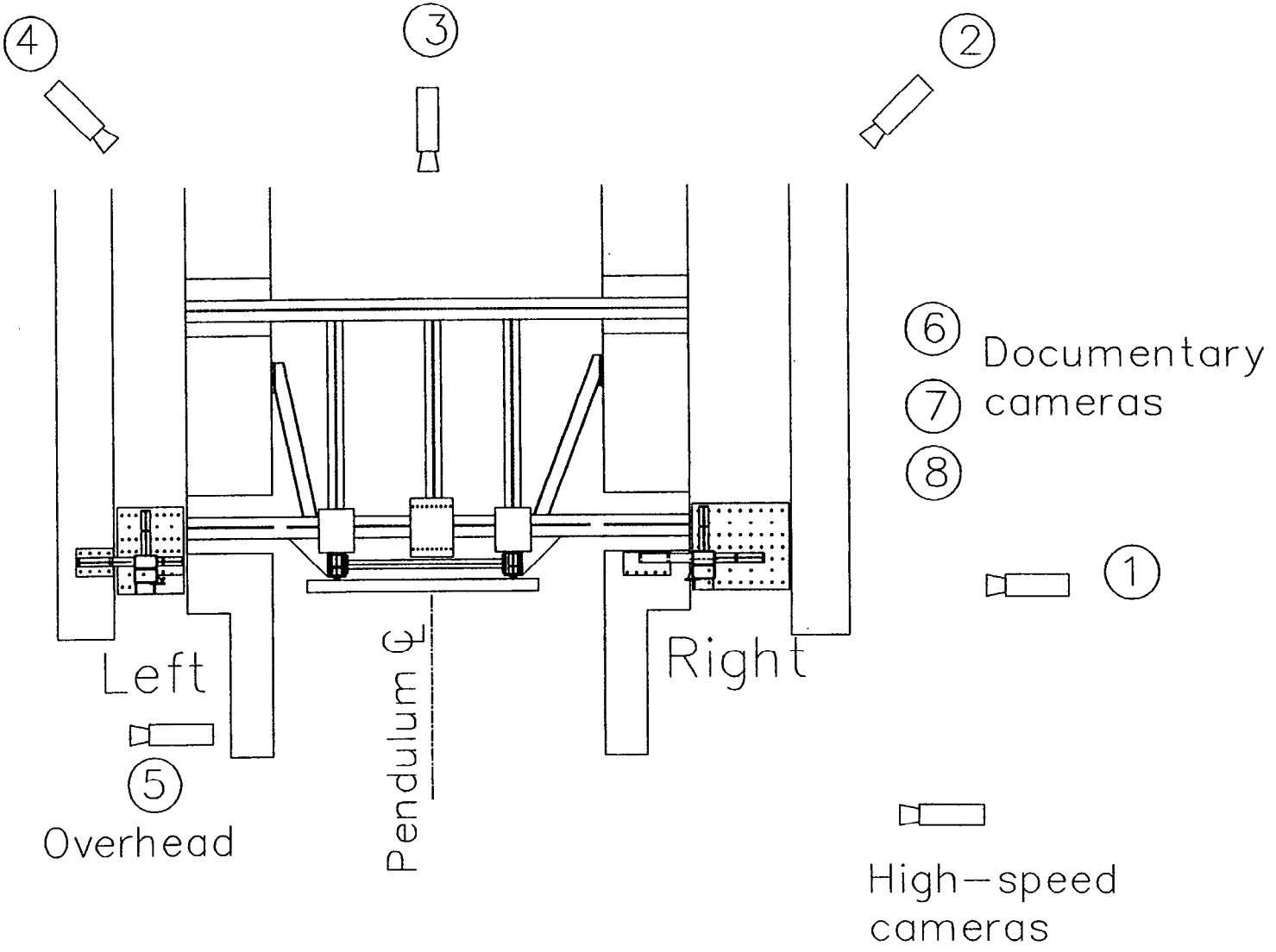

Figure 3. Overhead view of test setup and placement of high-speed cameras (continued).

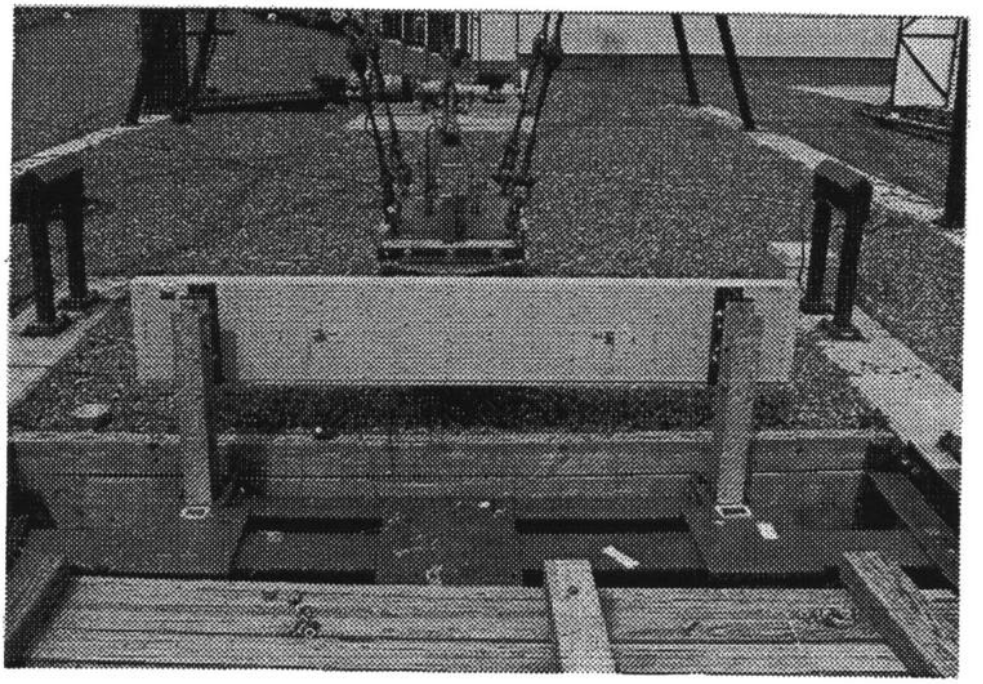

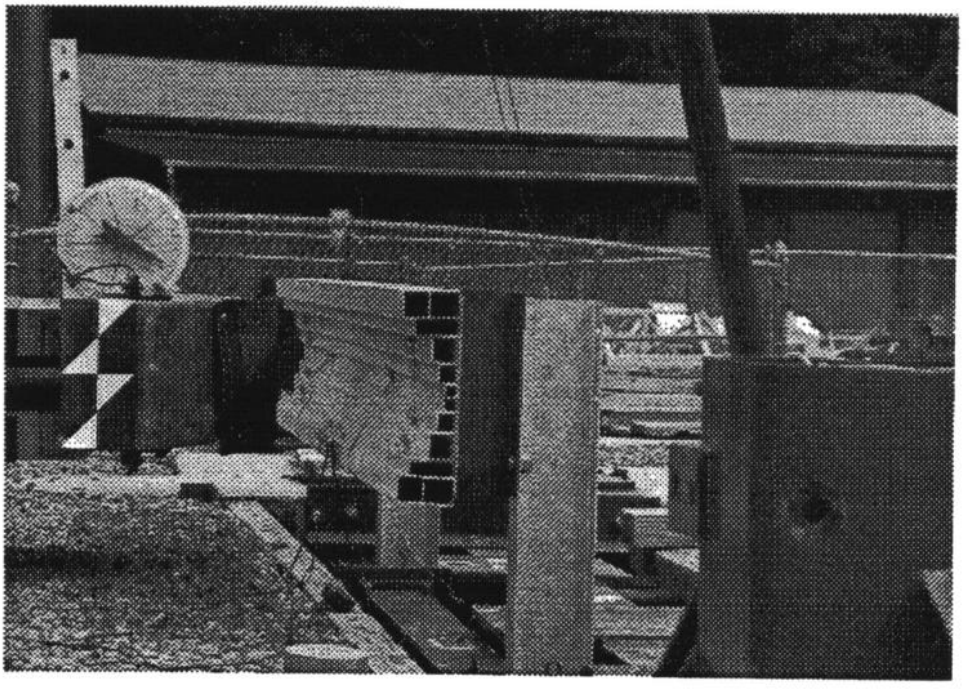

Figure 4. Typical test installation for the two-post setup.

Figure 5. Typical test installation for the four-post setup.

DATA ACQUISITION

For each pendulum test, a speed trap, accelerometers, strain gages, and high-speed film were used for data collection. Strain gages were placed on the FRP rail elements by CUA before delivery to the FOIL.

Speed Trap. The speed trap consisted of a set of four LED infrared emitter/receiver pairs fastened on opposite sides of the pendulum's swing path at 150-mm intervals. The scanner pairs were positioned before the impact area to measure the speed of the pendulum just prior to contact with the composite rail. Signals from the sensors were recorded on a Honeywell model 5600E analog tape recorder. The signals were stored on analog tape for future analysis.

Accelerometers. Two longitudinal (x-axis) 100-g accelerometers were mounted at the center of the rear face of the pendulum. The accelerometer signals were recorded by the FOIL onboard data acquisition system (ODAS) III/8. The ODAS III/8 is a self-contained data acquisition system providing transducer excitation, signal conditioning, 4000-Hz pre-filtering, 12,500-Hz digital sampling, and digital storage for up to eight channels. Data were collected, then downloaded to a portable computer.

Strain Gages. Data from either two or four single-gage strain gages were recorded during the pendulum tests. The single-gage strain gages were attached to the FRP specimen. Specimens with four gages were configured with two gages placed on the front, and two gages placed on the back of the FRP rail. Each front and back pair were placed at the same location vertically and laterally. The gages were placed at the same locations for each test. The specimens with two gages were configured with the gages attached only at the two right-side locations described in the four-gage configuration. During tests with only two strain gages, the strain gage data were recorded via the ODAS III system. During tests with four strain gages, the strain gage signals were conditioned using Vishay model 2310 amplifiers and recorded on analog tape using a Honeywell 5600E tape recorder for later analysis. Figure 2 shows the locations of the single-gage strain gages on the FRP composite rail.

High-Speed Photography. The tests were photographed using five high-speed cameras, one real-time camera, and two 35-mm still cameras. All high-speed cameras were loaded with Kodak 2253 color daylight film and the real-time camera was loaded with Kodak 7239 color film. One 35-mm camera was loaded with black-and-white print film and the other with 35-mm color slide film. The camera placements are summarized in table 2. The camera numbers in table 2 are also shown in figure 3.

Table 2. Camera configuration and placement.				
Camera Number	Type	Film Speed (frames/s)	Lens (mm)	Location
1	Locam II	500	50	90° to impact rt side
2	Locam II	500	25	45° to impact rt side
3	Locam II	500	75	180° to impact
4	Locam II	500	25	45° to impact left side
5	Locam II	500	25	overhead
6	Bolex	24	zoom	documentary
7	Canon A-1 (prints)	still	zoom	documentary
8	Canon A-1 (slides)	still	zoom	documentary

DATA ANALYSIS

For each pendulum test, a speed trap, accelerometers, strain gages, and high-speed film were used for data collection.

Speed Trap. The speed trap consisted of a set of four LED infrared emitter/receiver pairs fastened on opposite sides of the pendulum's swing path at 150-mm intervals just prior to the FRP composite specimen. As the pendulum passed through the infrared scanners, electronic pulses were recorded on analog tape. The tape was played back through a Data Translation analog-to-digital (A/D) converter and the time between pulses was determined. Time-displacement data were entered into a computer spreadsheet and a linear regression was performed on the data to determine the pendulum speed.

Accelerometers and Strain Gages. The data from the accelerometers and strain gages were digitally recorded and converted to the ASCII format. The sampling rate during data acquisition was 4000 Hz for data recorded via the FOIL umbilical cable and tape recorder (four-gage specimen strain gages) and 12,500 Hz for data recorded via the ODAS III onboard system (accelerometers and two-gage specimen strain gages). The ASCII files were processed, which included removal of zero-bias, storing the region of interest, and digitally filtering the data to 300 Hz (Class 180). Strain gage data were digitally filtered at 100 Hz (Class 60). Data were imported into a spreadsheet for plotting and analysis.

High-Speed Photography. The crash event was recorded on 16-mm film by five high-speed cameras. Primarily, the overhead camera was the only camera used for high-speed film analysis. Analysis of the crash event was performed using an NAC film motion analyzer model 160-F in conjunction with an IBM PC-AT. The motion analyzer digitized the 16-mm film, reducing the image to Cartesian coordinates. Using the Cartesian coordinate data, a time-displacement history of the test was obtained. The time-displacement data were then imported into a computer spreadsheet and a linear regression was performed to determine the impact velocity of the pendulum. Using the Cartesian coordinate data, the deflection of the rail could be measured directly. Film analysis data could be used in the event of electronic data channel failure. The speed-trap data were used as the primary measurement for impact velocity.

RESULTS

For each test, the pendulum was accelerated to the target speed and made contact at the intended location on the FRP rail. The first two tests were conducted at 20 km/h. The lower speed tests were conducted to observe the dynamic performance of the FRP rail to ensure that nothing unpredictable would occur. One test was conducted on a non-anchored rail (test 96P019), and one test was conducted on an end-anchored rail (test 96P020). During test 96P019, the pendulum struck the FRP rail and collapsed the FRP box-sections. The built-up forces caused the strong-posts to twist and bend backwards. The pendulum continued forward, loading the FRP rail until the pendulum stopped at approximately 0.250 s. During test 96P020, the pendulum struck the FRP rail and collapsed the FRP box-sections. The built-up forces caused the strong-posts to twist and bend backwards. The pendulum continued forward, loading the FRP rail and cable anchors until the pendulum stopped at approximately 0.090 s. The FRP rails behaved in a predictable manner; therefore, a 35-km/h test was conducted on an end-anchored rail.

During test 96P021, the pendulum struck the FRP rail with a velocity of 35.3 km/h. The pendulum collapsed the FRP box-sections. The built-up forces caused the strong-posts to twist and bend backwards. The pendulum continued forward, loading the FRP rail, and as the load began to transfer to the anchor cables, the edge of one of the cable anchor brackets cut one of the anchor cables. The cable failure allowed for a large rail deflection and caused the pendulum to yaw clockwise. Before additional fixed-end testing was conducted, modifications were made to the cable anchor brackets to prevent the brackets from cutting the anchor cables. Two more fixed-end tests (97P001 and 97P002) were conducted after conducting two additional non-fixed-end tests (96P022 and 96P023).

Tests 96P022 and 96P023 were tests conducted on non-fixed-end specimens at impact speeds of 25.2 and 35.7 km/h, respectively. During test 96P022, the pendulum collapsed the FRP box-sections and loaded the rail until the strong-posts failed in bending and torsion. The FRP rail stopped the pendulum at approximately 0.240 s. During test 96P023, the pendulum collapsed the FRP box-sections and loaded the rail until the strong-posts failed in bending and torsion. The two bolts attaching the blockout to the left-side strong-post failed, and the pendulum swung through the specimen and climbed to a height of approximately 3 m.

The FRP rails tested in tests 97P001 and 97P002 had modified cable anchor brackets. Two small slots were made in the corners of each cable anchor bracket. These slots would prevent the anchor cable failure experienced in test 96P021. The test speeds during tests 97P001 and 97P002 were 35.6 km/h and 35.2 km/h, respectively. The response of the FRP rail was similar during these two tests. The pendulum struck the FRP rail and collapsed the FRP box-sections. The built-up forces in the rail led to the eventual torsional and bending failure of the two standard strong-posts approximately 0.040 s after initial contact. The force relaxed until the cables engaged and stopped the pendulum (0.115 s). The pendulum rebounded with a small velocity. A portion of the rebound velocity may be attributed to the pendulum's natural return to equilibrium. The data from the pendulum testing are summarized in table 3. Pretest and post-test photographs from one non-fixed-end and one fixed-end test (test 96P022 and test 97P002) are shown in figures 6 through 9. Photographs taken from high-speed film during the same two tests are shown in figures 10 and 11. Data plots of data obtained from the pendulum accelerometers and FRP rail strain gages are shown in appendix A.

CONCLUSIONS

The data summarized in table 3 and shown in the data plots in appendix A suggests a high degree of repeatability in the dynamic response of end-anchored or fixed-end FRP rail. The two similar tests, 97P001 and 97P002, are comparable in peak force and rail deflection. Acceleration histories from each of the FRP composite rail 35-km/h tests are plotted together in figure 12. The results from these two tests are comparable to the results from three 35-km/h pendulum tests of cable-anchored steel w-beam guardrail. The points plotted in figure 12 demonstrate the similar loading characteristic. The two-hump shape signifies the events during impact. The first hump may be attributed to the rise in force prior to buckling and torsional failure of the strong-posts and blockouts, while the second hump may be attributed to the load transfer to the anchor cables. This two-stage event is also evident in the steel w-beam tests. An average acceleration history of the two FRP tests and an average acceleration history of three steel w-beam tests are plotted

together in figure 13. The dynamic response of steel w-beam rail is closely replicated by the FRP composite rail during impact tests with a 912-kg pendulum traveling at 35 km/h. The two significant peak loads occur at approximately the same time for both types of rail. The peak loads vary between the two types of rail; however, maximum deflection of the two types of rails is similar. The data also establishes that the energy from a pendulum with a mass of 912 kg and a velocity of 35 km/h is not enough to produce the forces necessary to load the FRP rail element to failure. A heavier, faster pendulum is needed to generate sufficient forces to fail the FRP composite rail.

Table 3. Summary of pendulum testing of FRP composite rail.

Test number	Speed (km/h)		E, (kJ)	Rail Pretension ($\mu\epsilon$)		Peaks		Rail deflection(mm)			Work F•d (kJ)
	Trap	Film		Left gage	Right gage	g's	Force (1000 N)	Accel	Film	Static measure	
96P019	20.3	20.3	14.5	NA	NA	4.6	40.9	890	813	838	14.4
96P020	20.2	20.6	14.4	500	500	11.8	105.6	340	281	152	14.2
96P021	35.3	35.2	43.8	500	500	15.6	139.6	1190	402	705	43.6
96P022	25.2	25.2	22.3	NA	NA	5.2	46.8	1060	984	910	22.3
96P023	35.7	35.2	44.7	NA	NA	8.1	72.6	NA	NA	NA	37.7
97P001	35.6	35.1	44.7	331	321	18.6	166.6	680	528	432	44.5
97P002	35.2	34.9	43.8	335	360	18.7	167.8	650	572	492	43.7

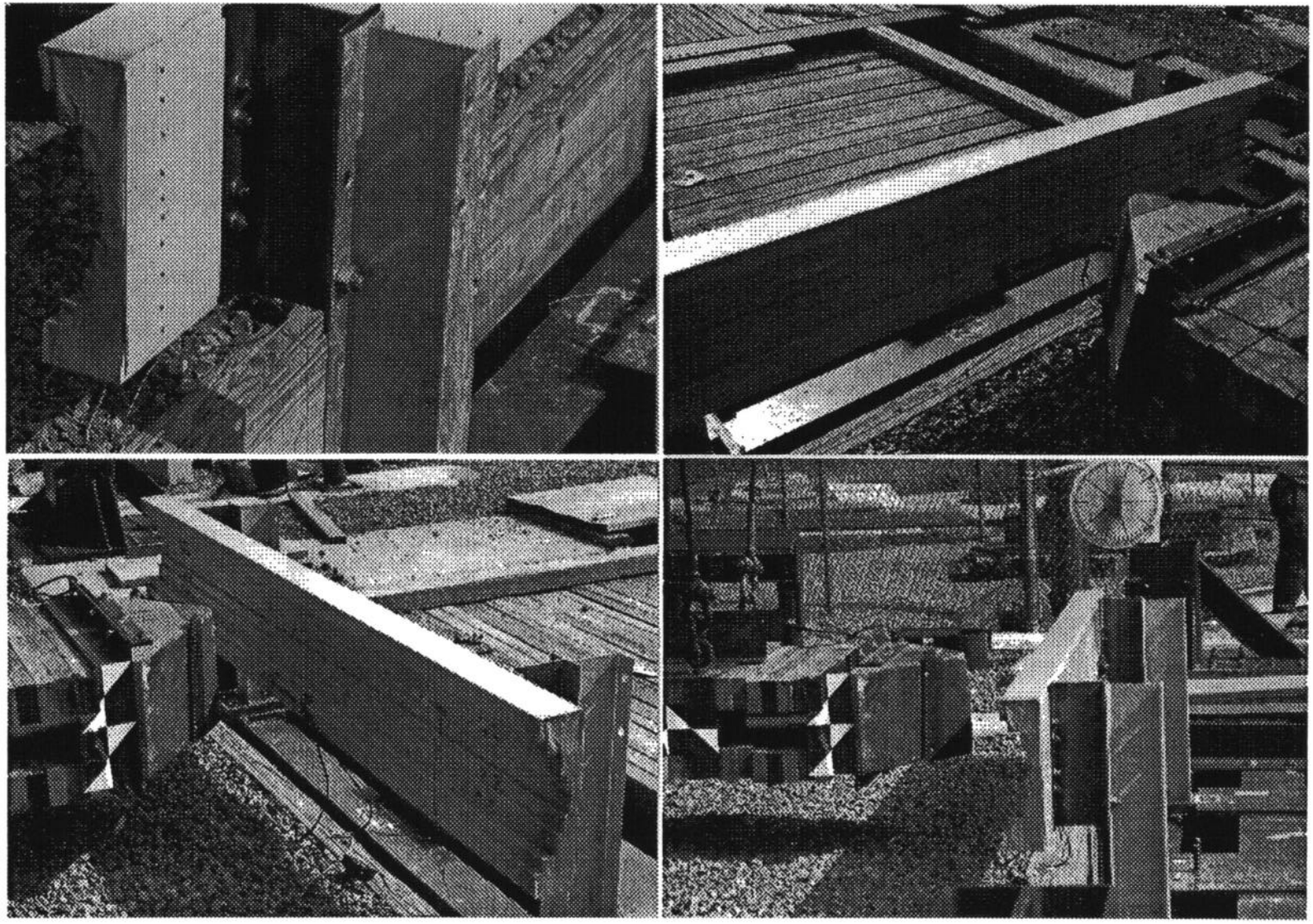

Figure 6. Pretest photographs, test 96P022.

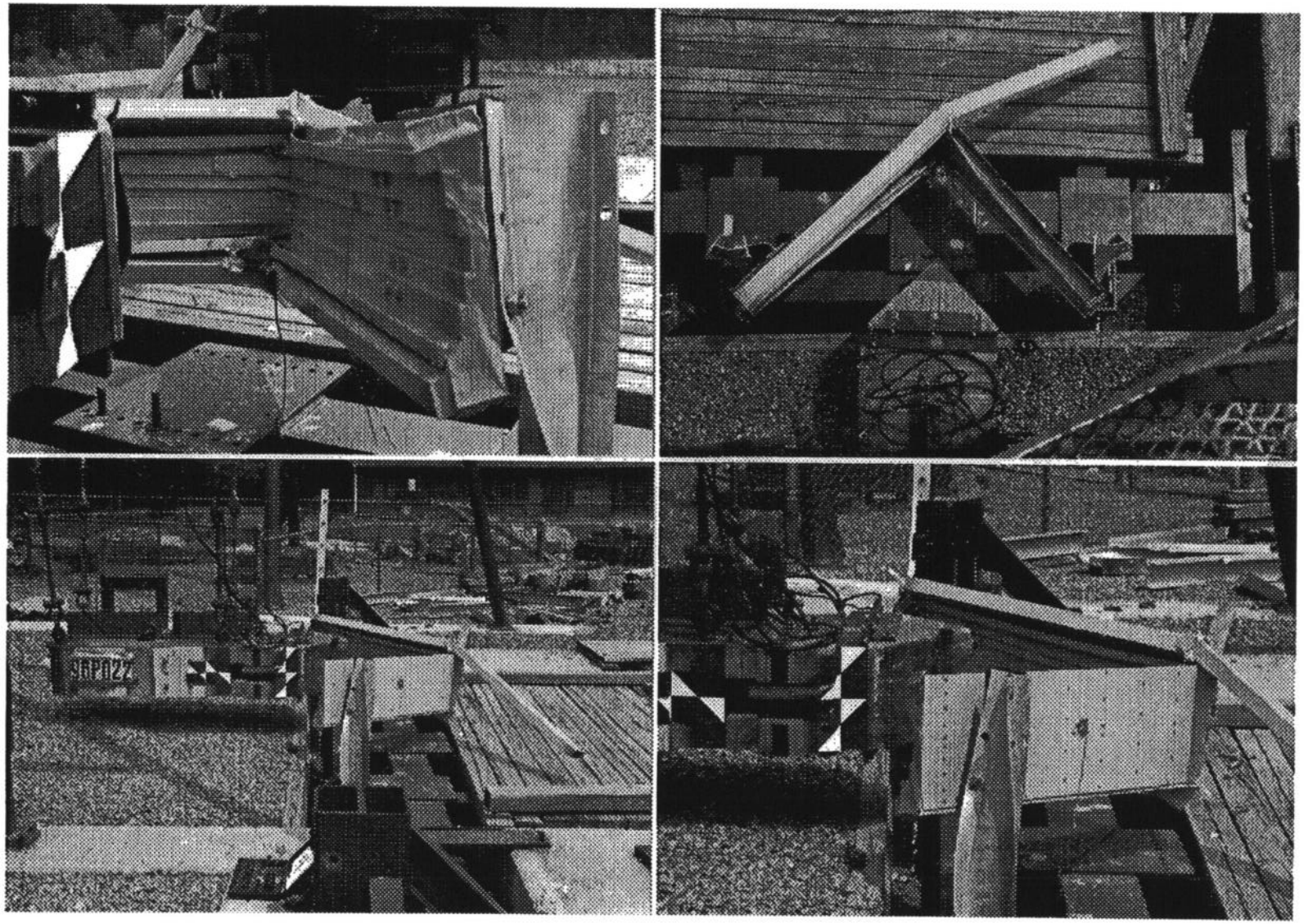

Figure 7. Post-test photographs, test 96P022.

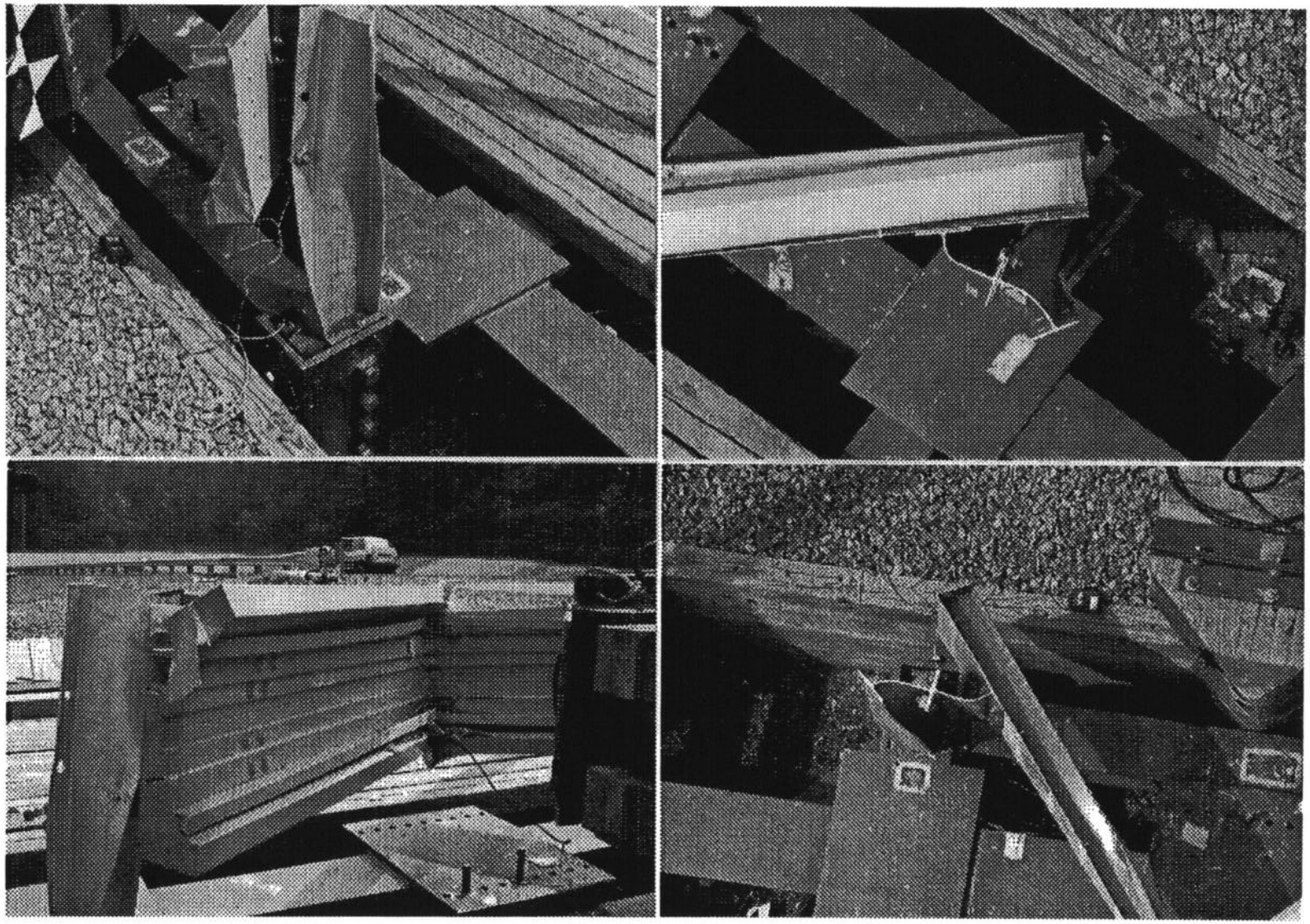

Figure 7. Post-test photographs, test 96P022 (continued).

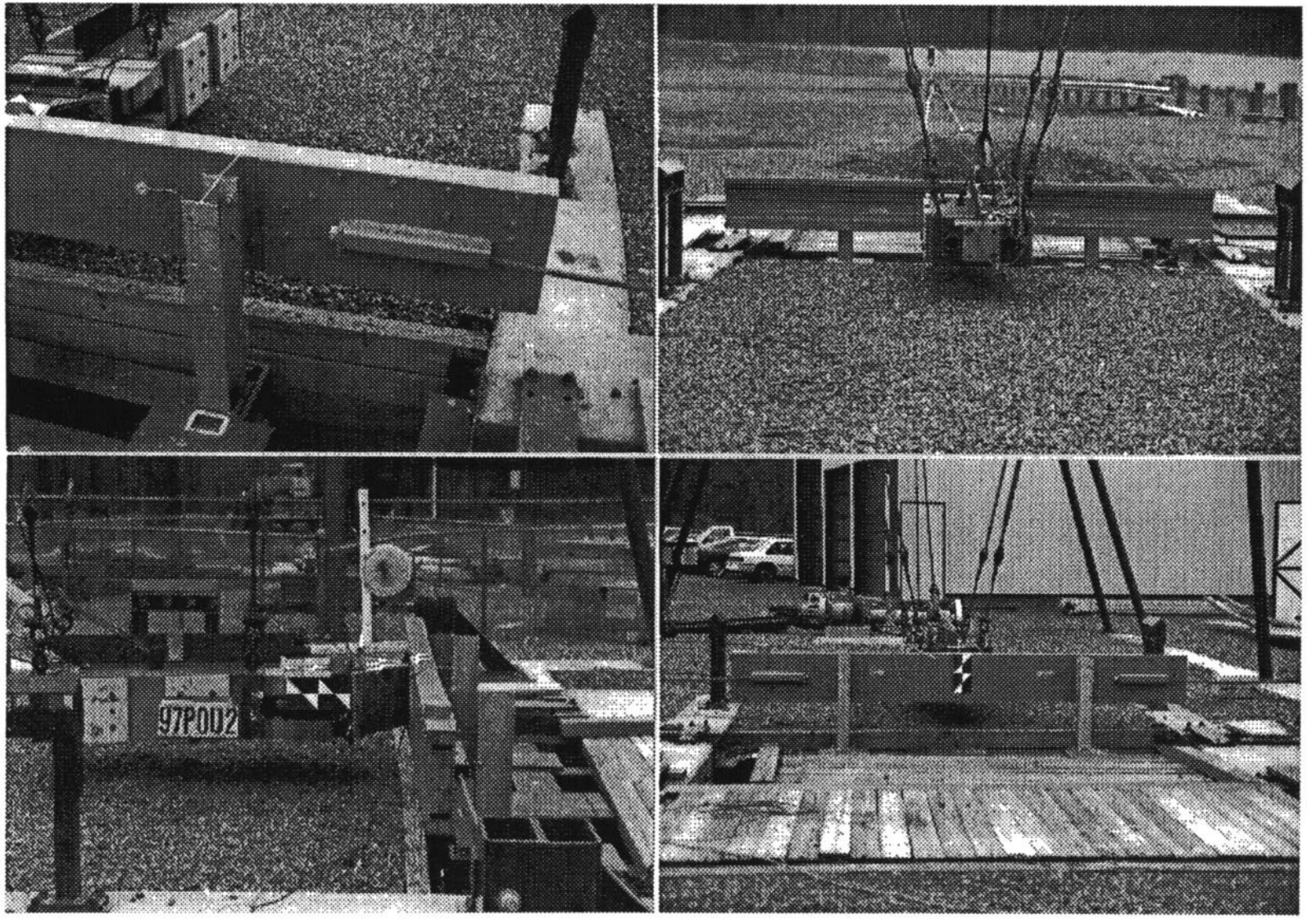

Figure 8. Pretest photographs, test 97P002.

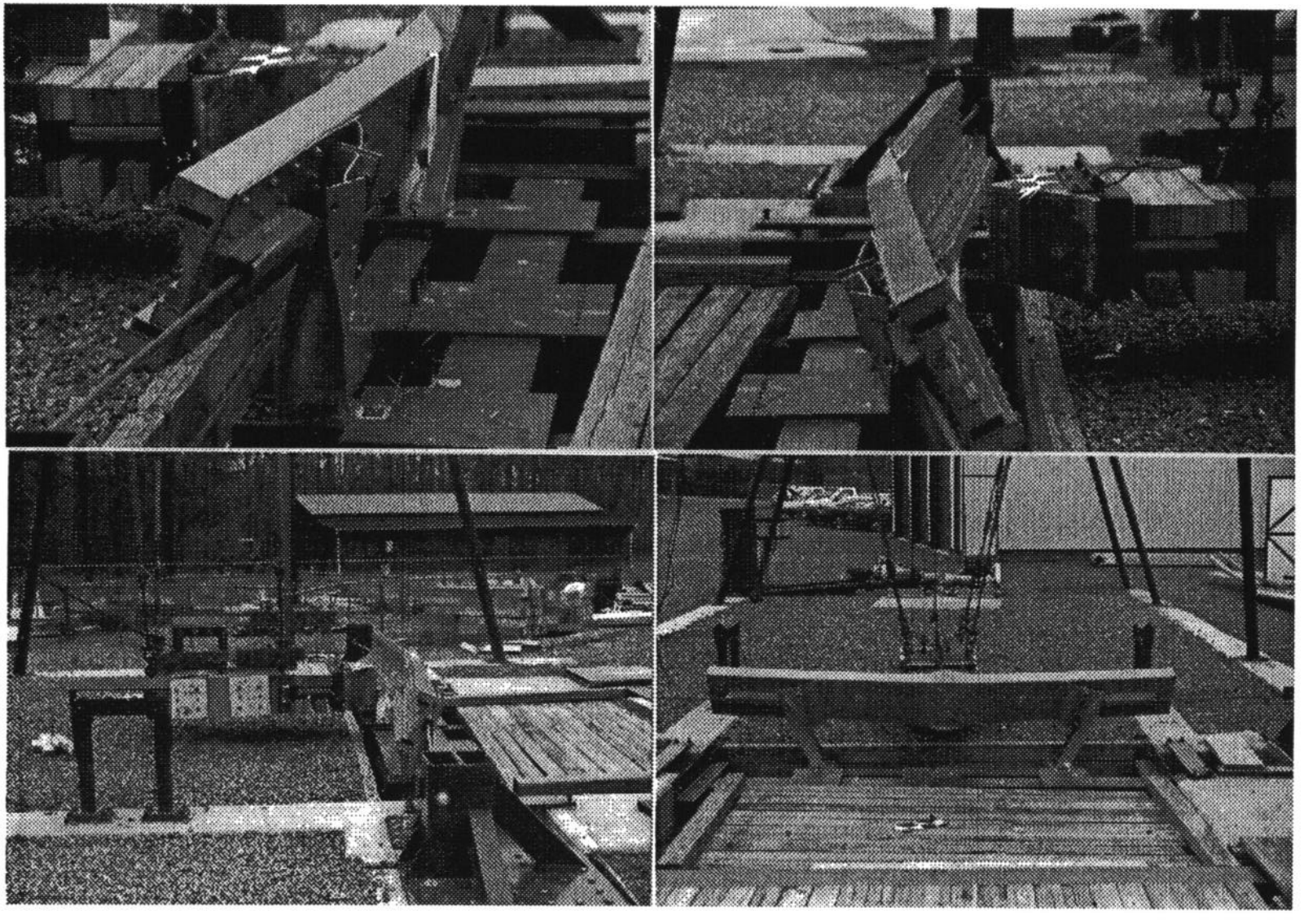

Figure 9. Post-test photographs, test 97P002.

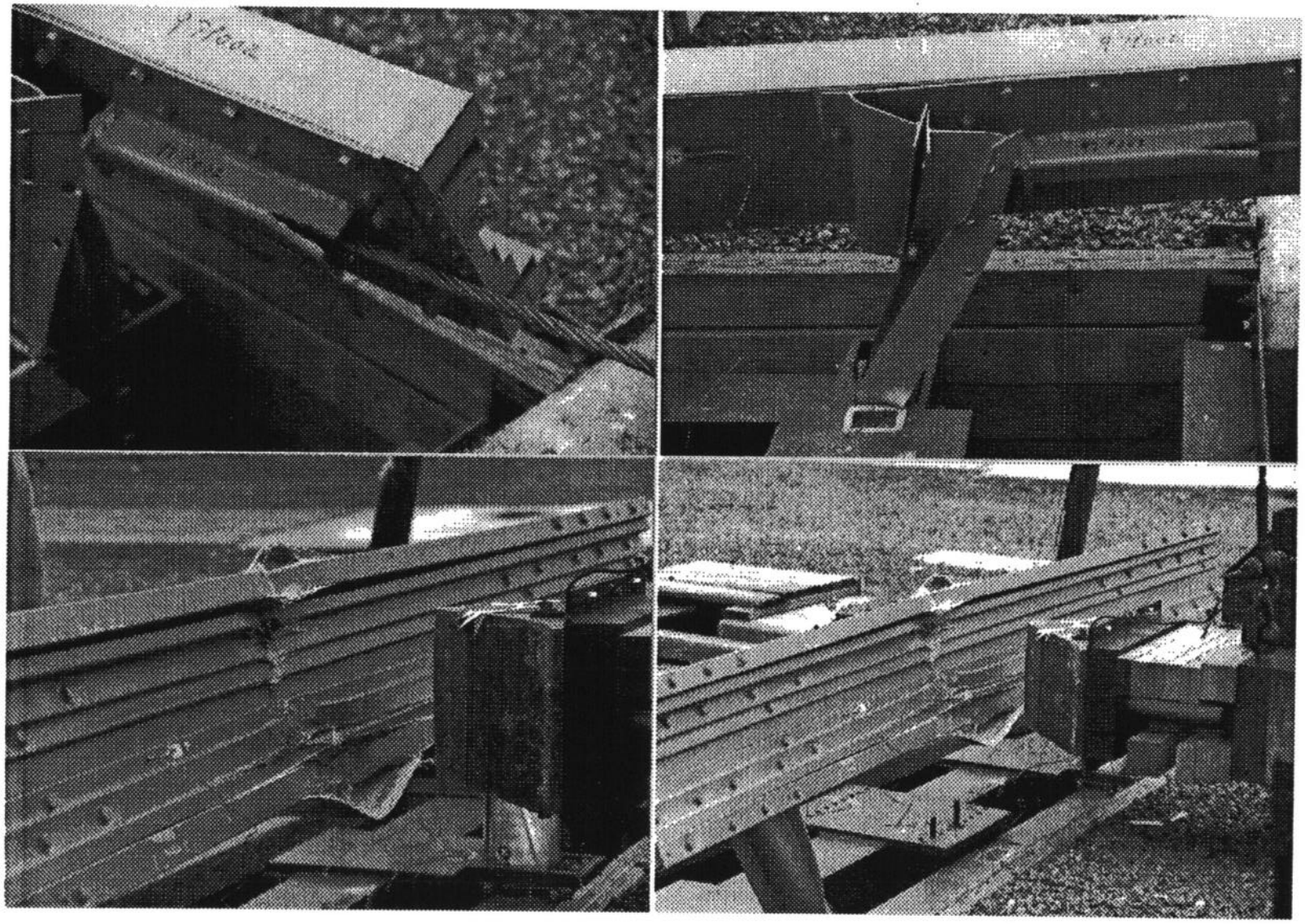

Figure 9. Post-test photographs, test 97P002 (continued).

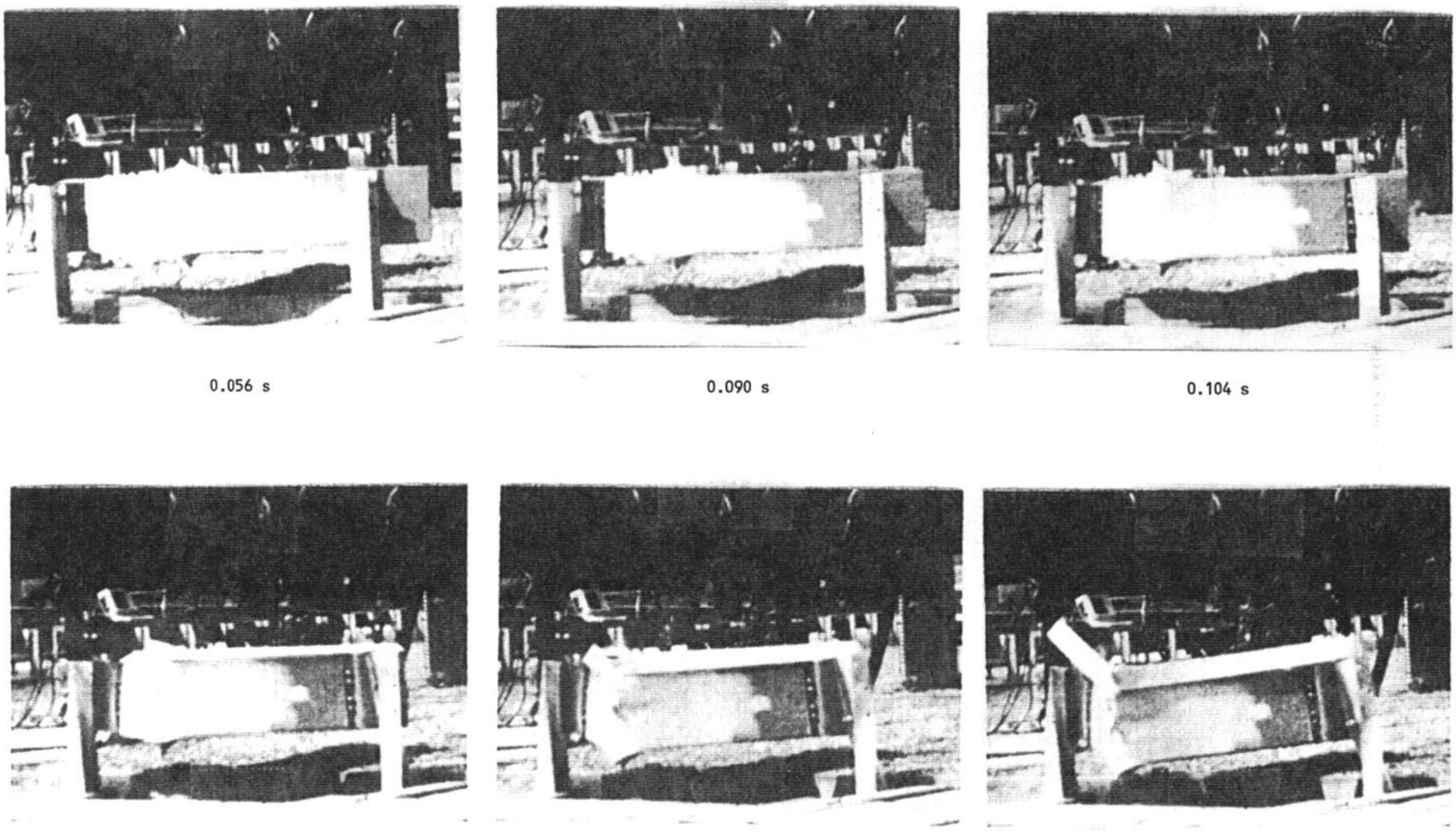

Figure 10. Test photographs during impact, test 96P022.

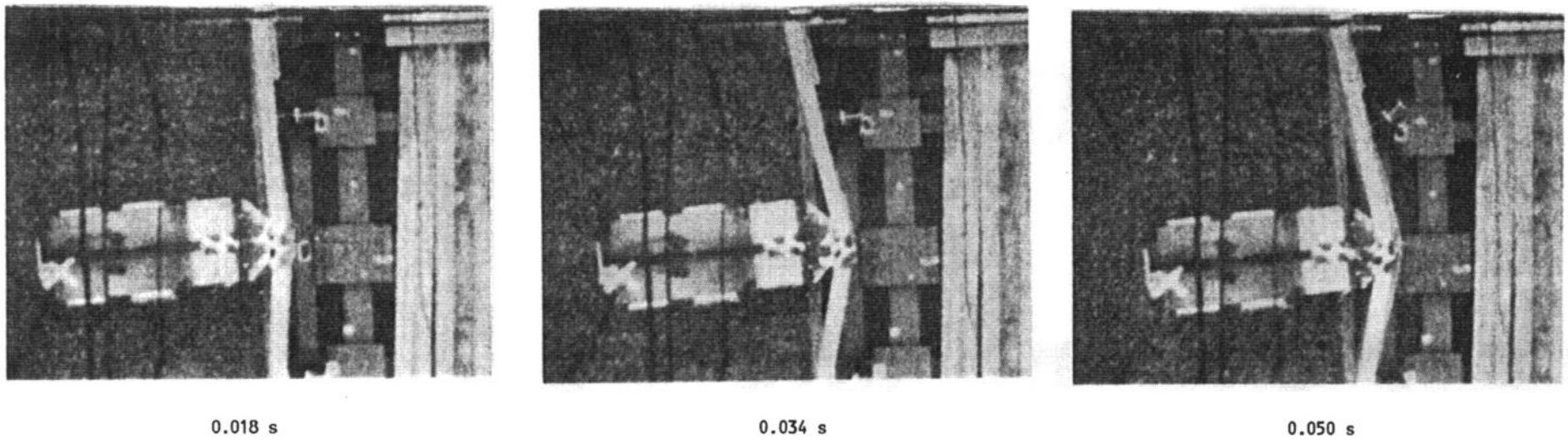

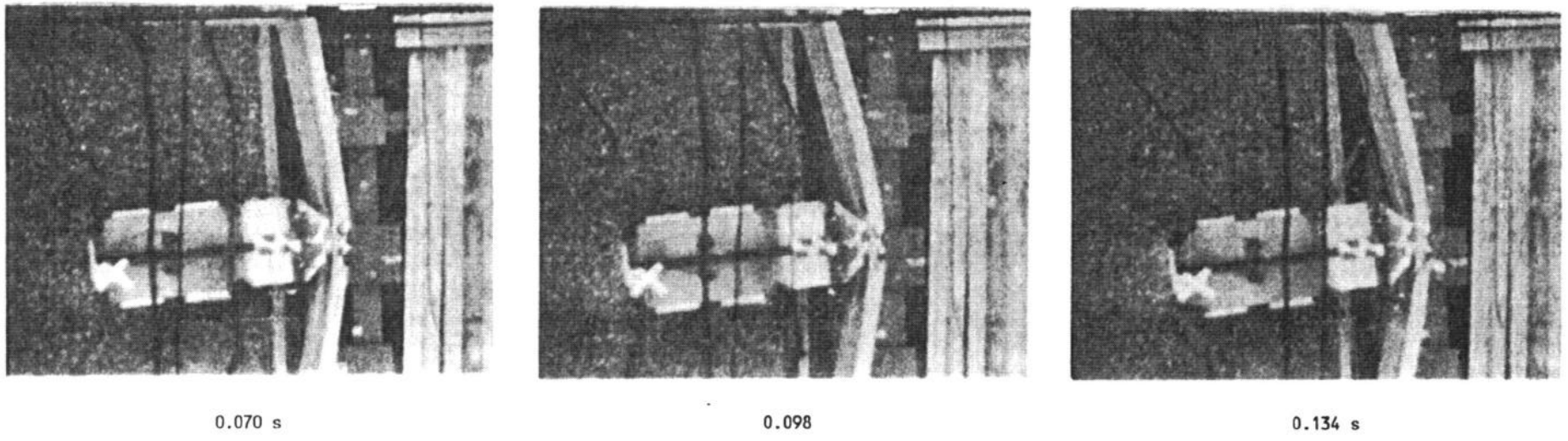

Figure 11. Test photographs during impact, test 97P002.

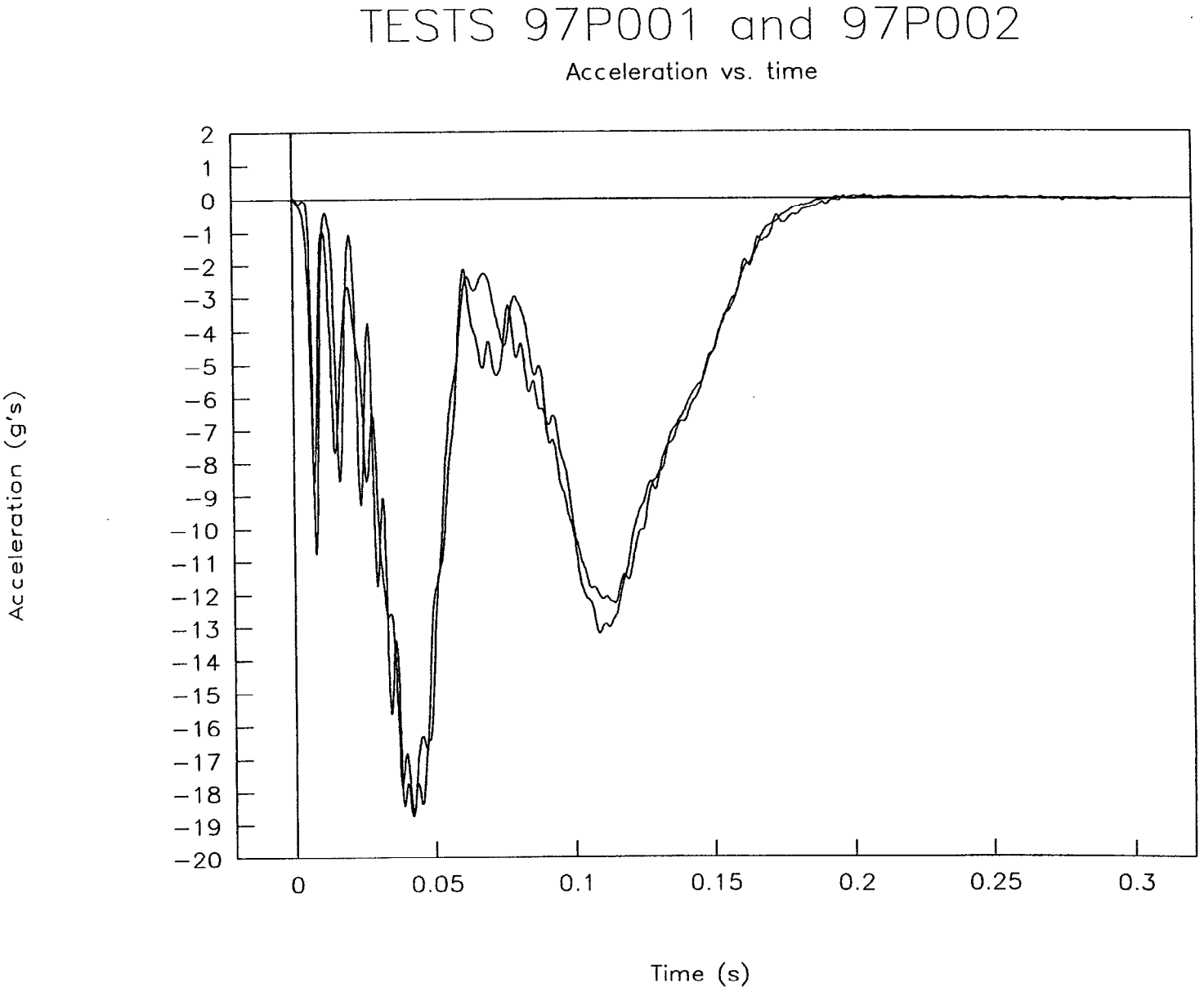

Figure 12. Acceleration histories, tests 97P001 and 97P002.

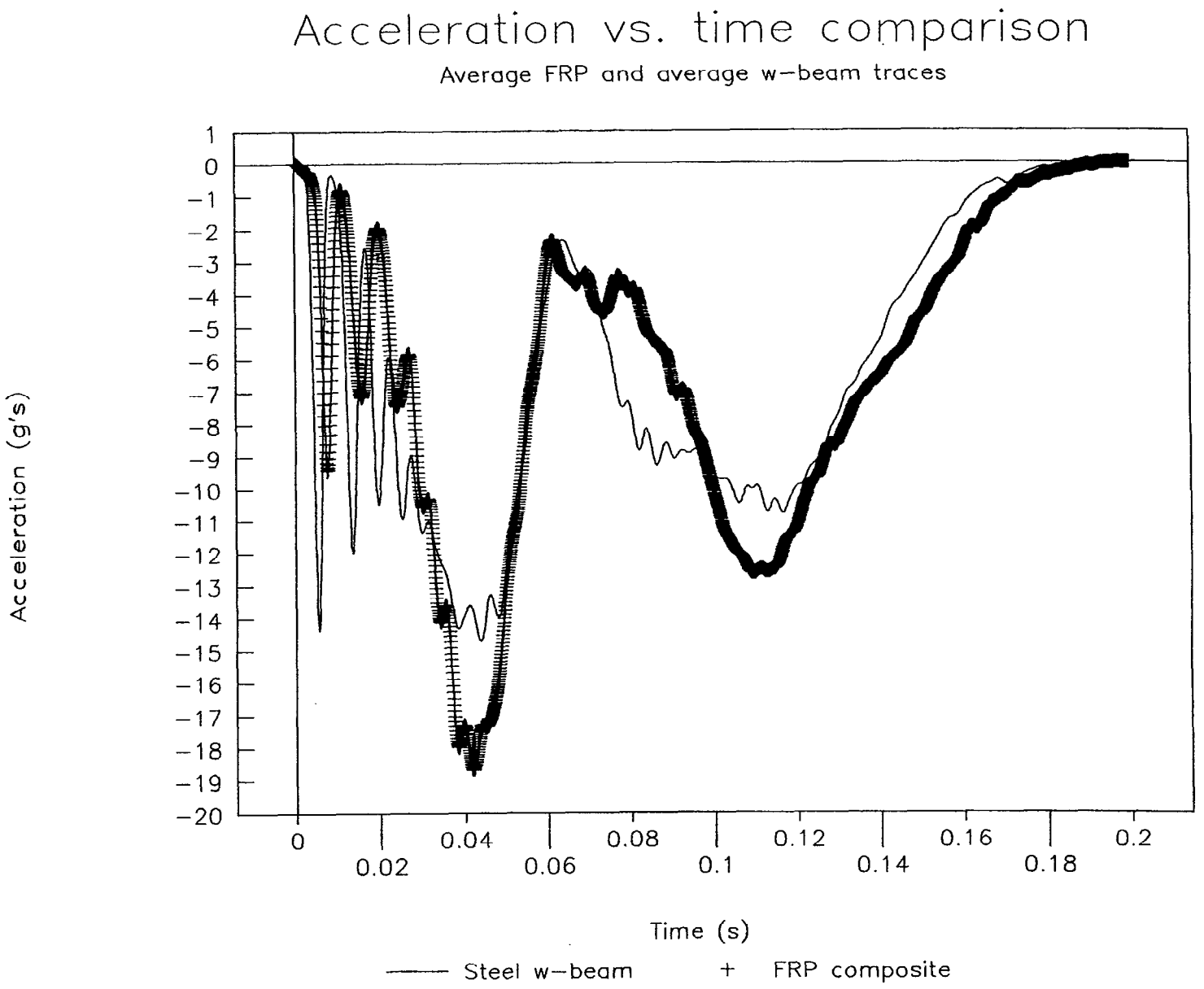

Figure 13. Average FRP and average w-beam traces.

APPENDIX A. DATA PLOTS FROM PENDULUM ACCELEROMETERS

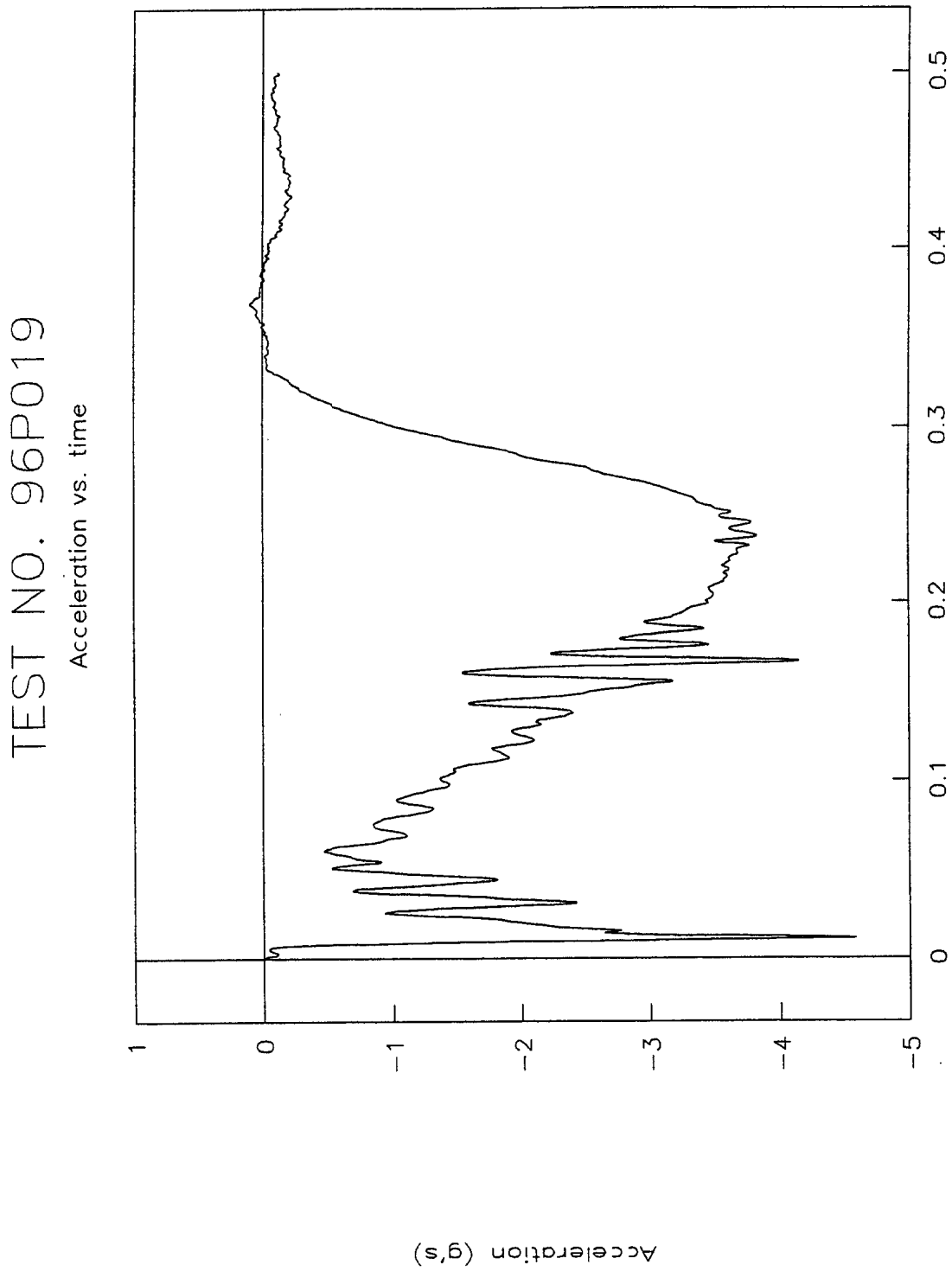

Figure 14. Acceleration vs. time, test 96P019.

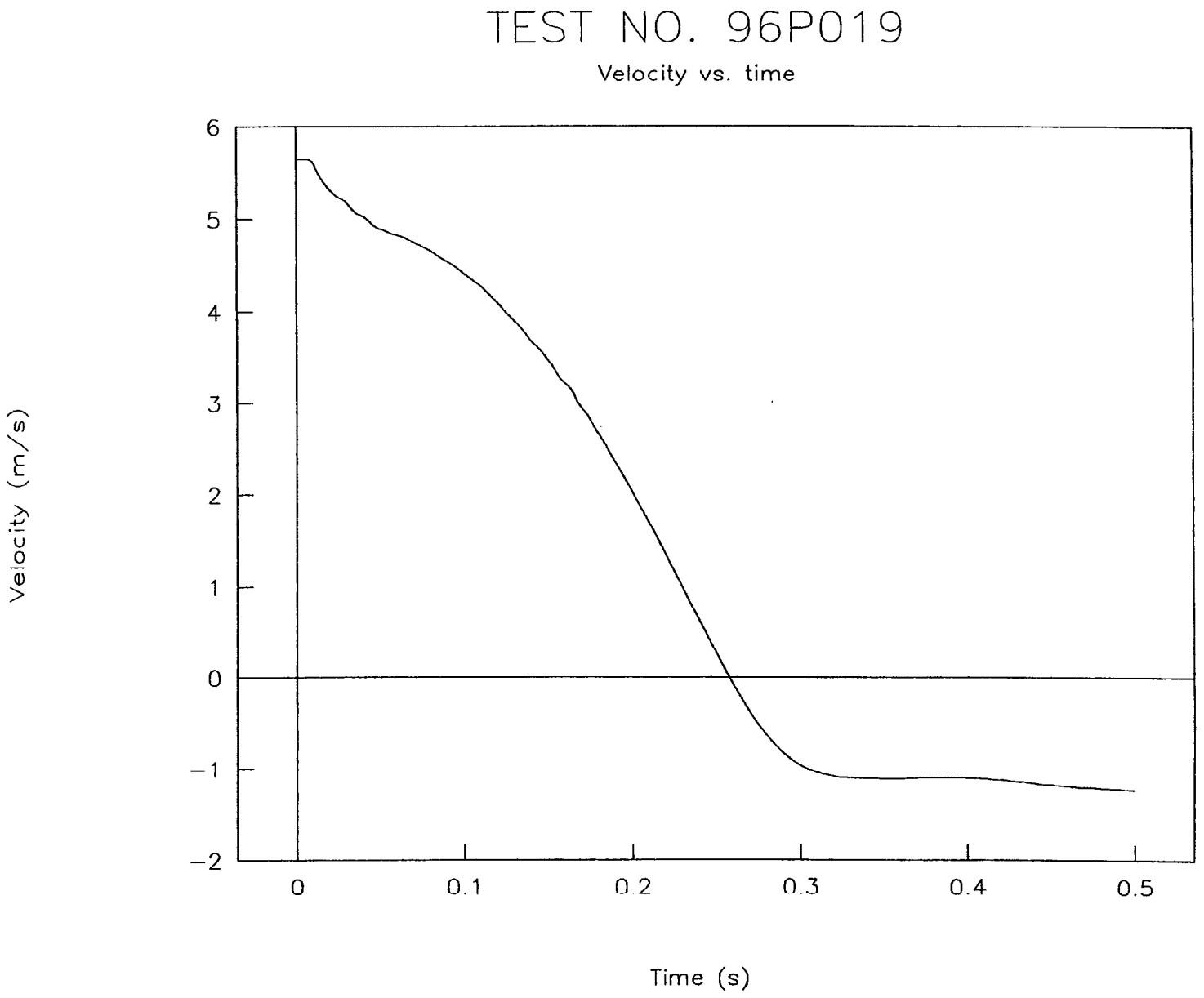

Figure 15. Velocity vs. time, test 96P019.

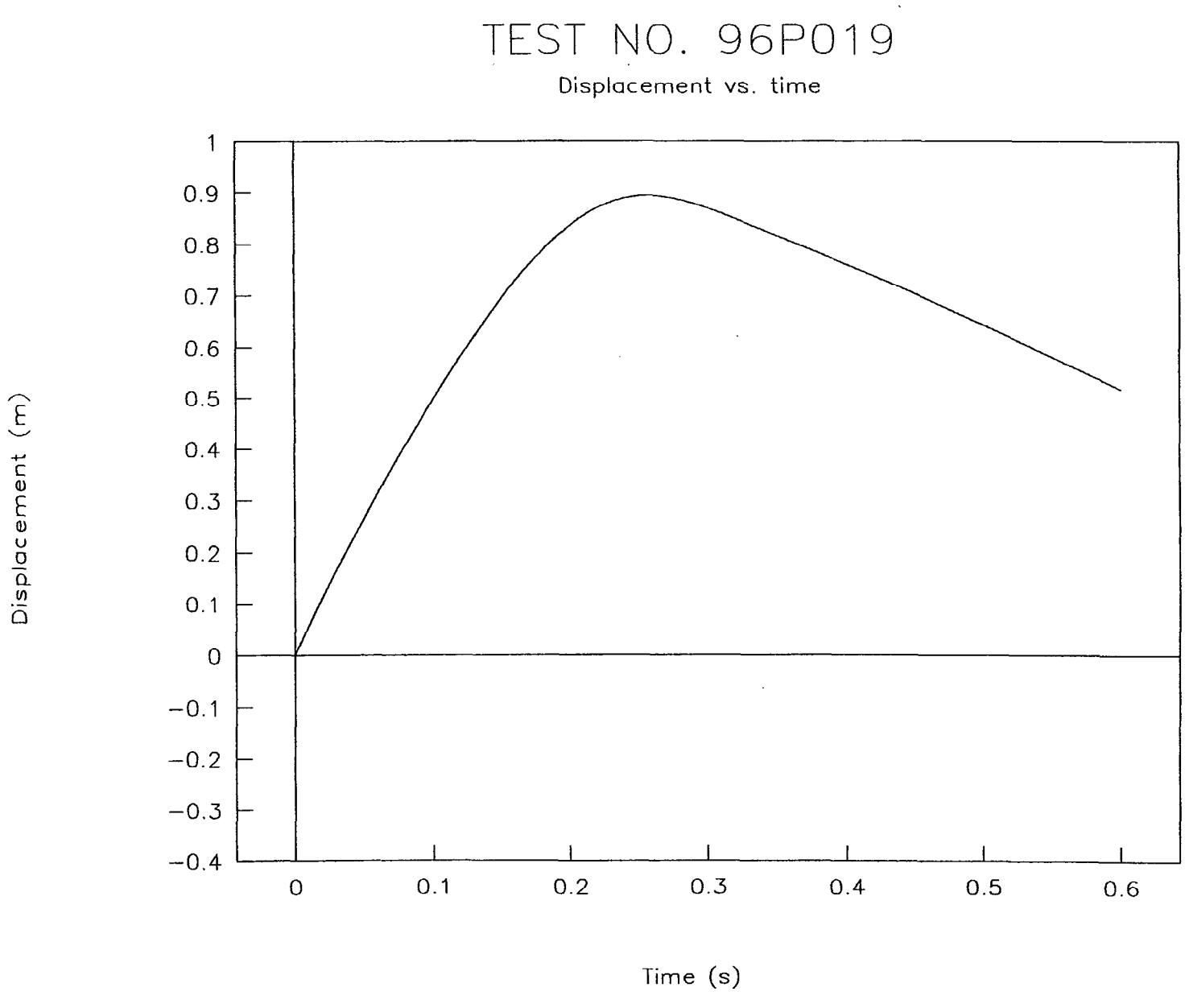

Figure 16. Displacement vs. time, test 96P019.

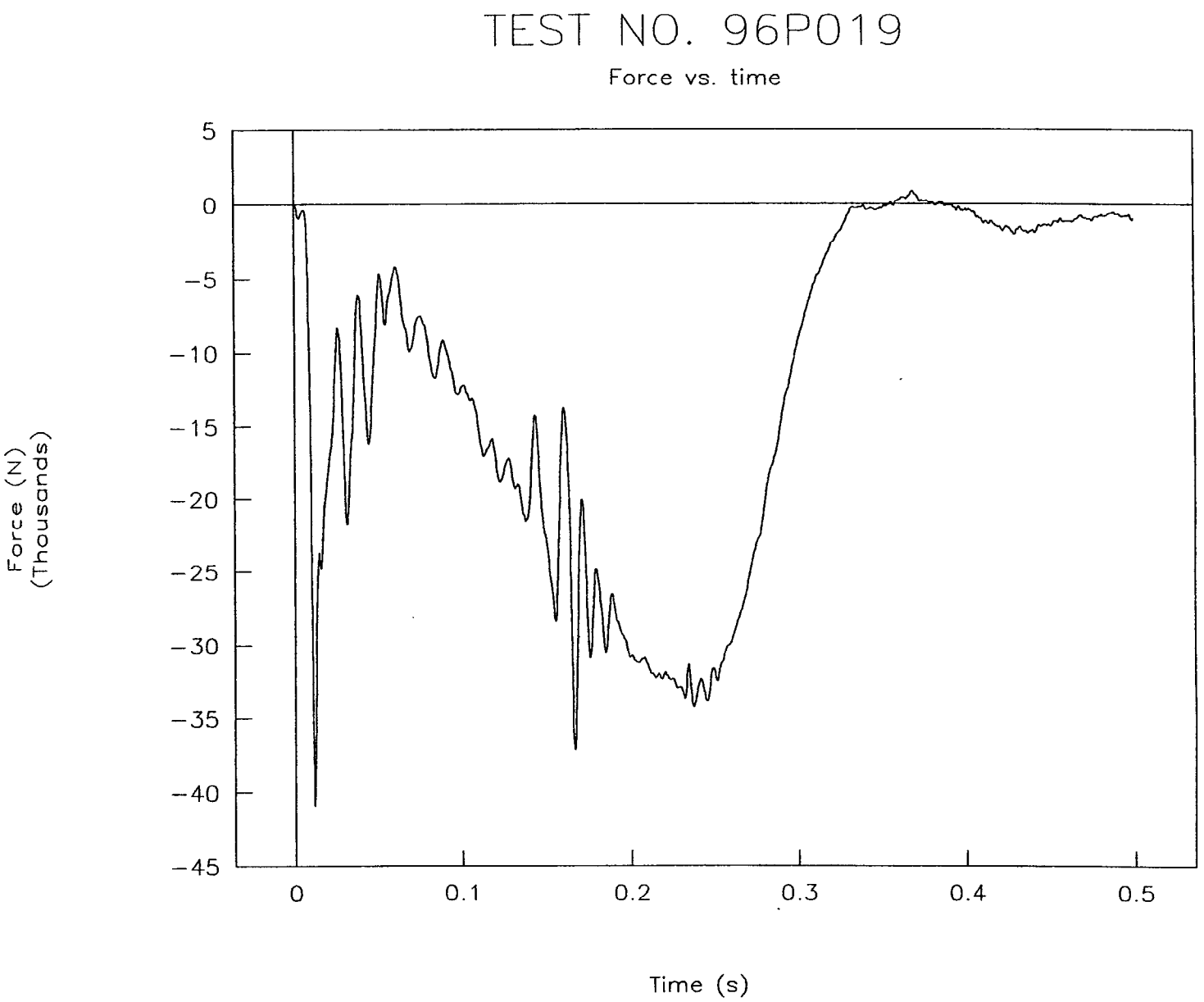

Figure 17. Force vs. time, test 96P019.

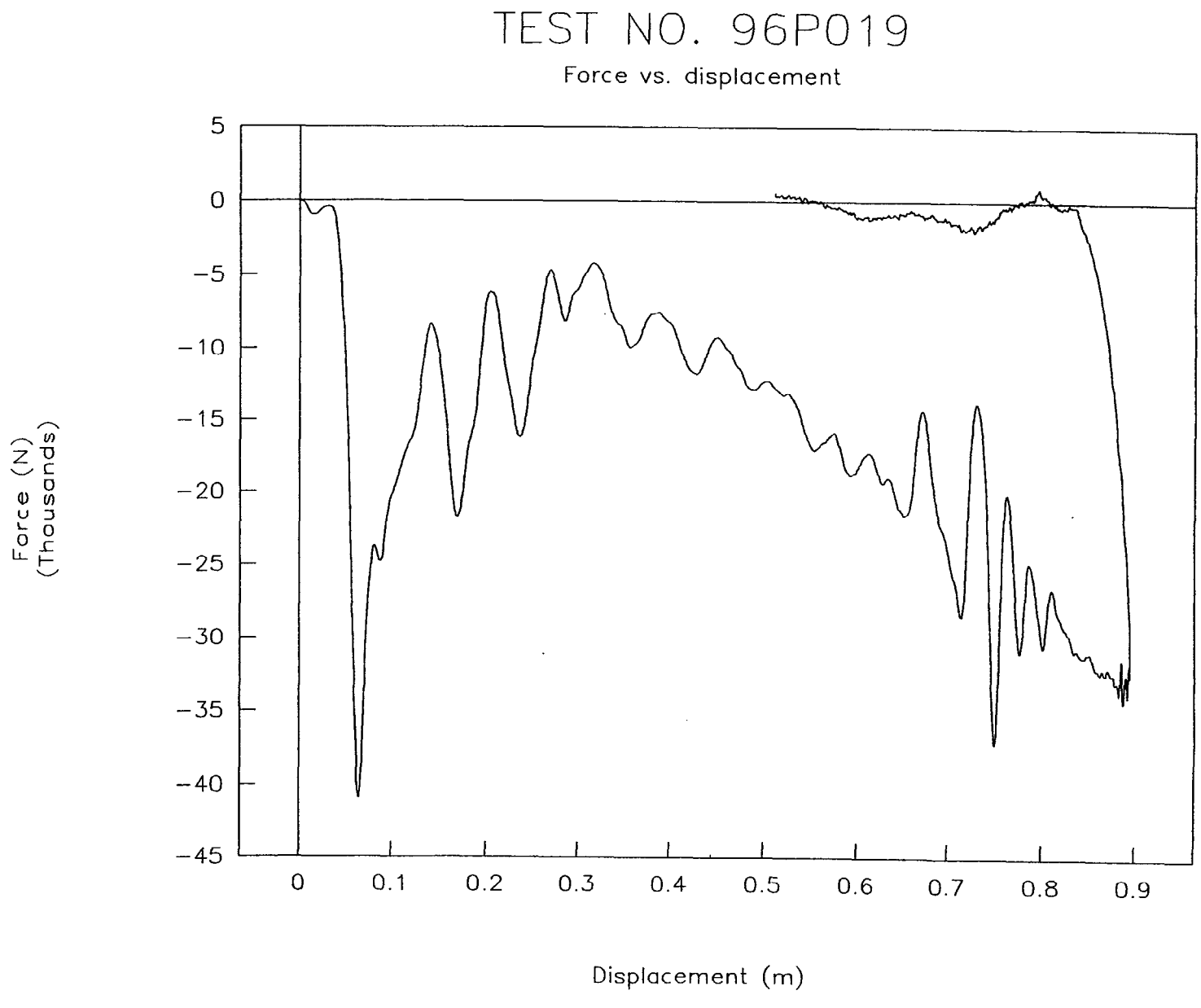

Figure 18. Force vs. displacement, test 96P019.

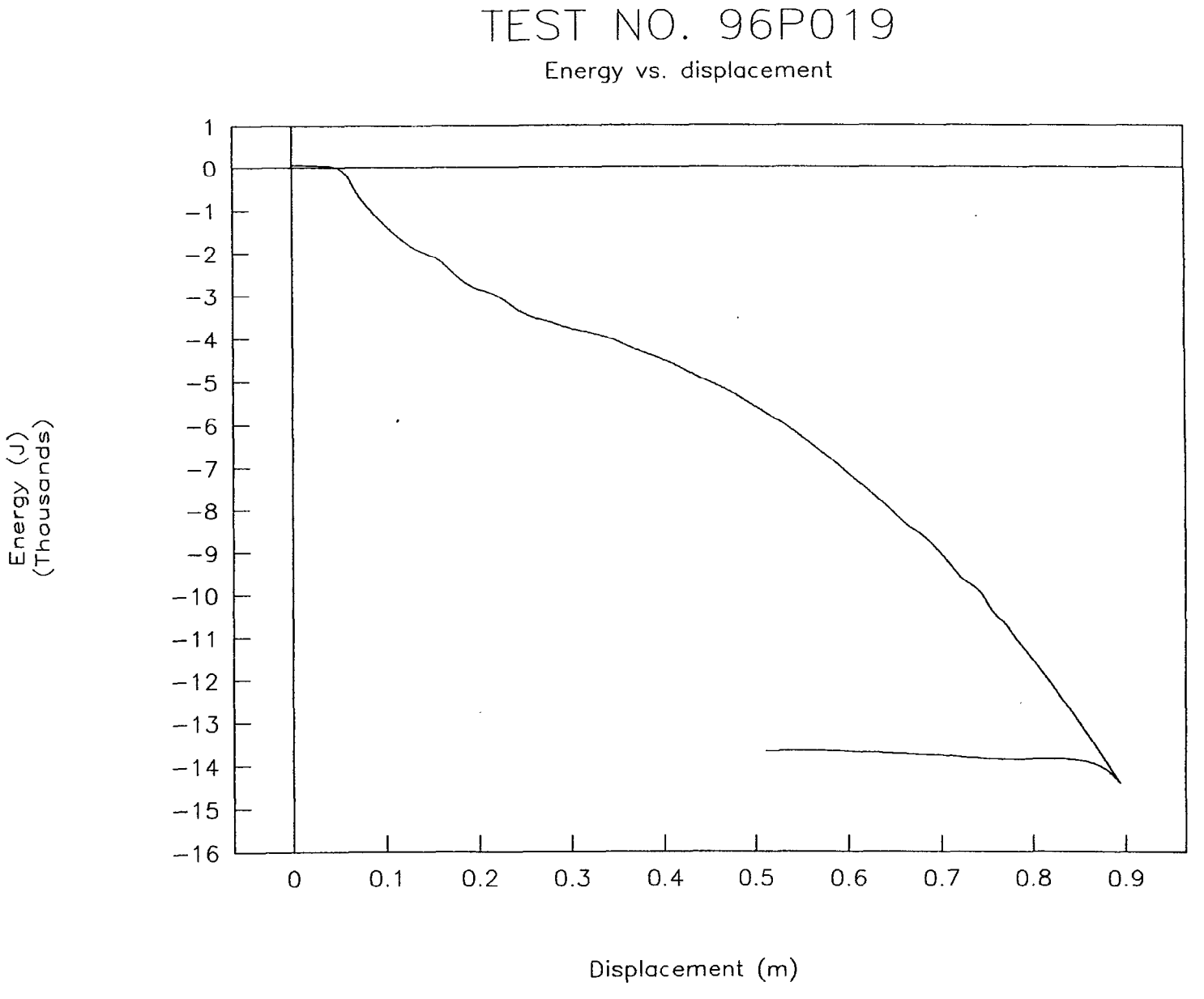

Figure 19. Energy vs. displacement, test 96P019.

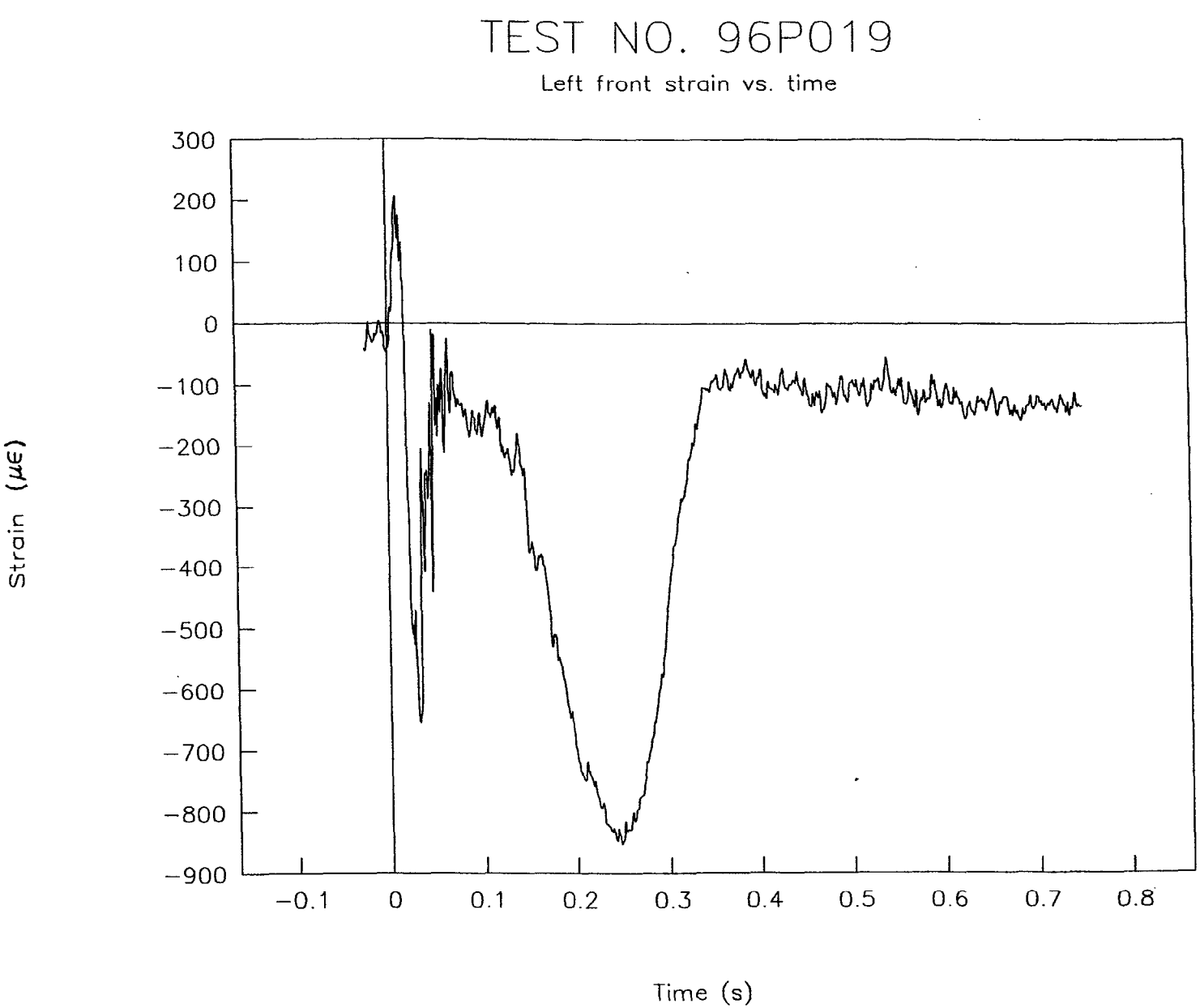

Figure 20. Strain vs. time, left front, test 96P019.

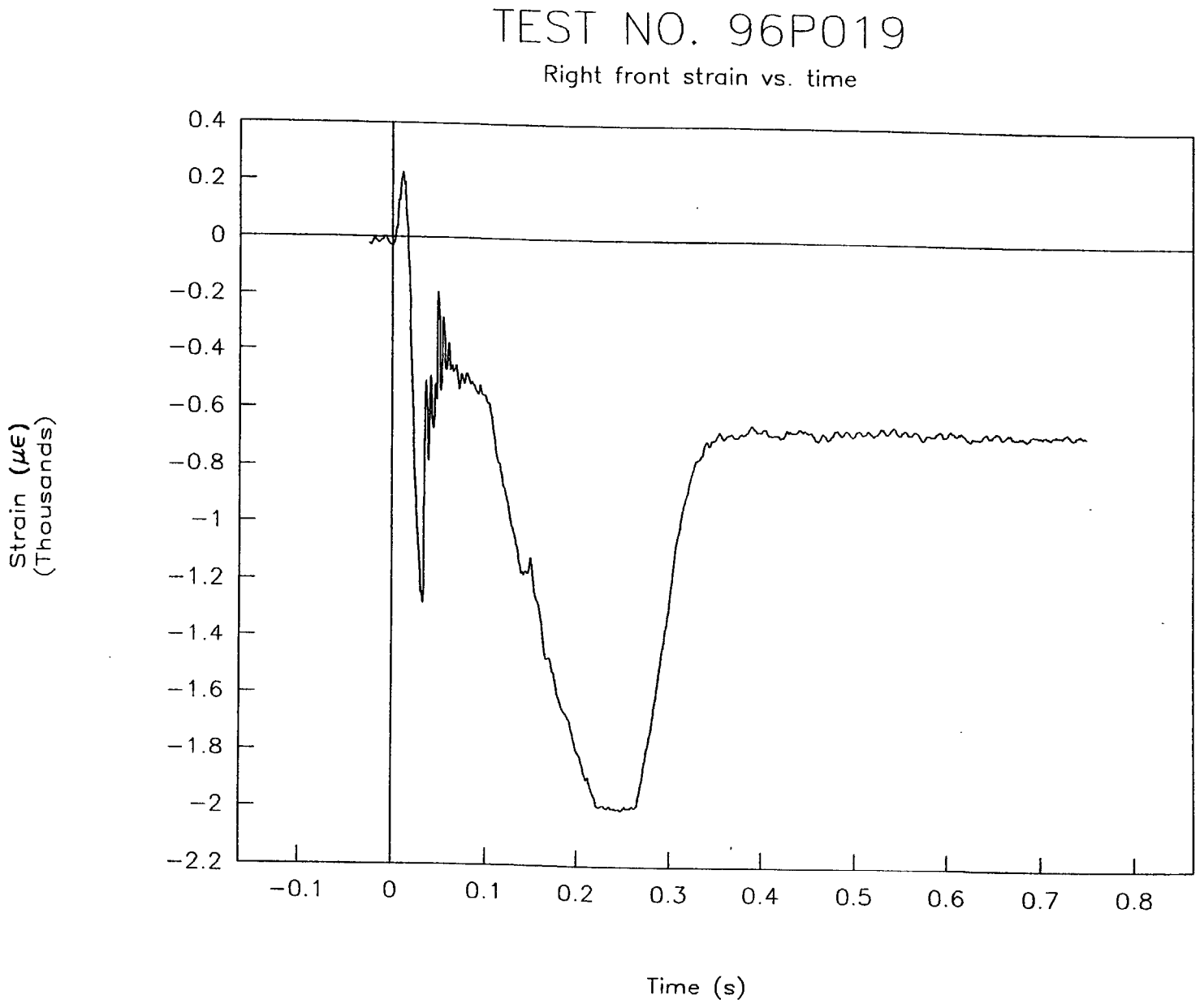

Figure 21. Strain vs. time, right front, test 96P019.

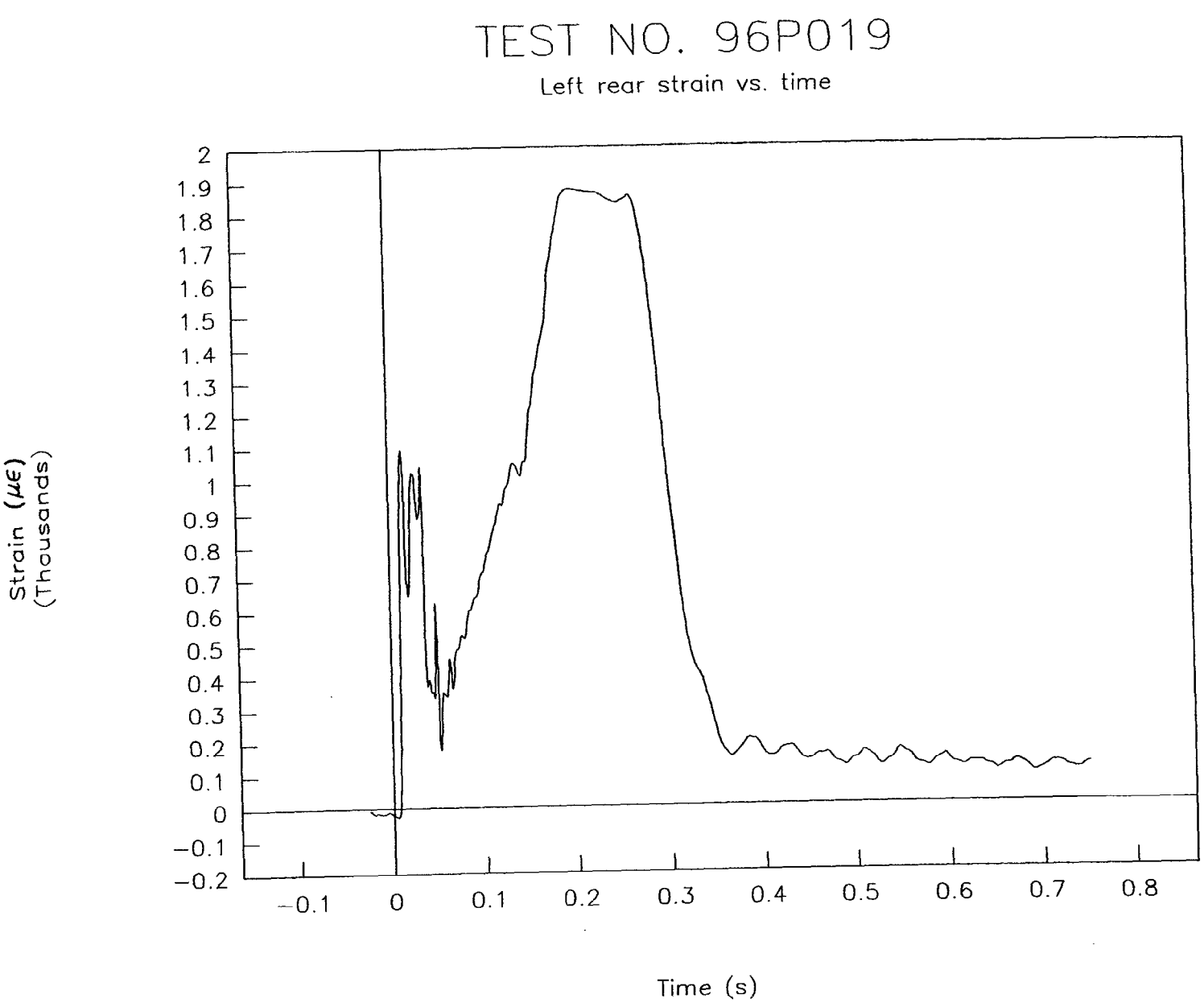

Figure 22. Strain vs. time, left rear, test 96P019.

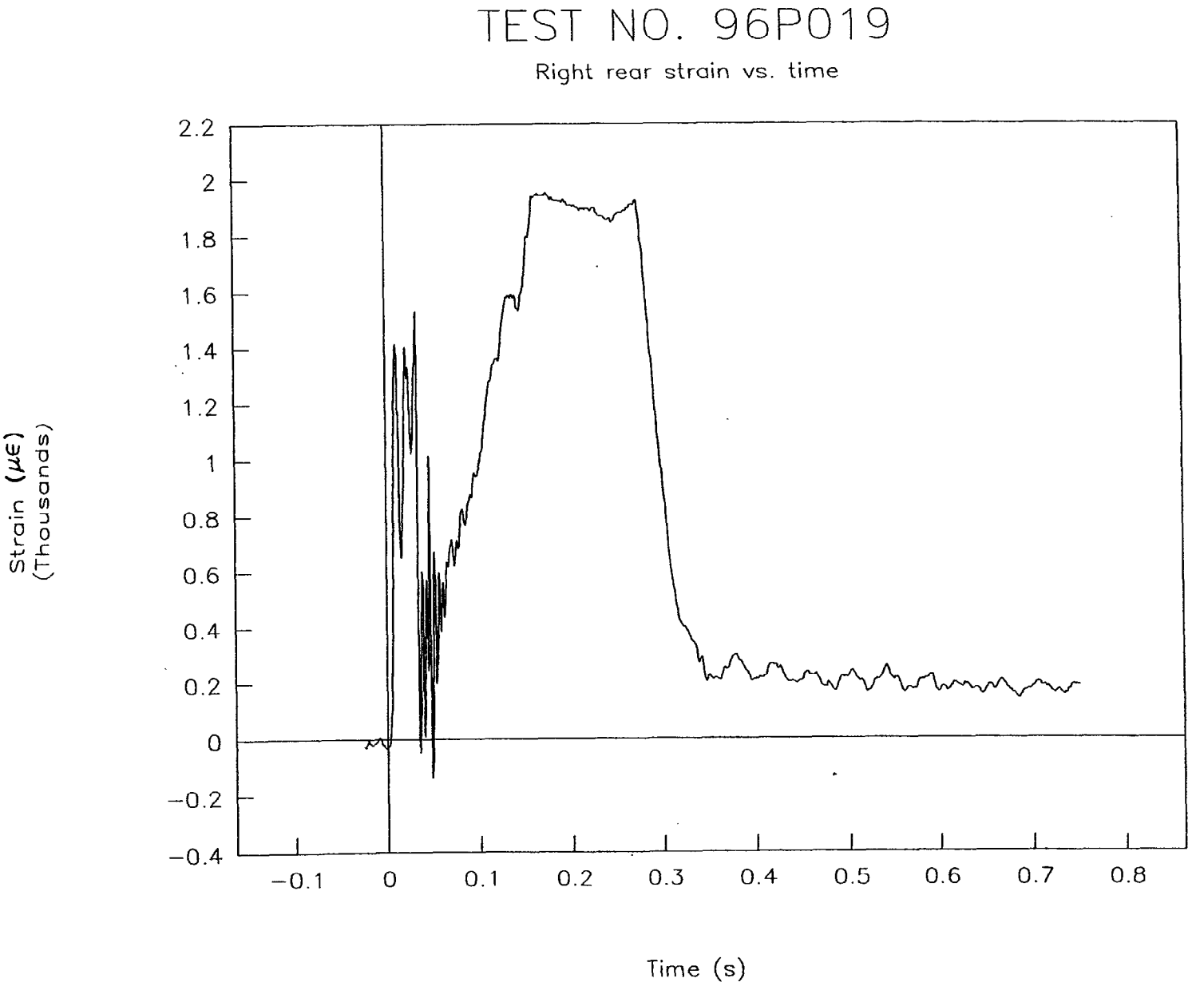

Figure 23. Strain vs. time, right rear, test 96P019.

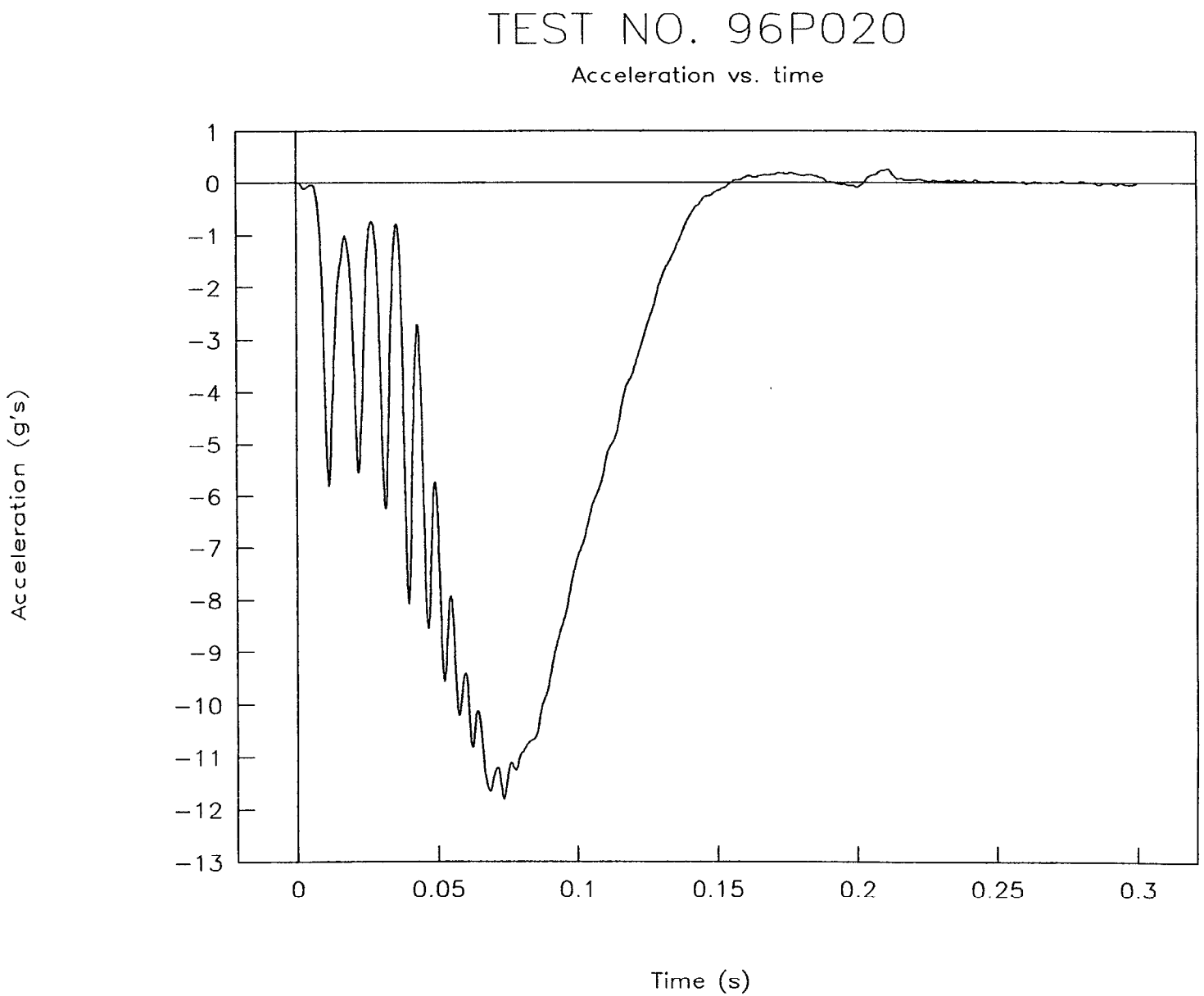

Figure 24. Acceleration vs. time, test 96P020.

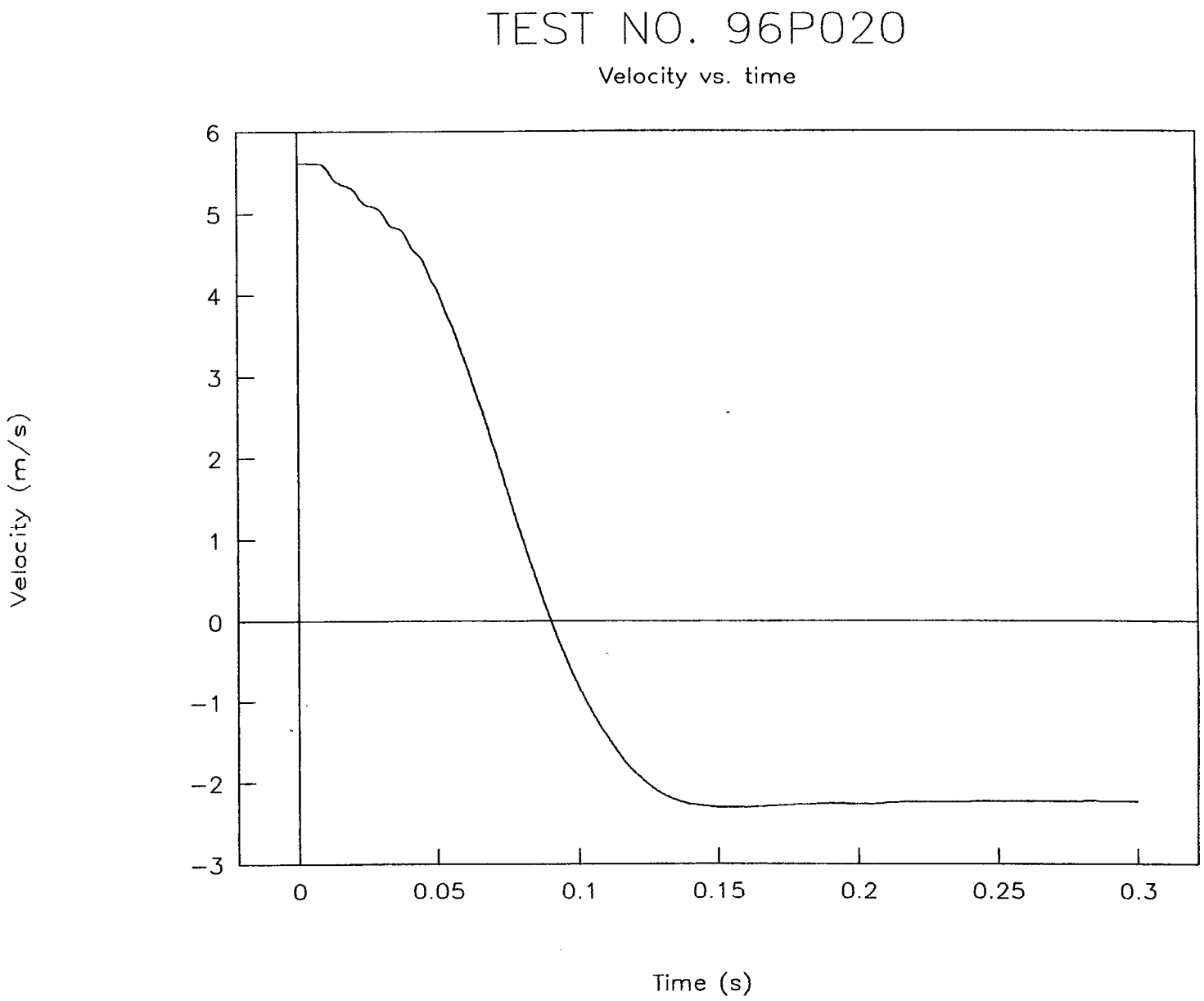

Figure 25. Velocity vs. time, test 96P020.

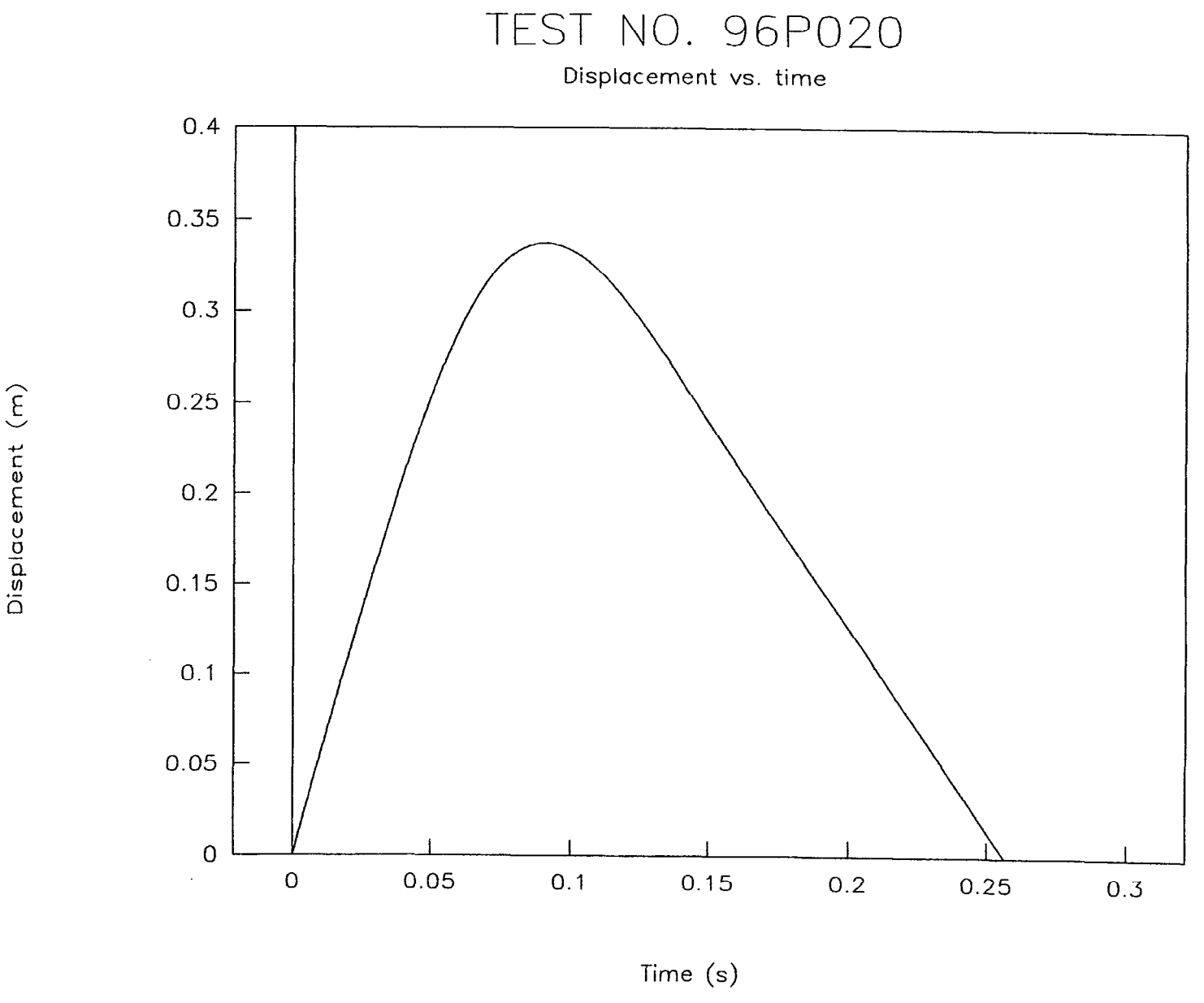

Figure 26. Displacement vs. time, test 96P020.

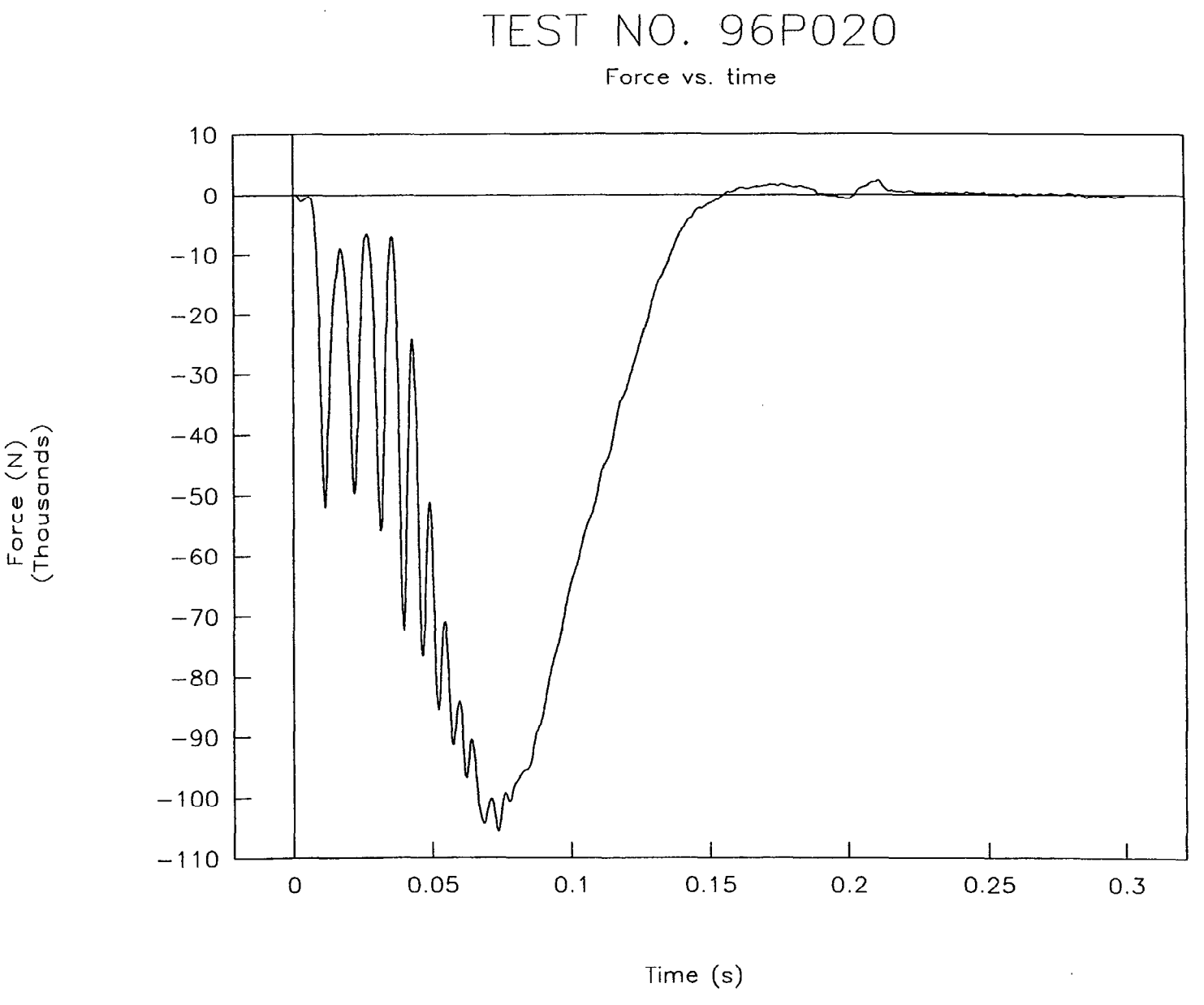

Figure 27. Force vs. time, test 96P020.

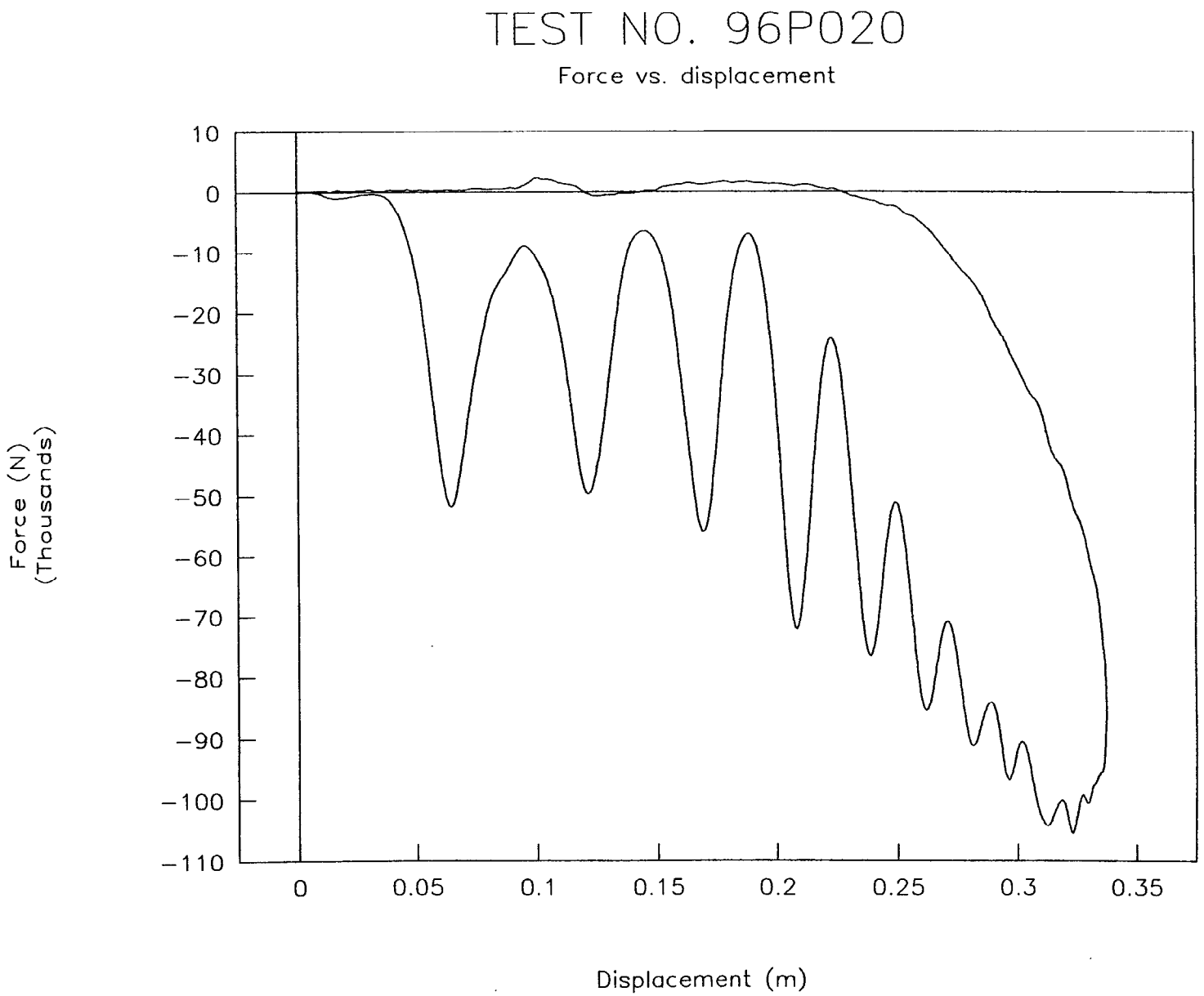

Figure 28. Force vs. displacement, test 96P020.

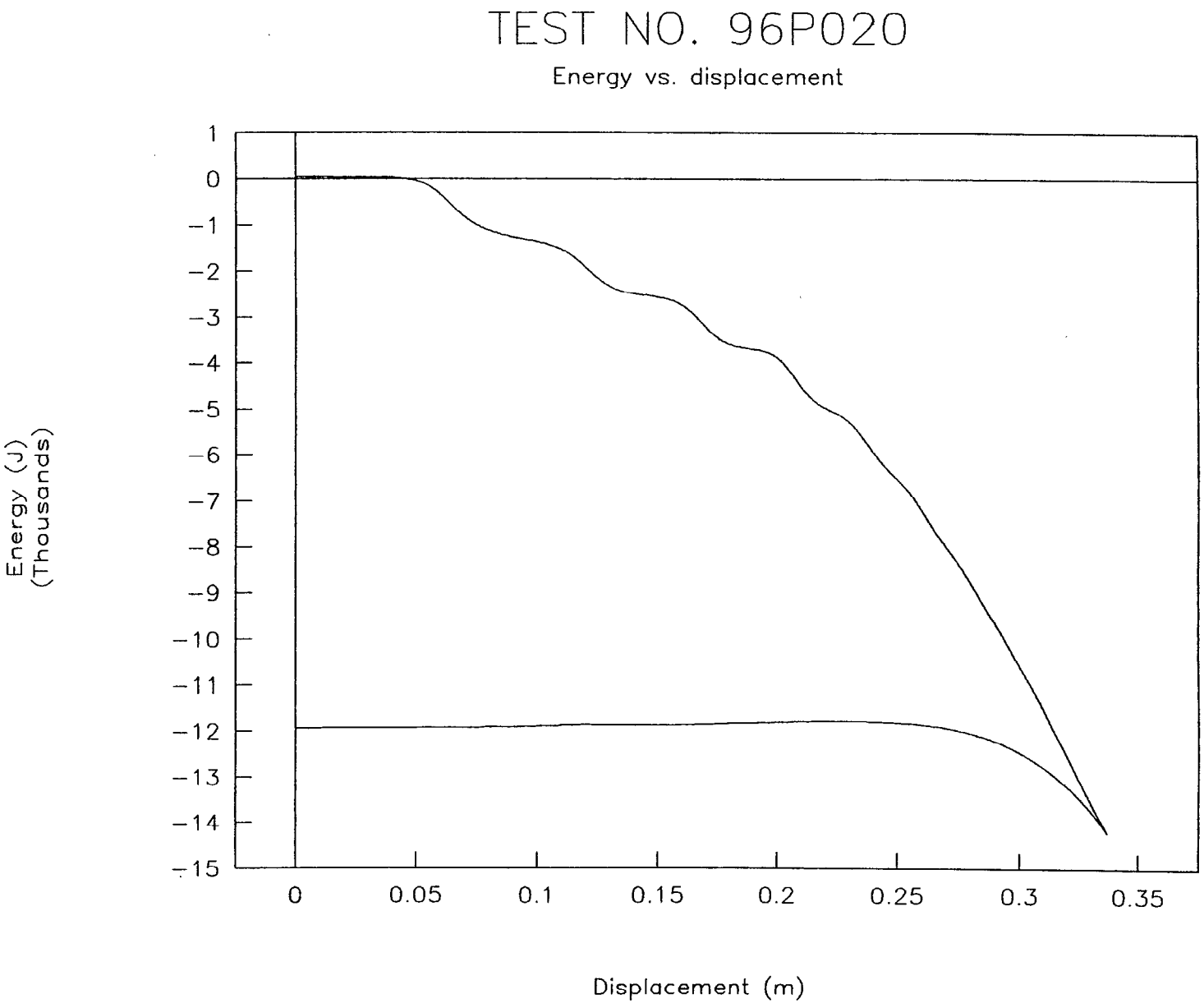

Figure 29. Energy vs. displacement, test 96P020.

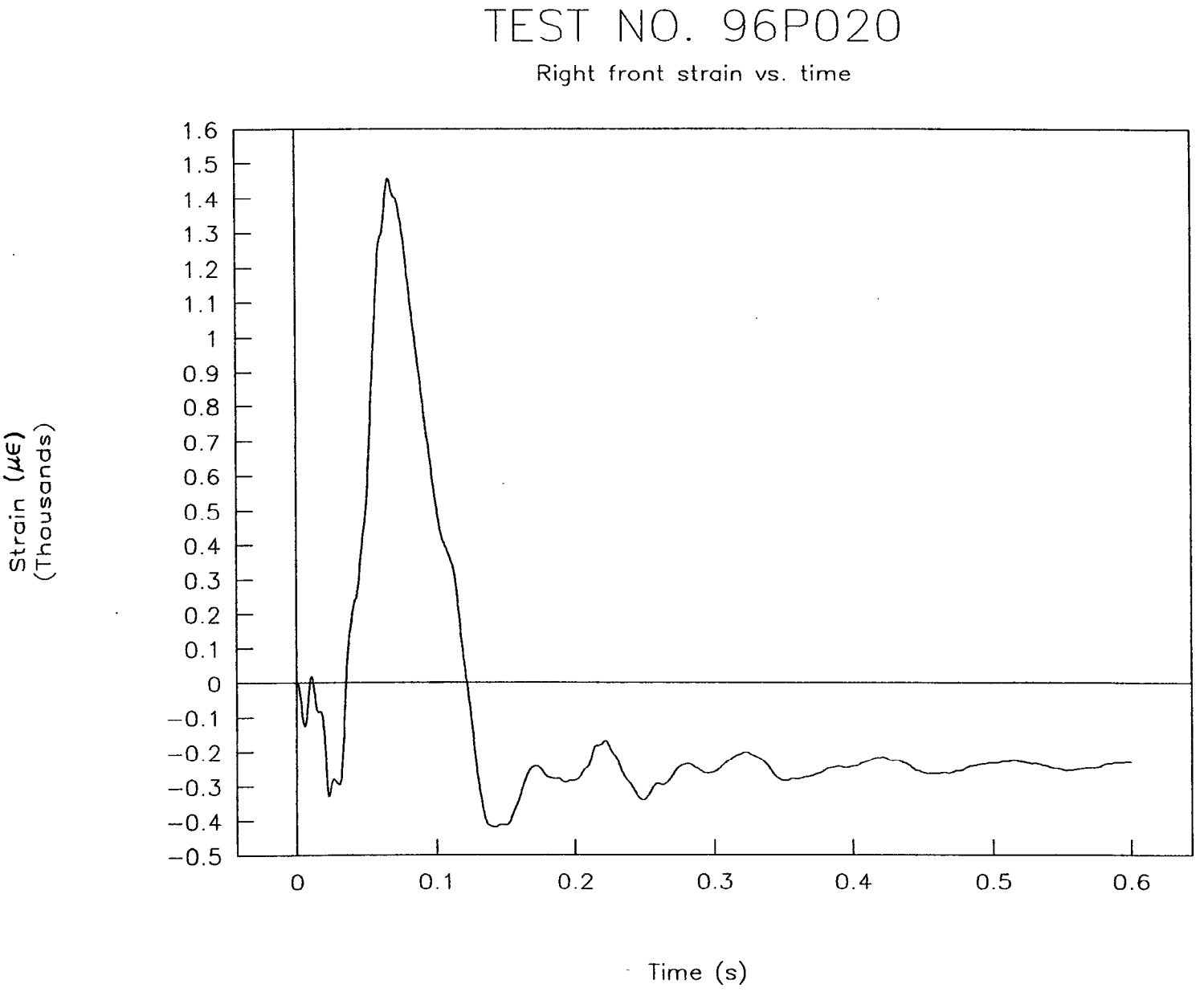

Figure 30. Strain vs. time, right front, test 96P020.

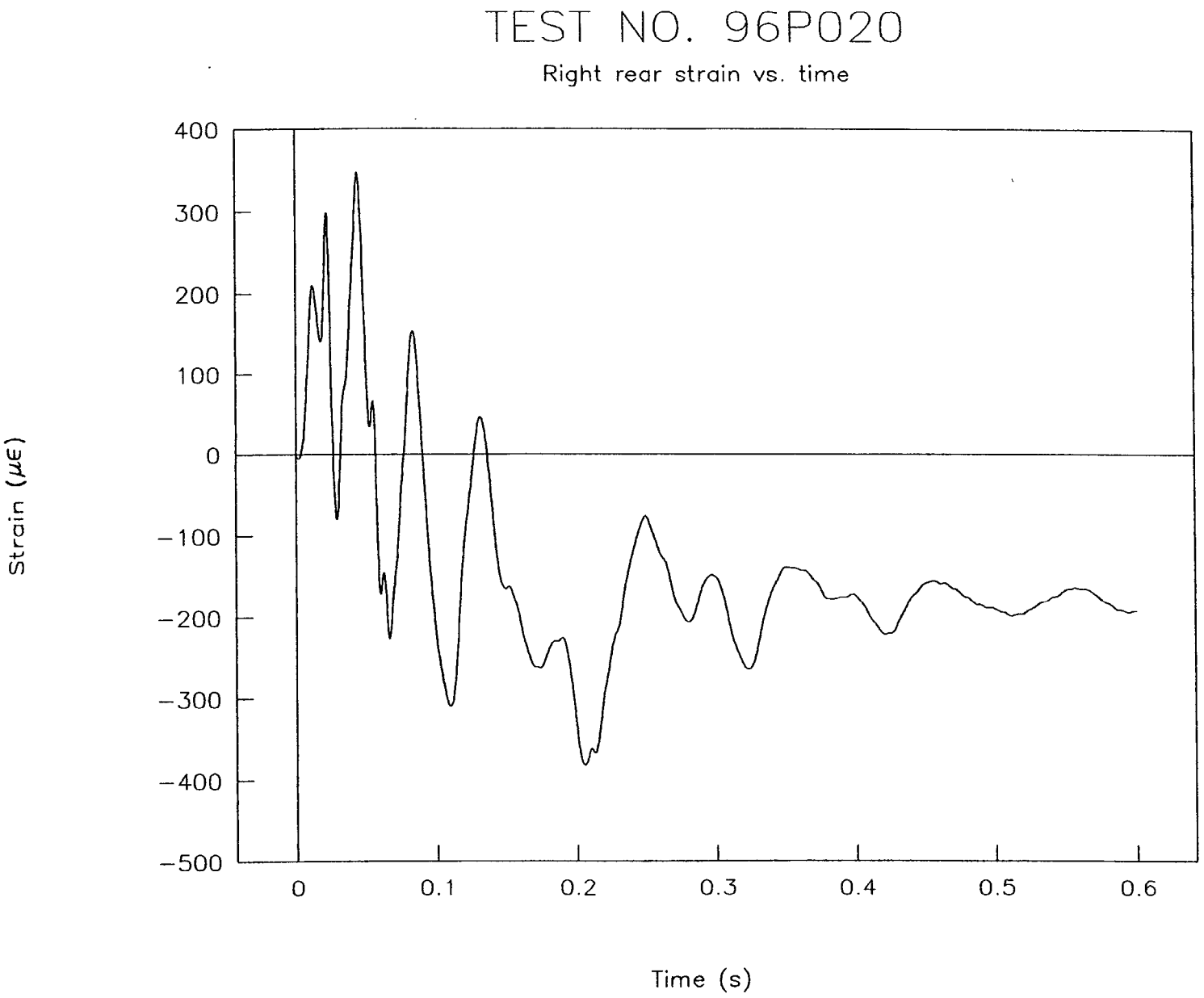

Figure 31. Strain vs. time, right rear, test 96P020.

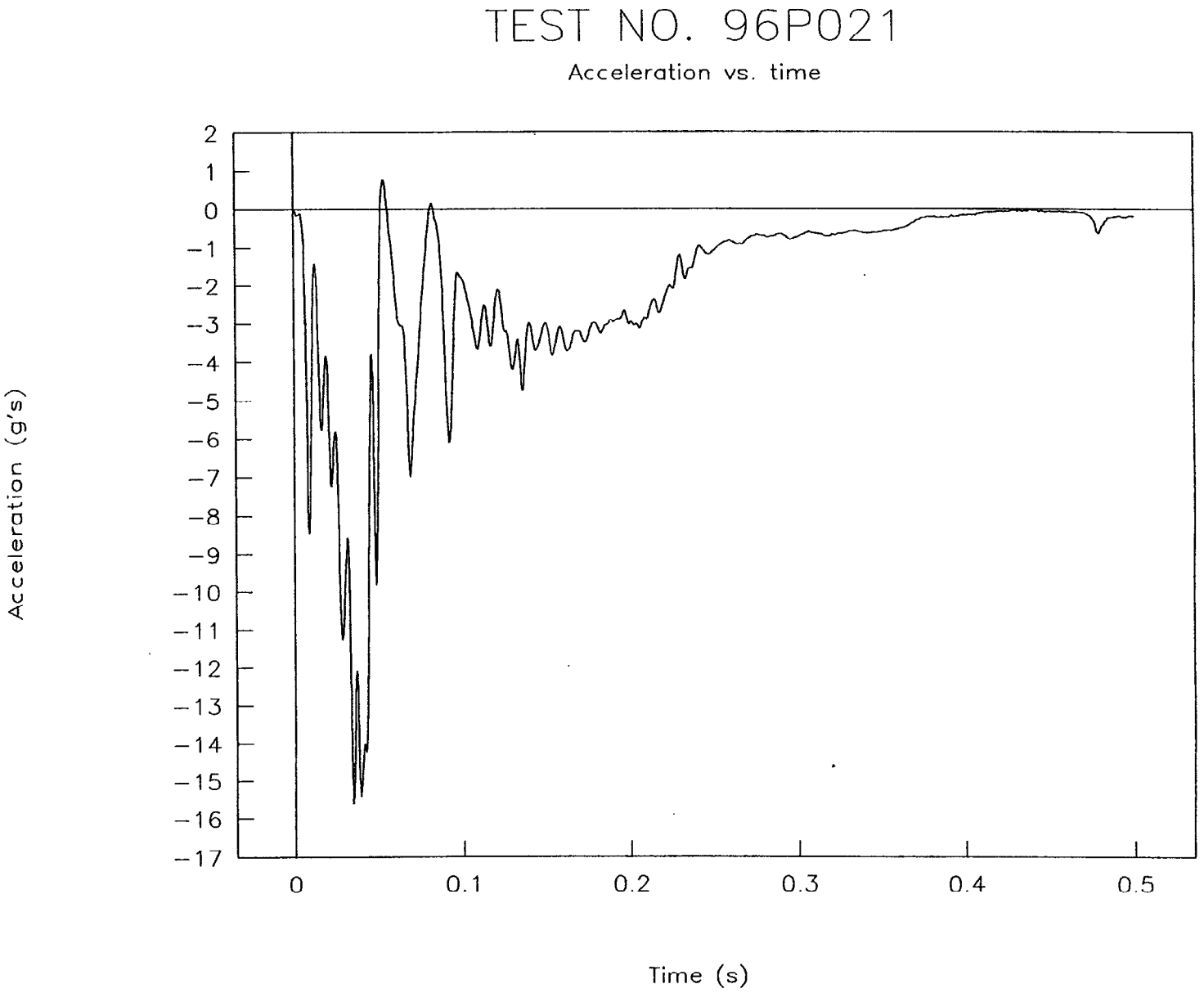

Figure 32. Acceleration vs. time, test 96P021.

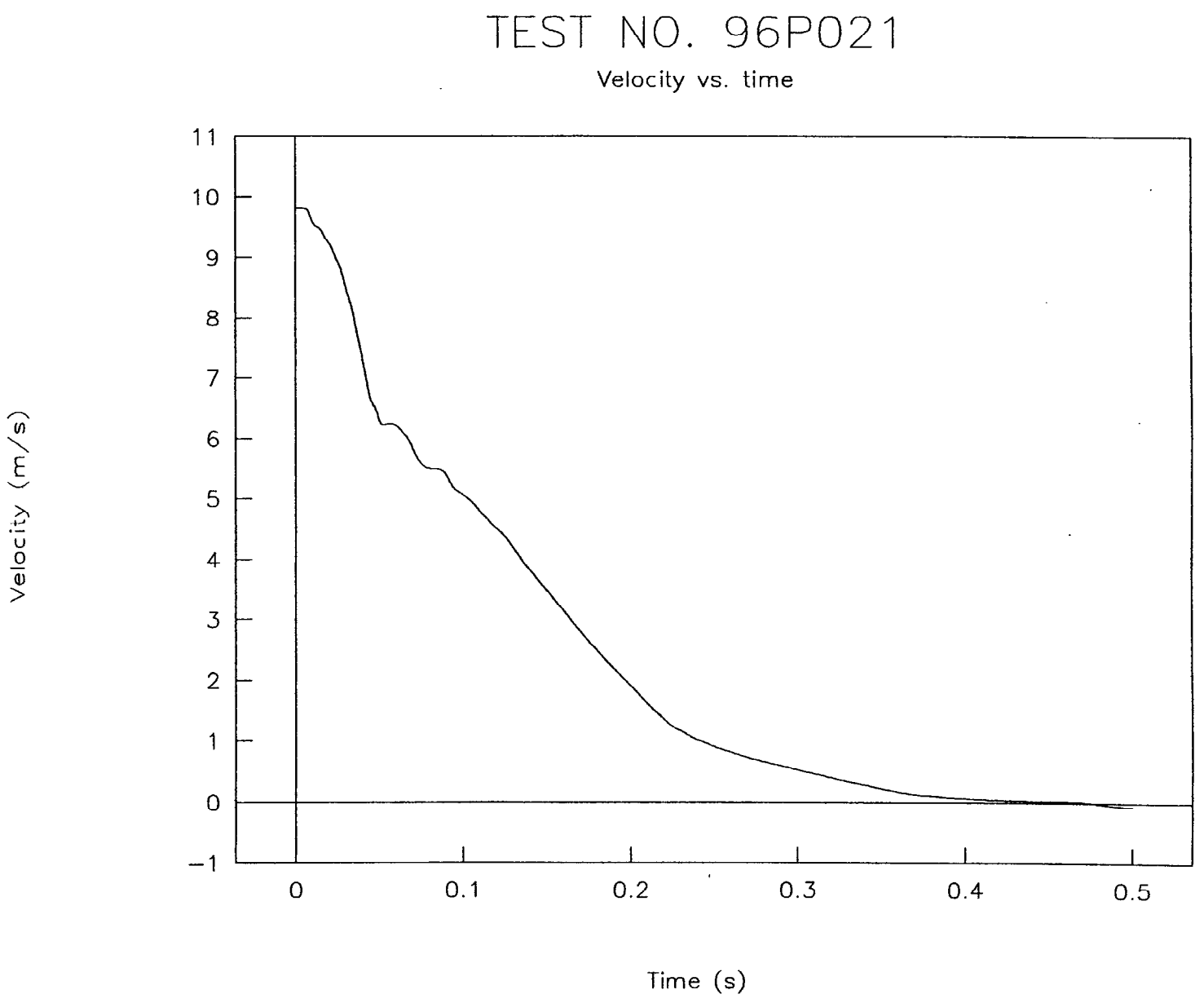

Figure 33. Velocity vs. time, test 96P021.

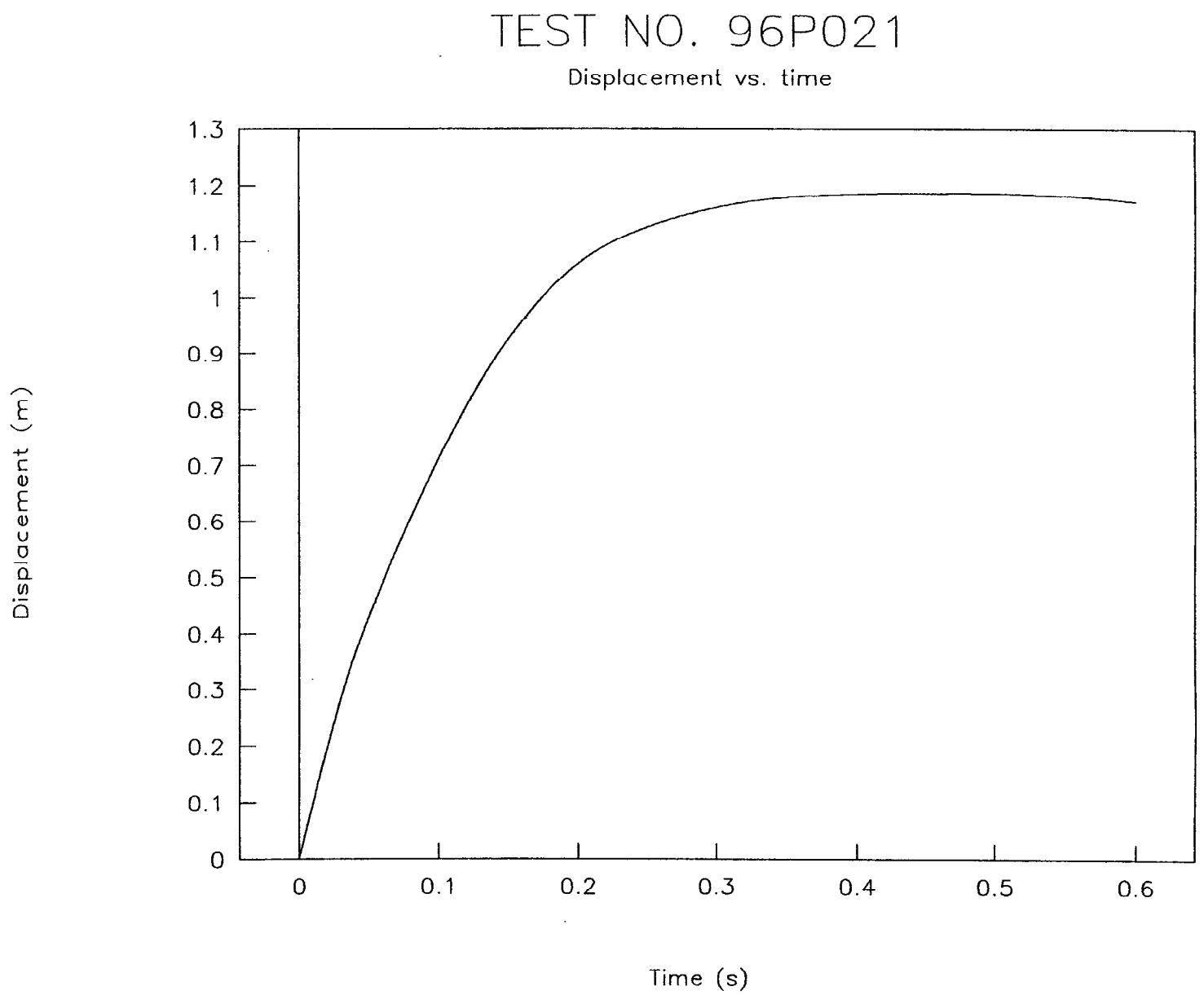

Figure 34. Displacement vs. time, test 96P021.

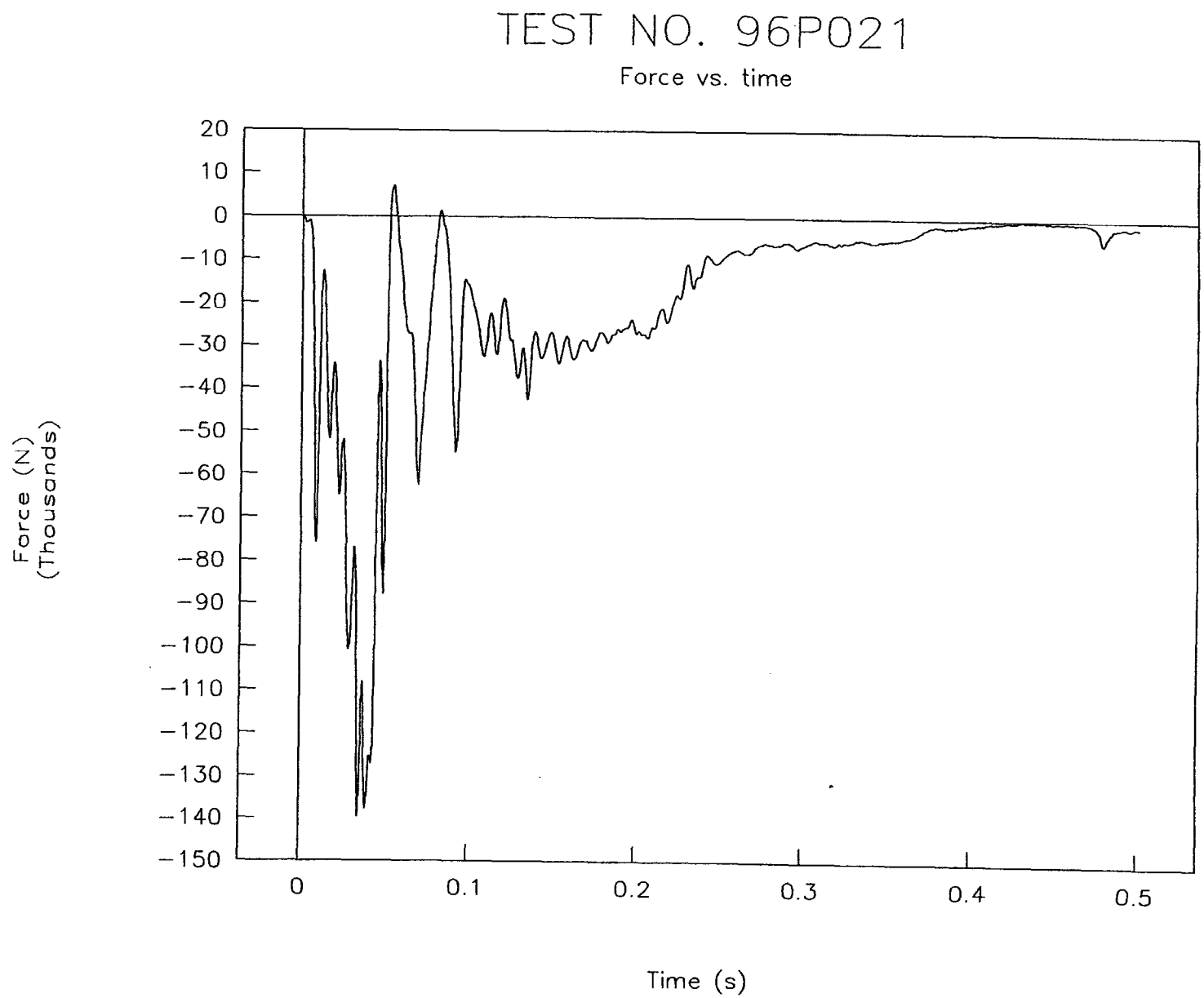

Figure 35. Force vs. time, test 96P021.

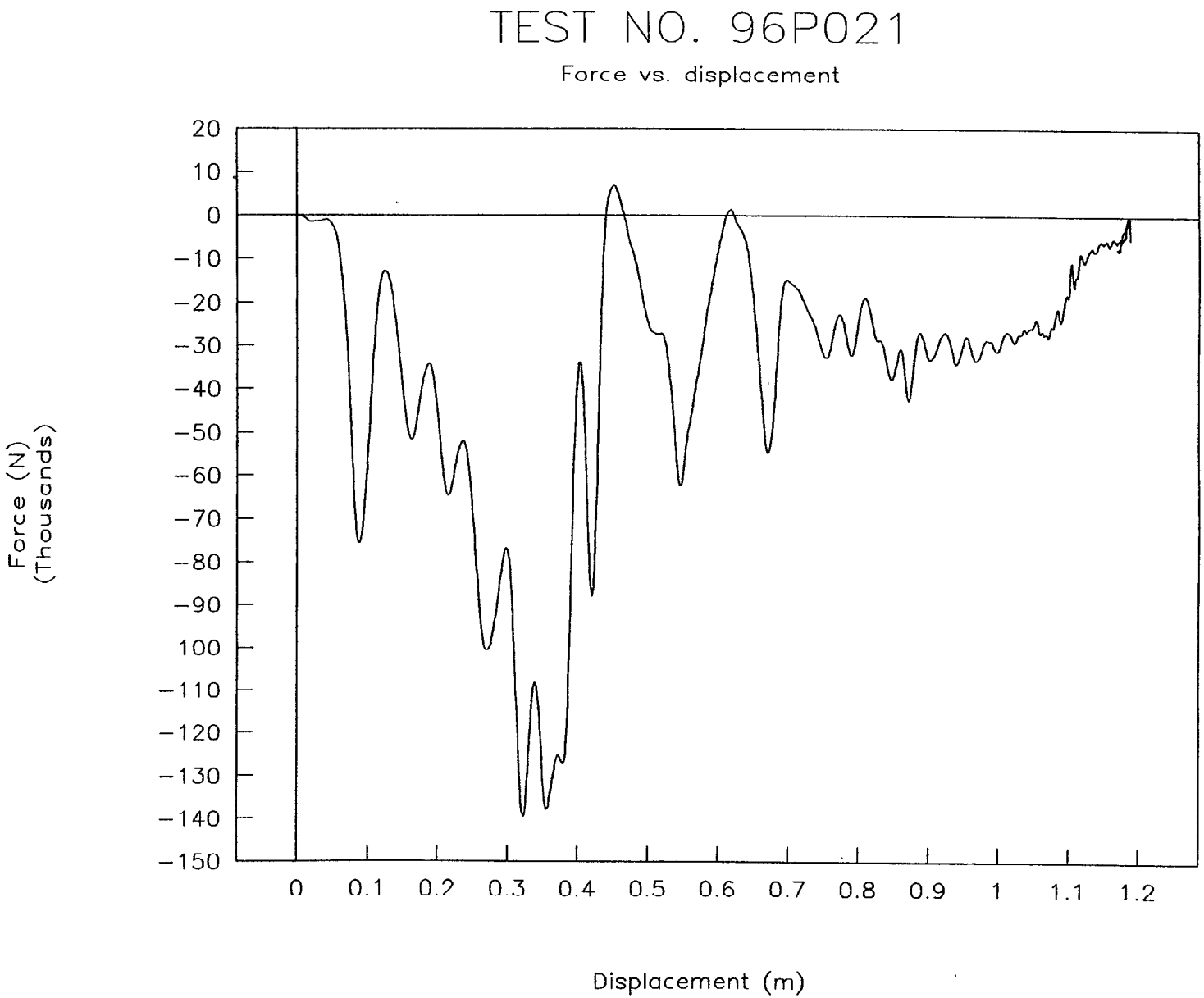

Figure 36. Force vs. displacement, test 96P021.

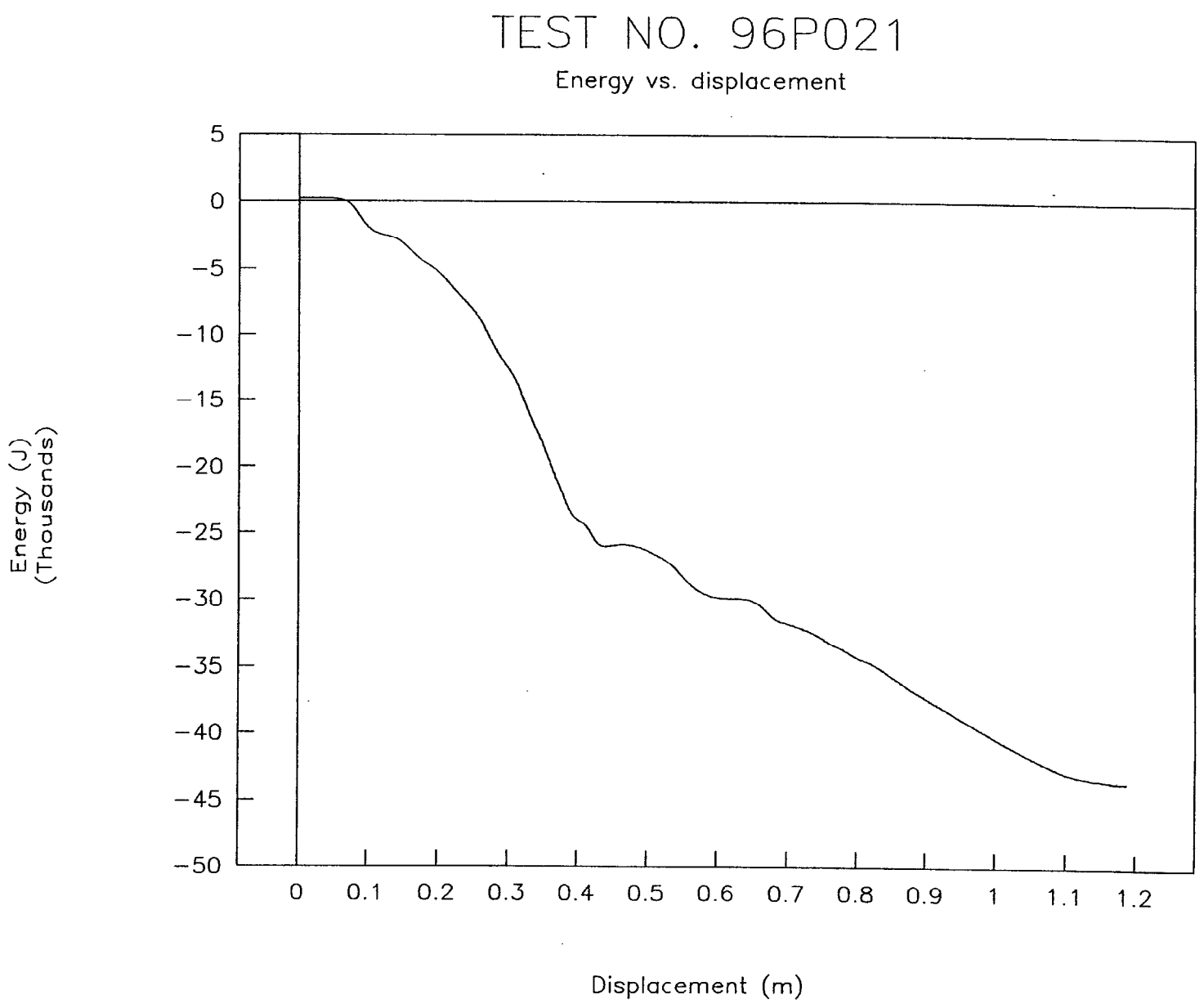

Figure 37. Energy vs. displacement, test 96P021.

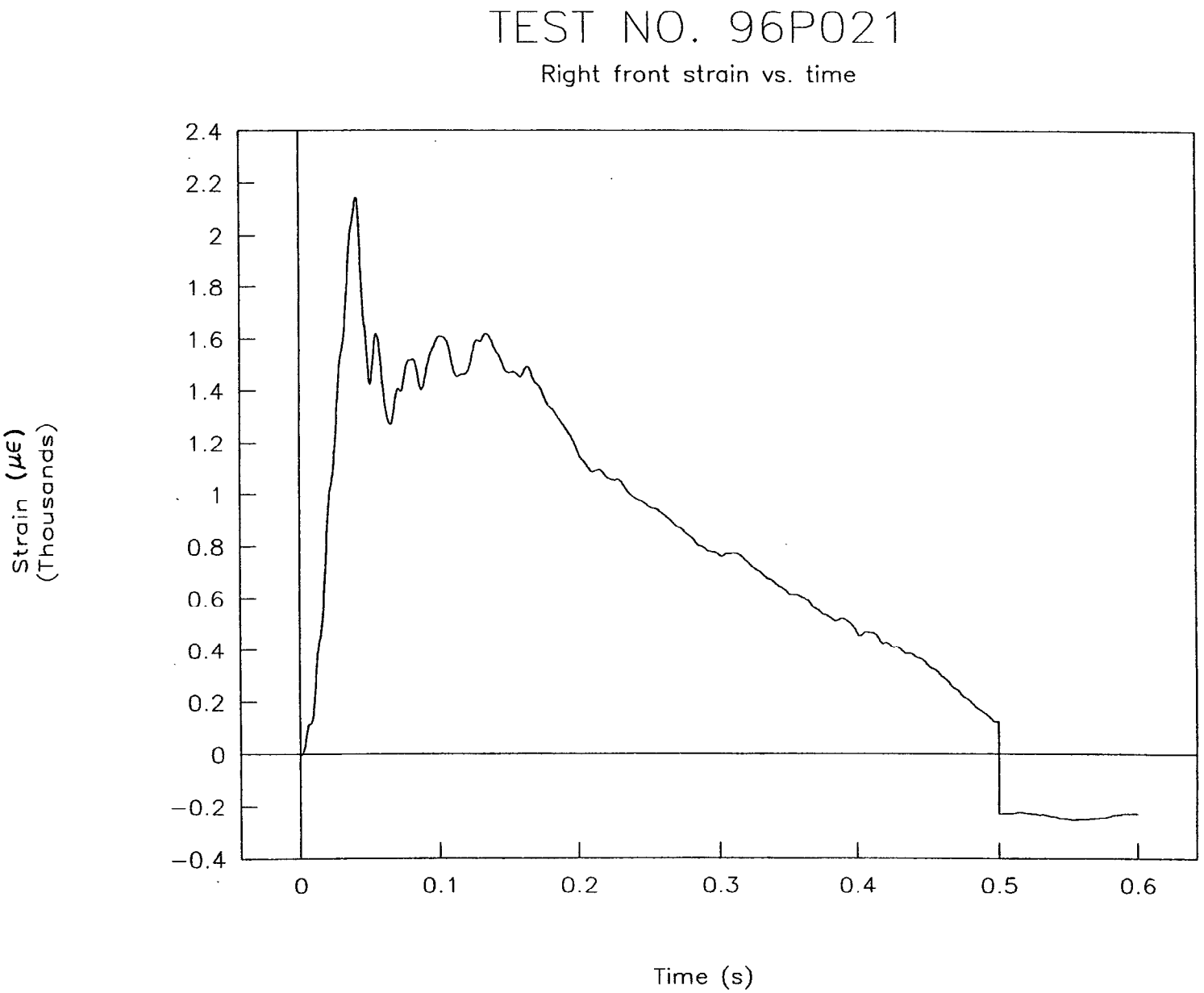

Figure 38. Strain vs. time, right front, test 96P021.

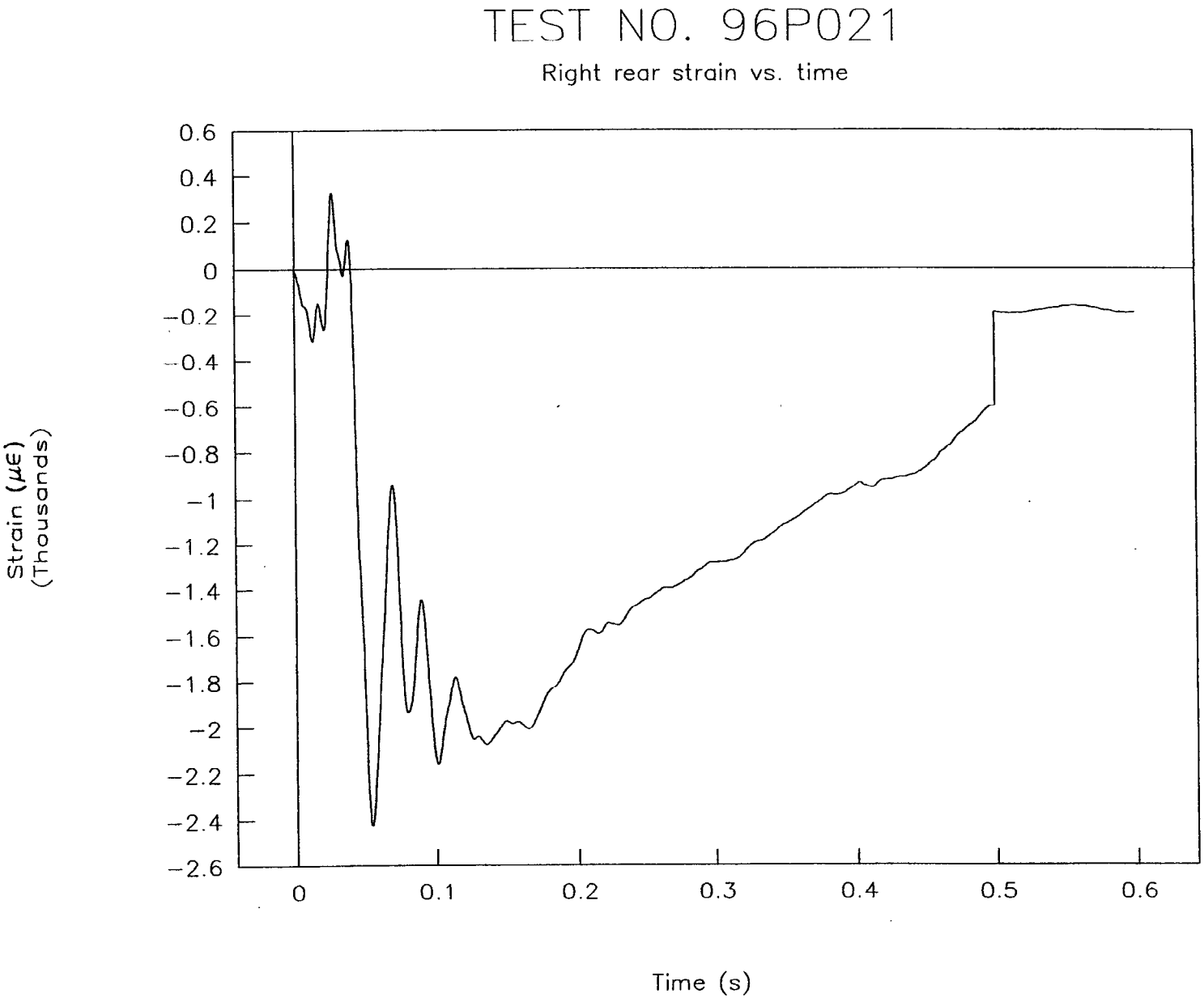

Figure 39. Strain vs. time, right rear, test 96P021.

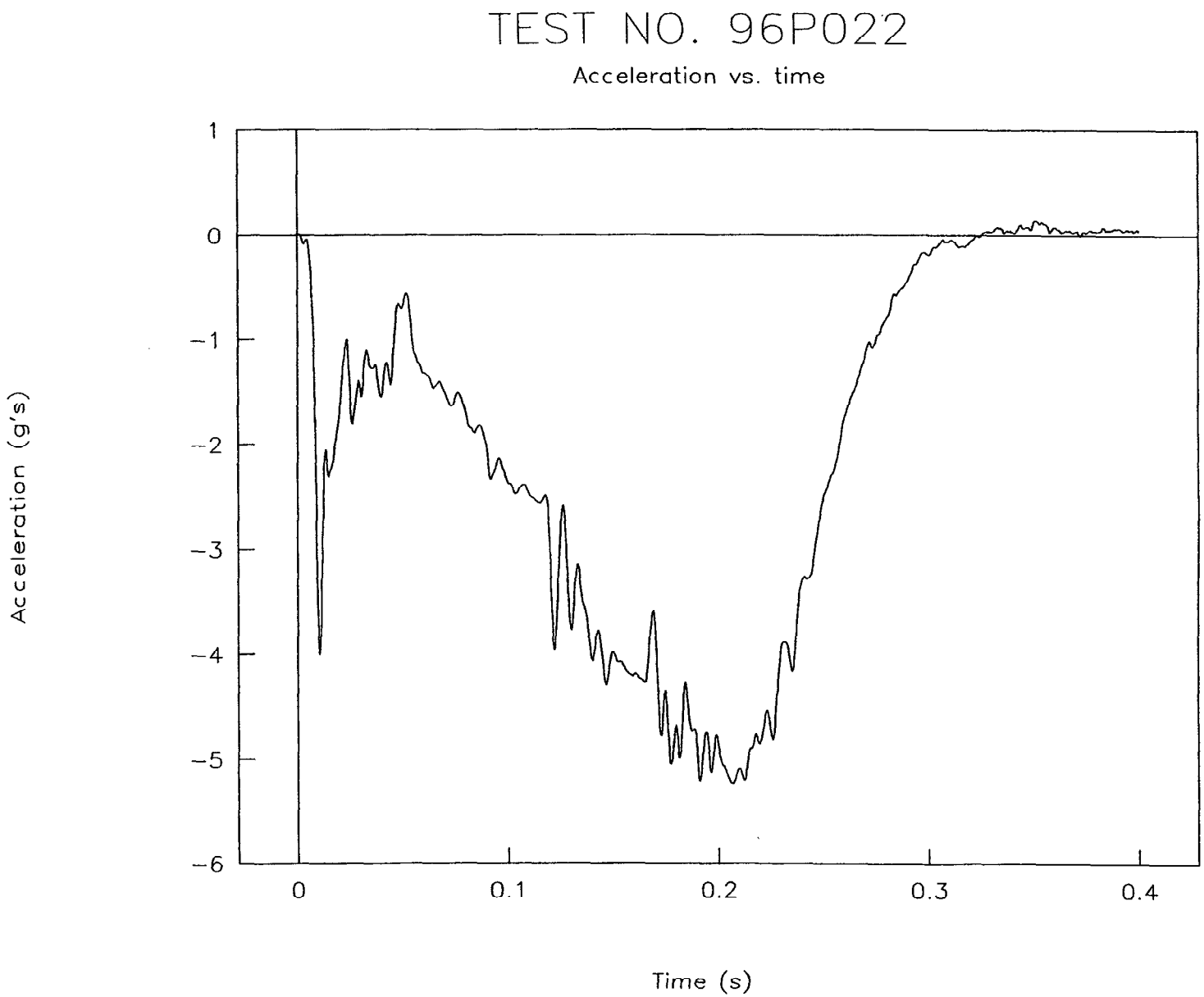

Figure 40. Acceleration vs. time, test 96P022.

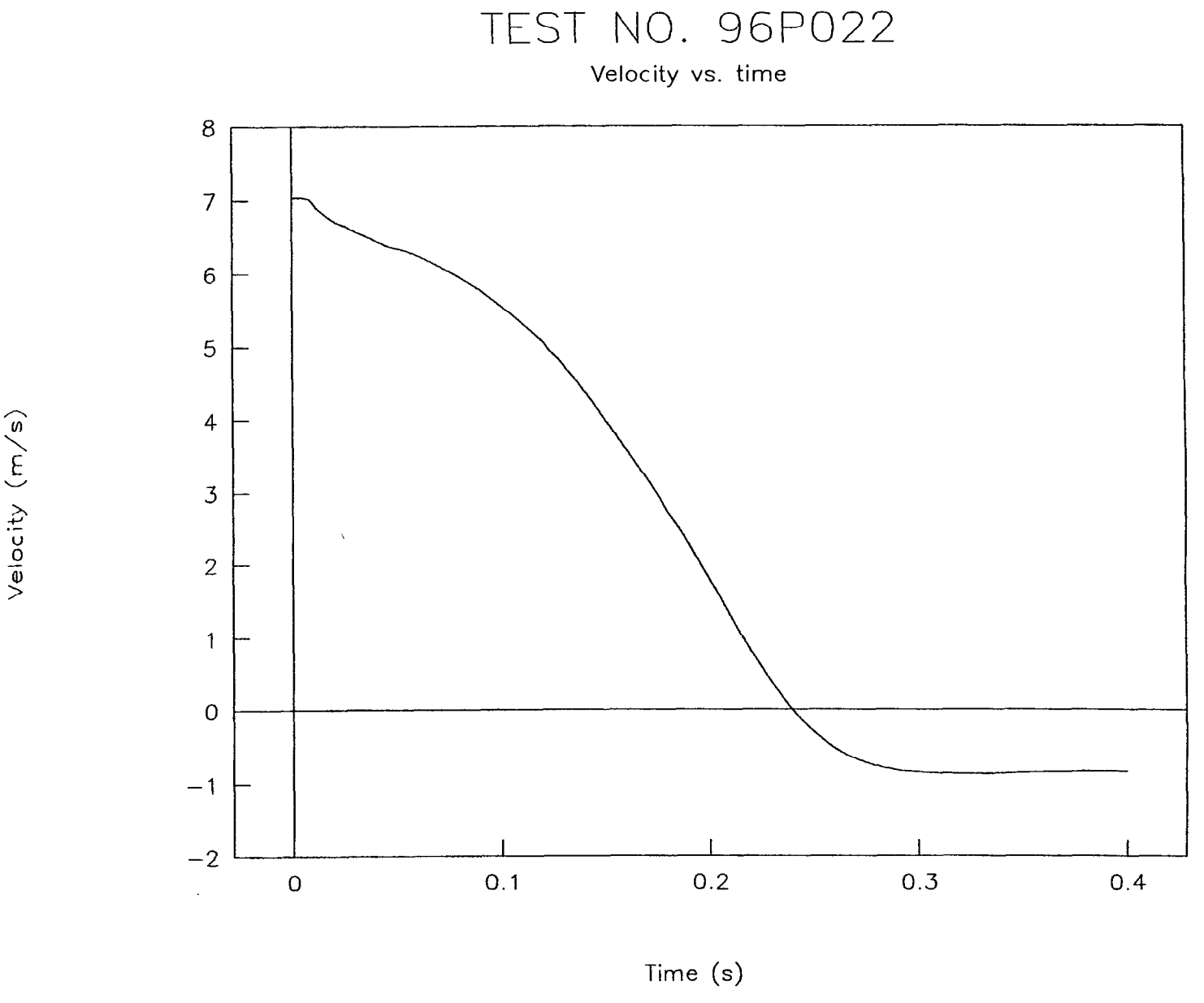

Figure 41. Velocity vs. time, test 96P022.

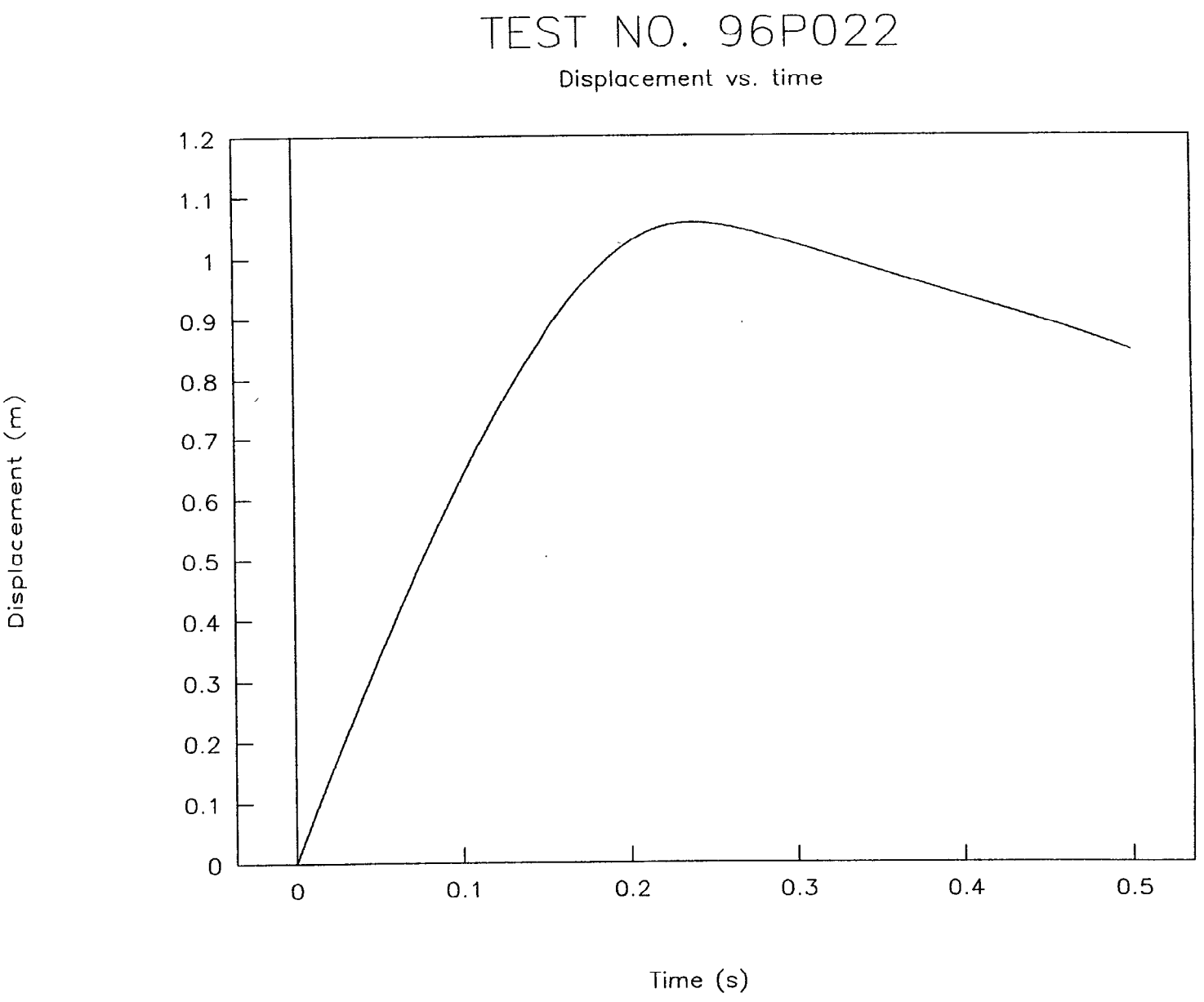

Figure 42. Displacement vs. time, test 96P022.

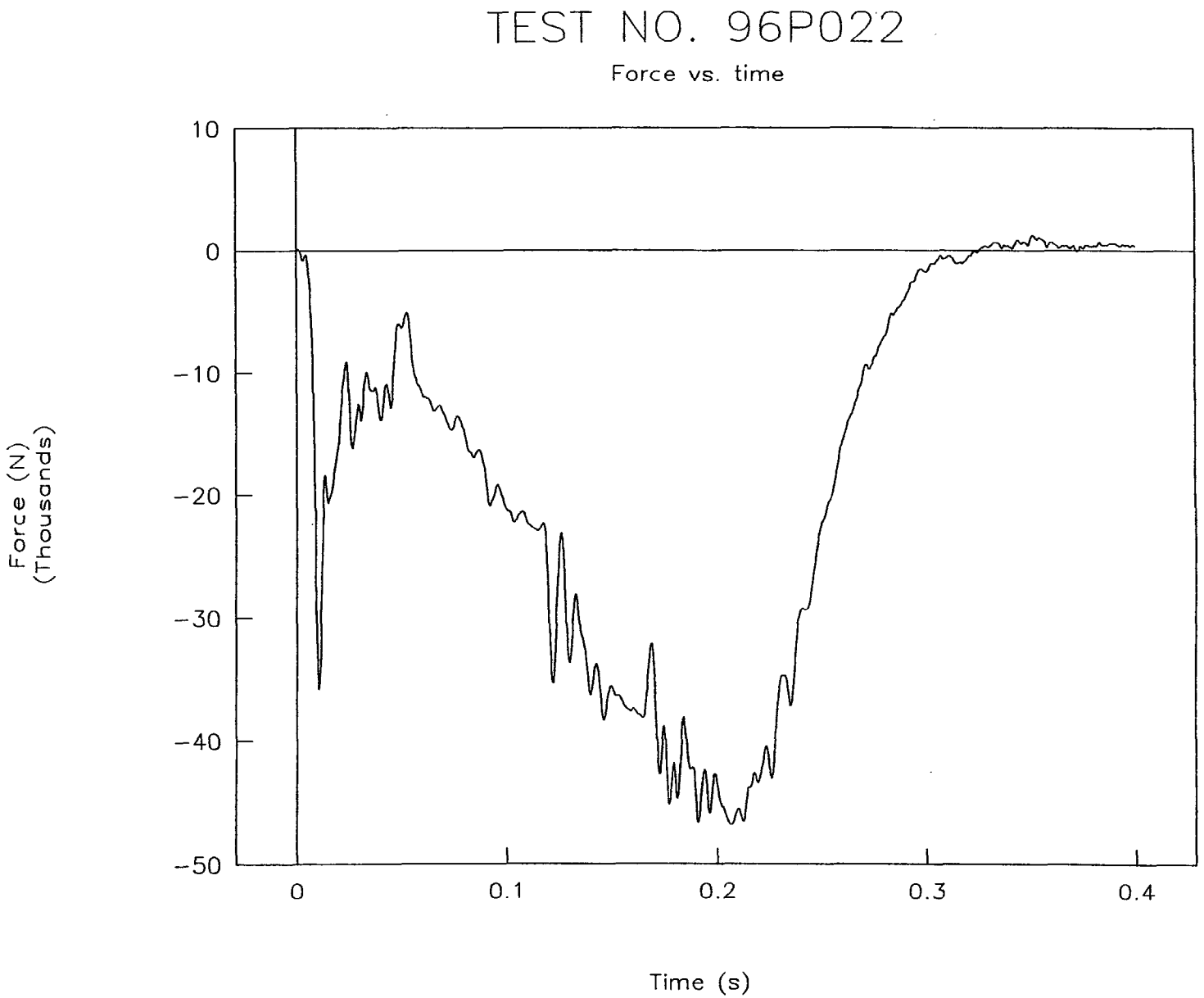

Figure 43. Force vs. time, test 96P022.

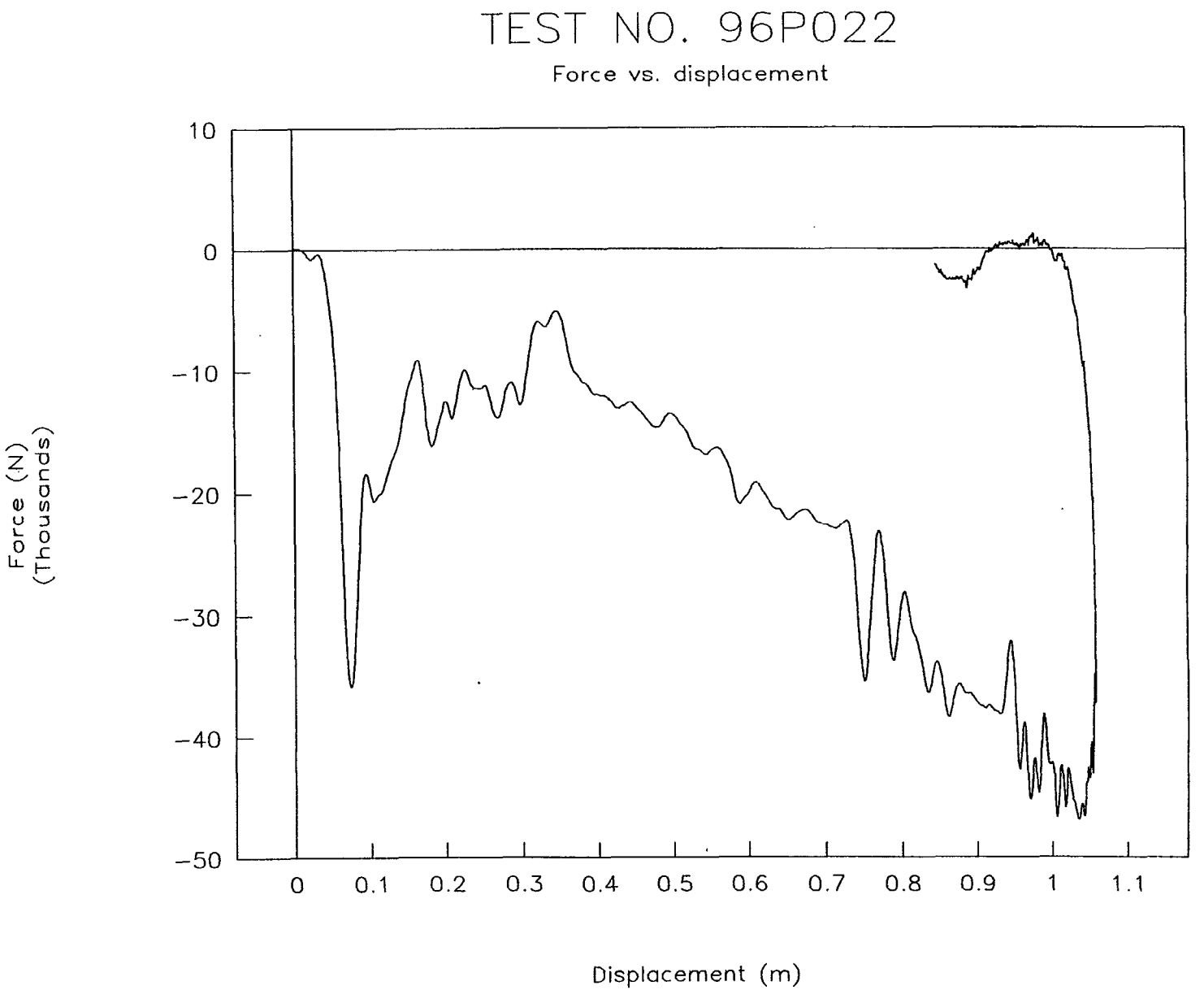

Figure 44. Force vs. displacement, test 96P022.

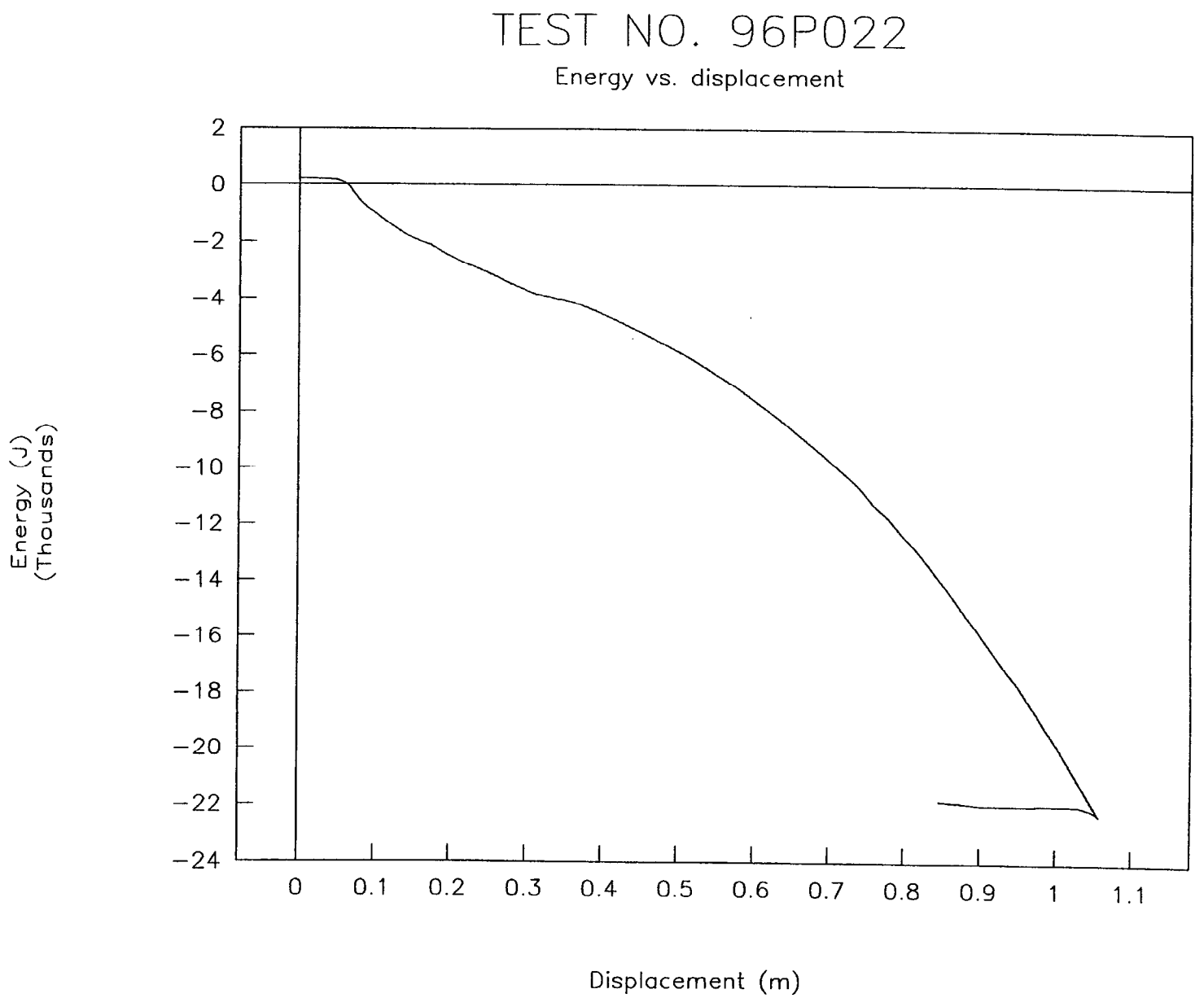

Figure 45. Energy vs. displacement, test 96P022.

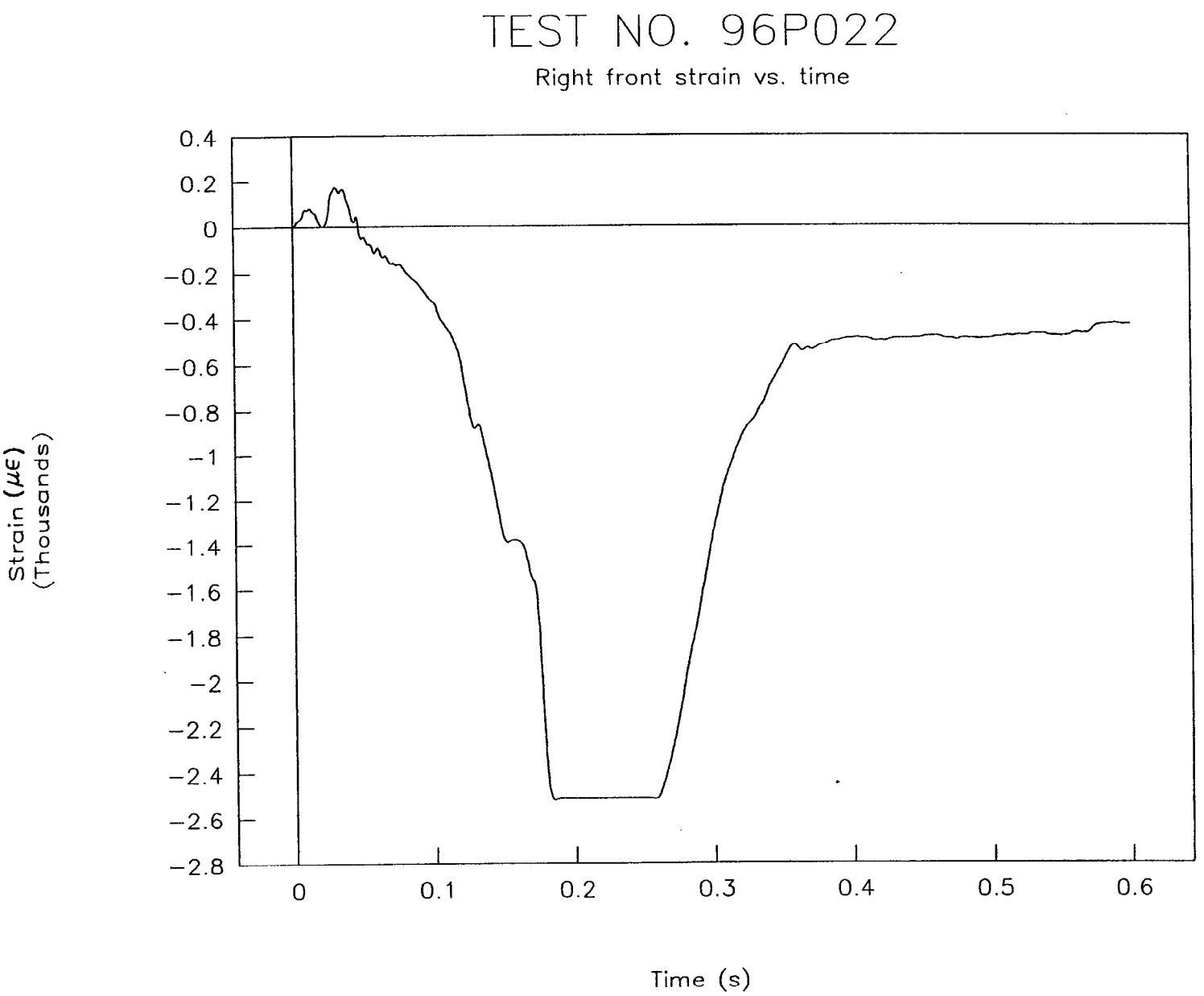

Figure 46. Strain vs. time, right front, test 96P022.

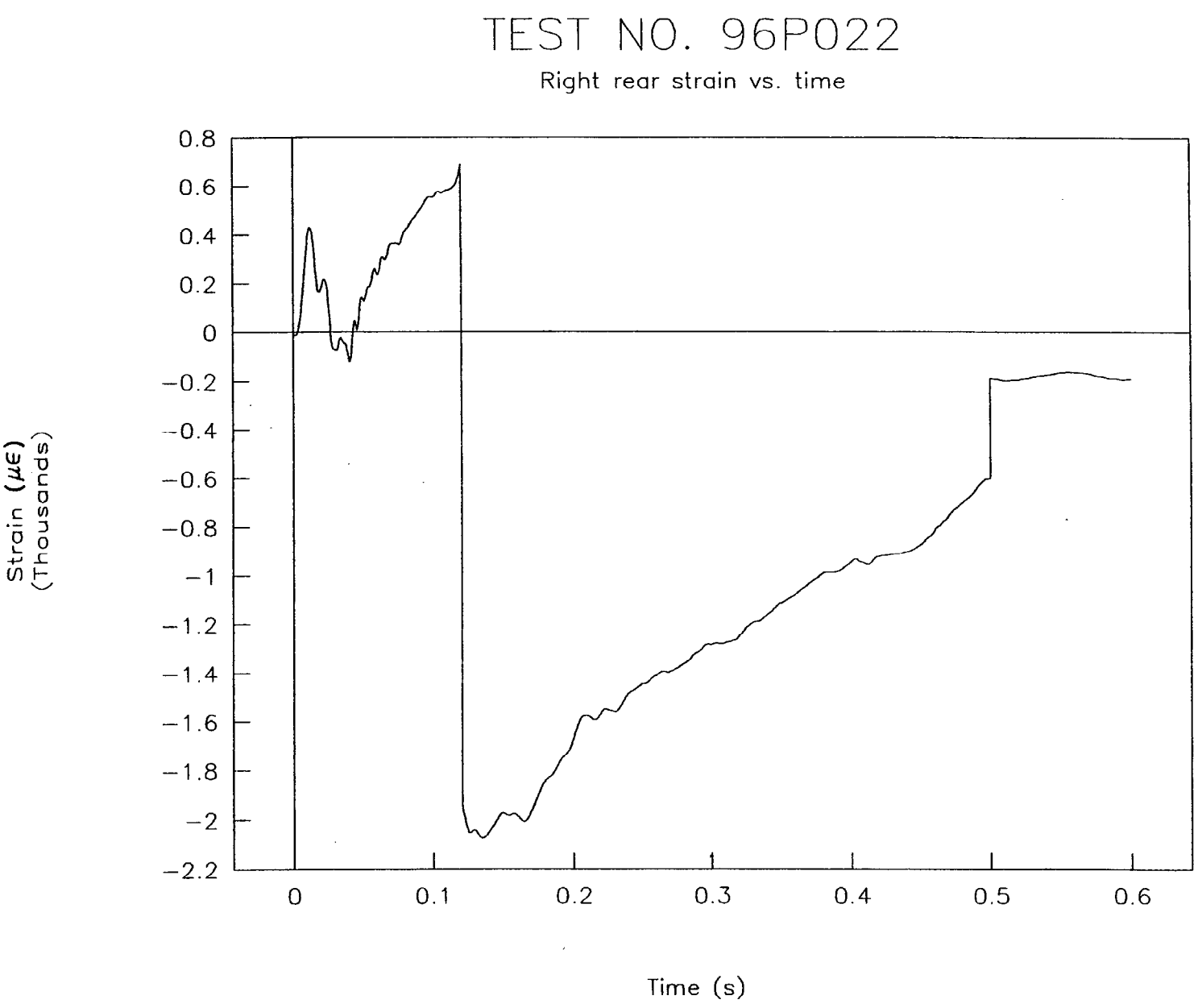

Figure 47. Strain vs. time, right rear, 96P022.

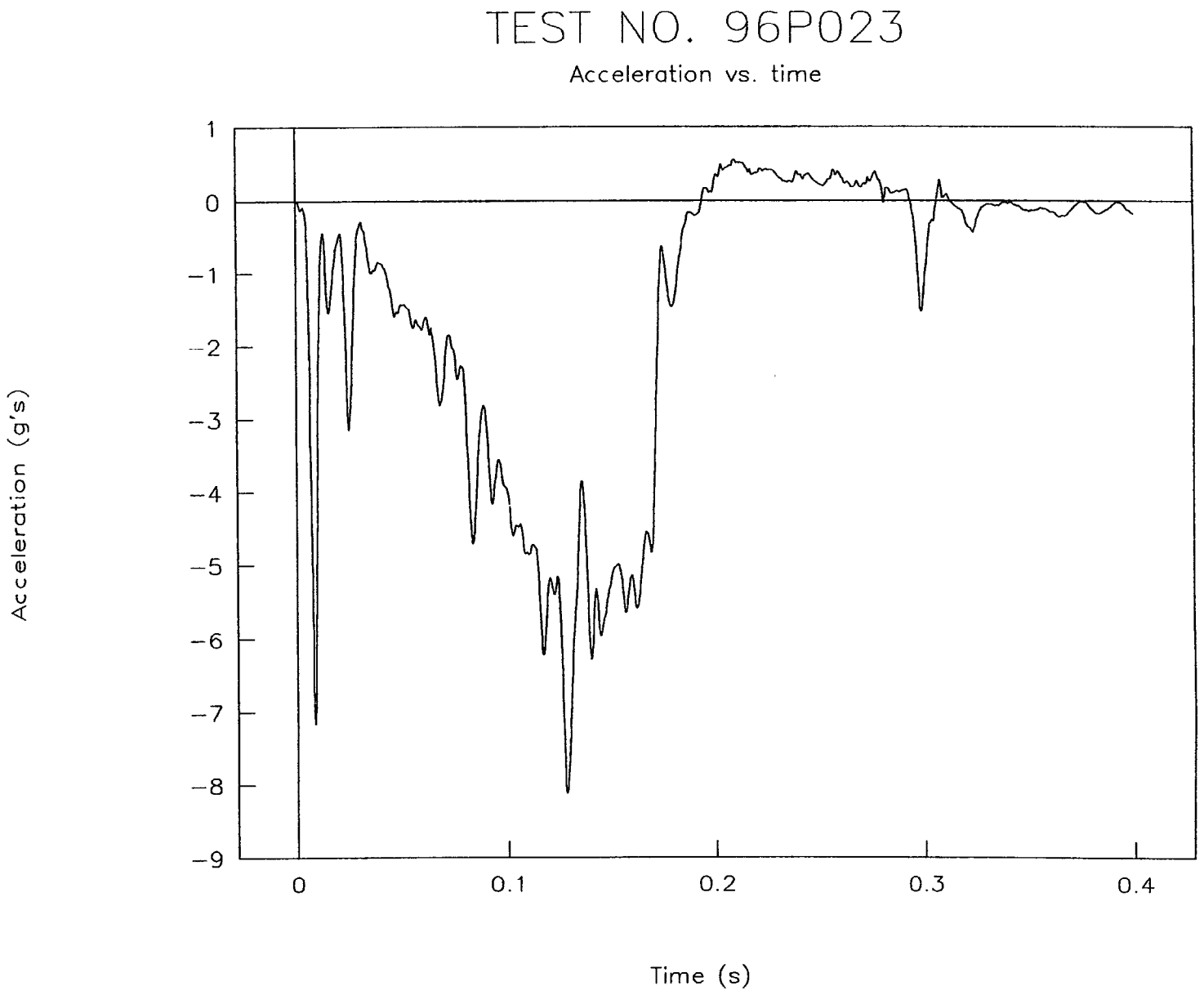

Figure 48. Acceleration vs. time, test 96P023.

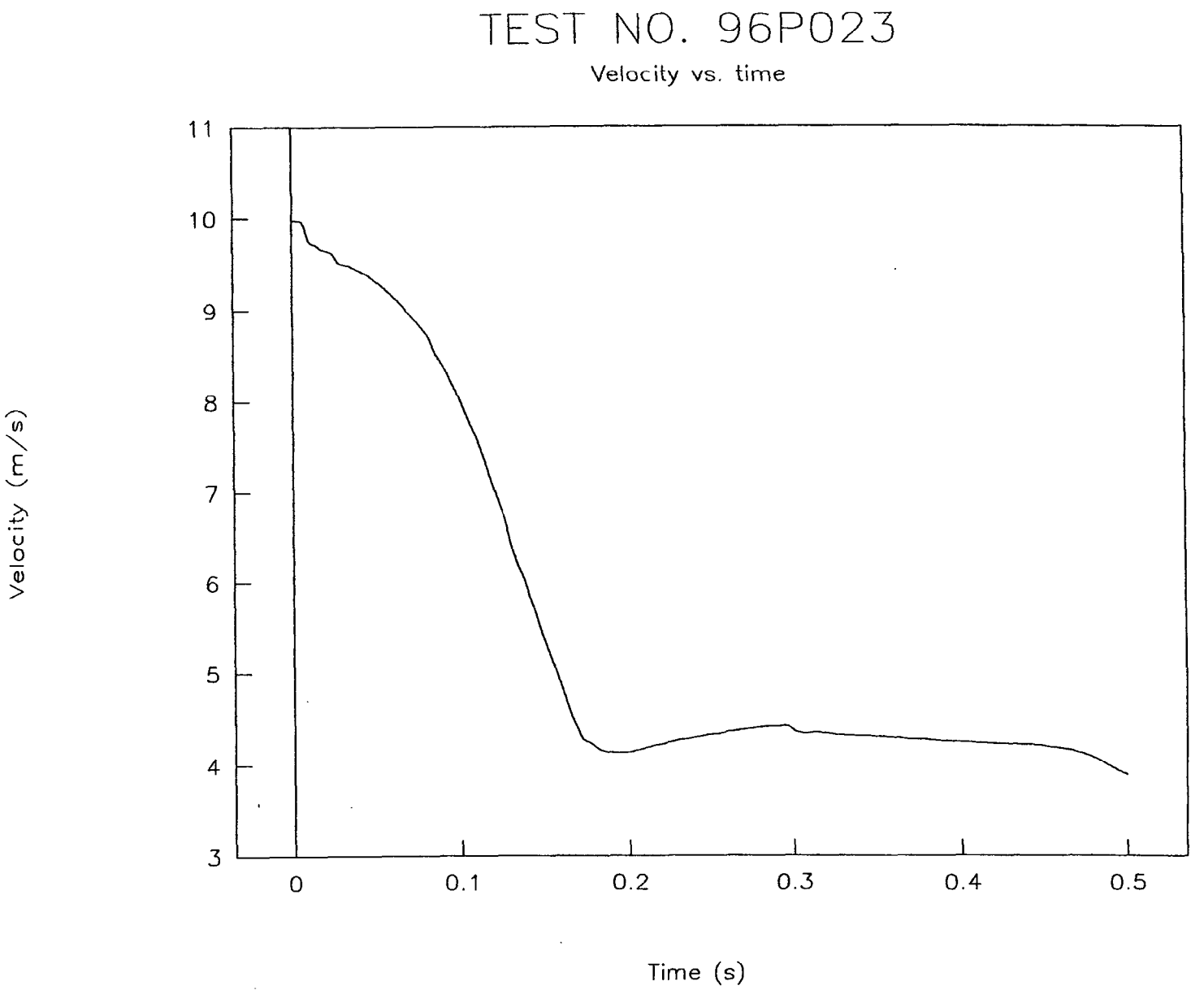

Figure 49. Velocity vs. time, test 96P023.

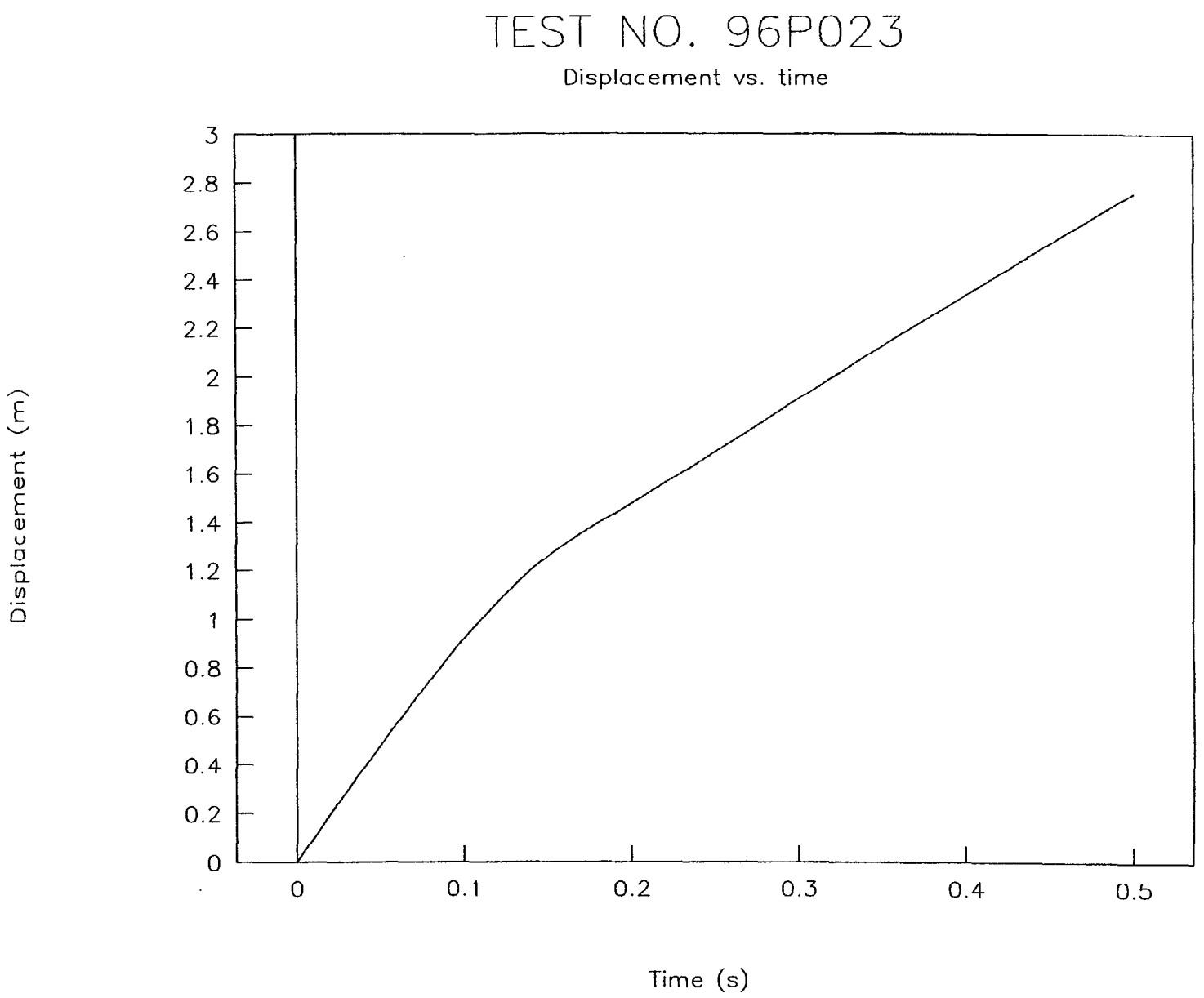

Figure 50. Displacement vs. time, test 96P023.

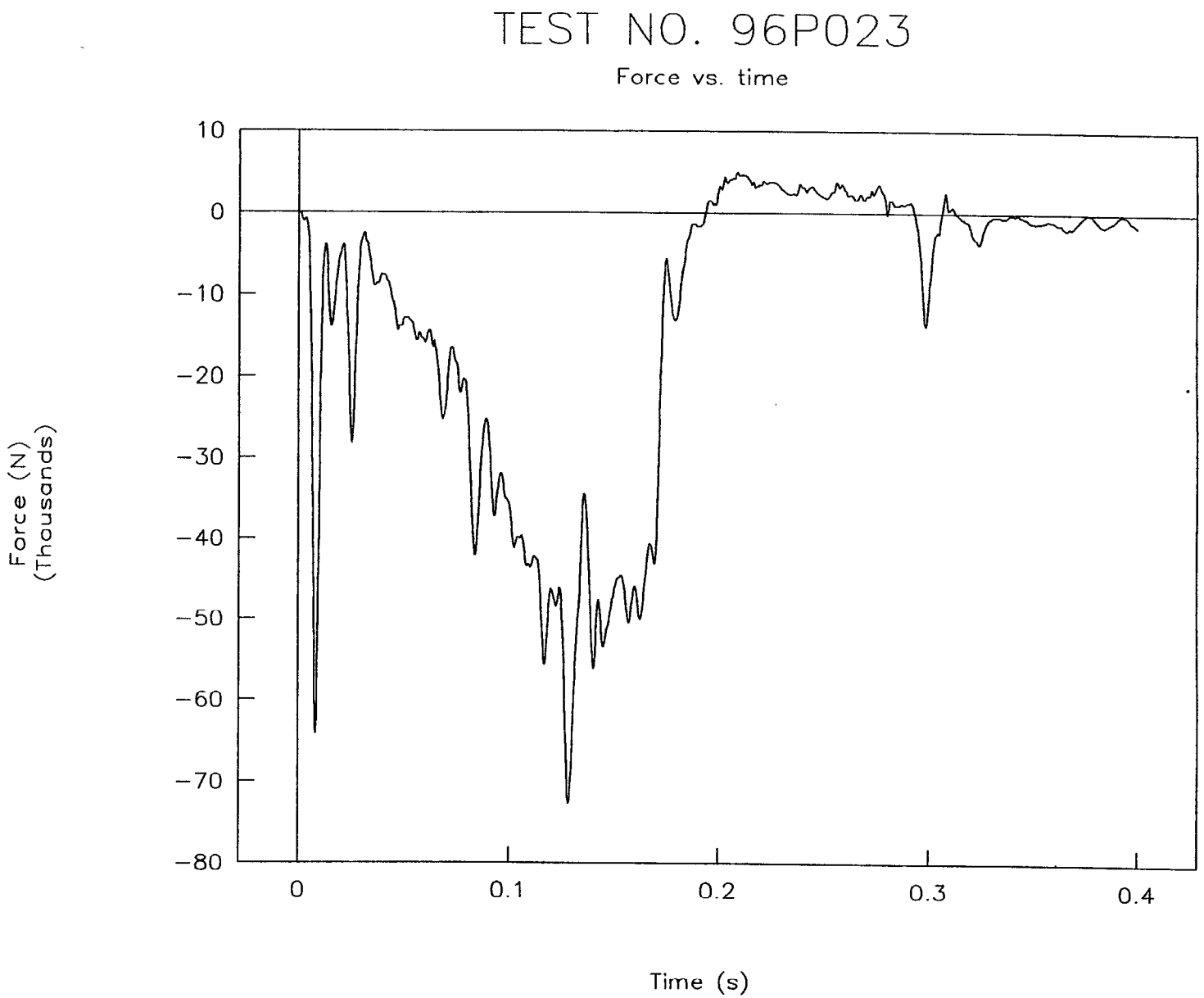

Figure 51. Force vs. time, test 96P023.

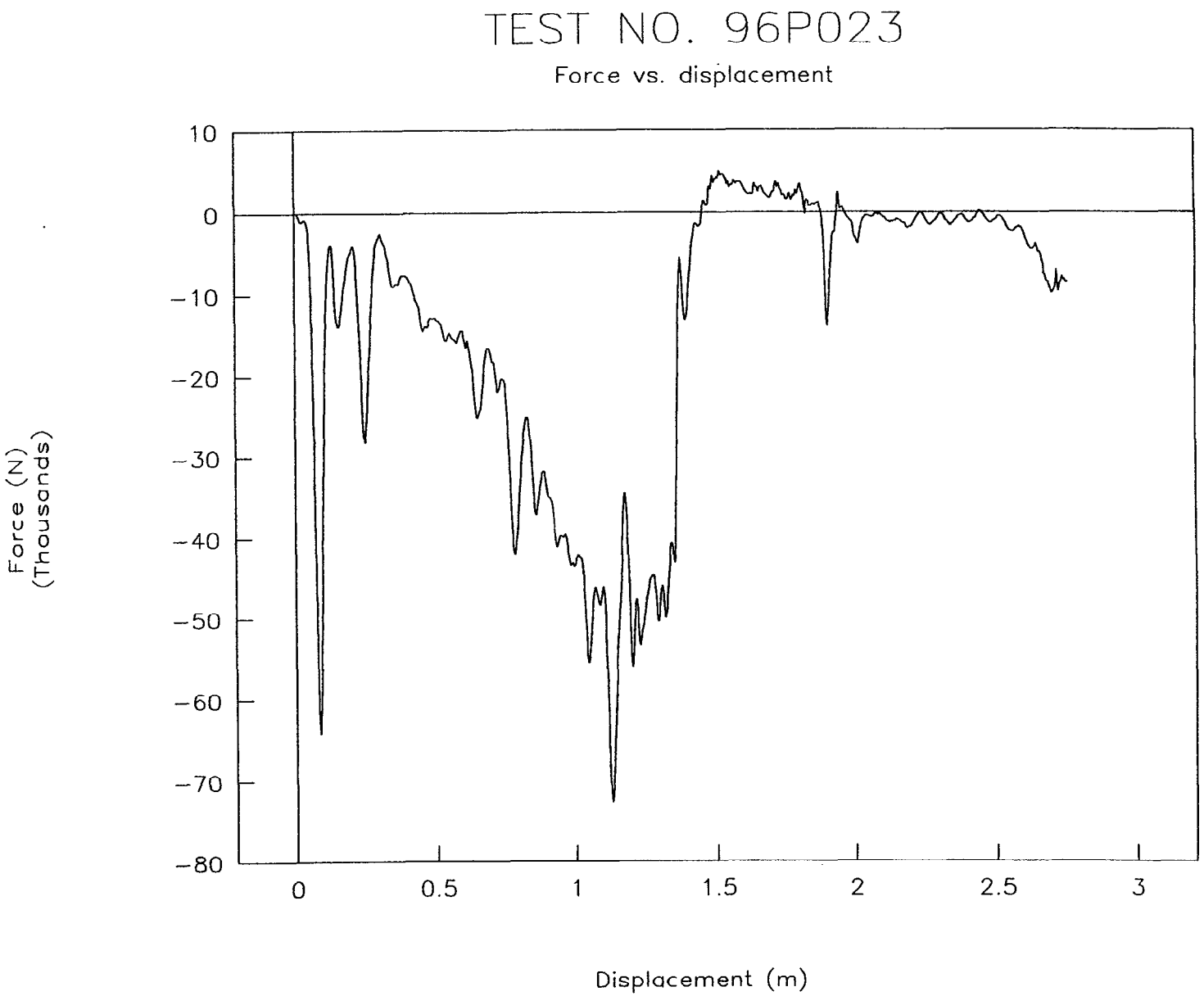

Figure 52. Force vs. displacement, test 96P023.

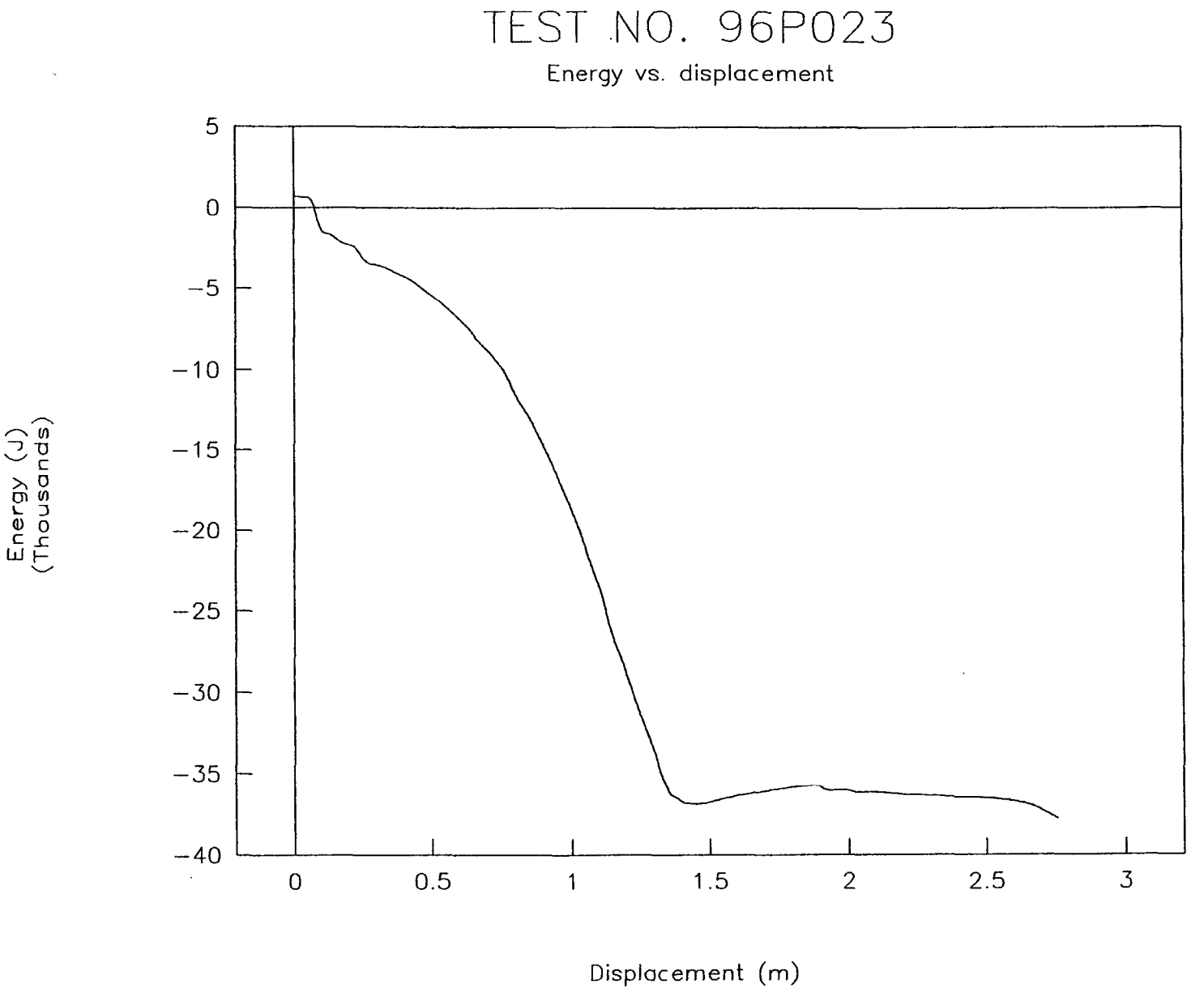

Figure 53. Energy vs. displacement, test 96P023.

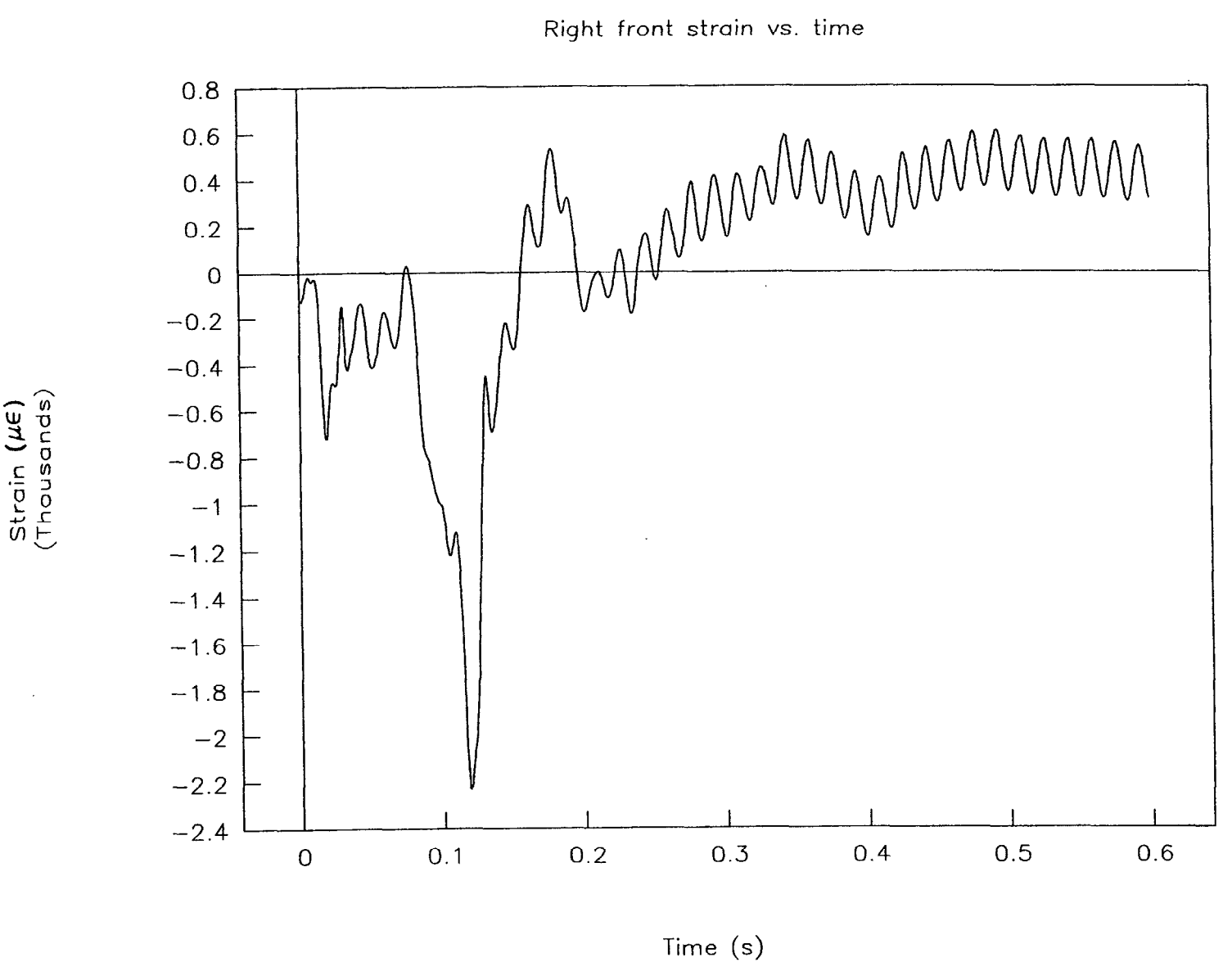

Figure 54. Strain vs. time, right front, test 96P023.

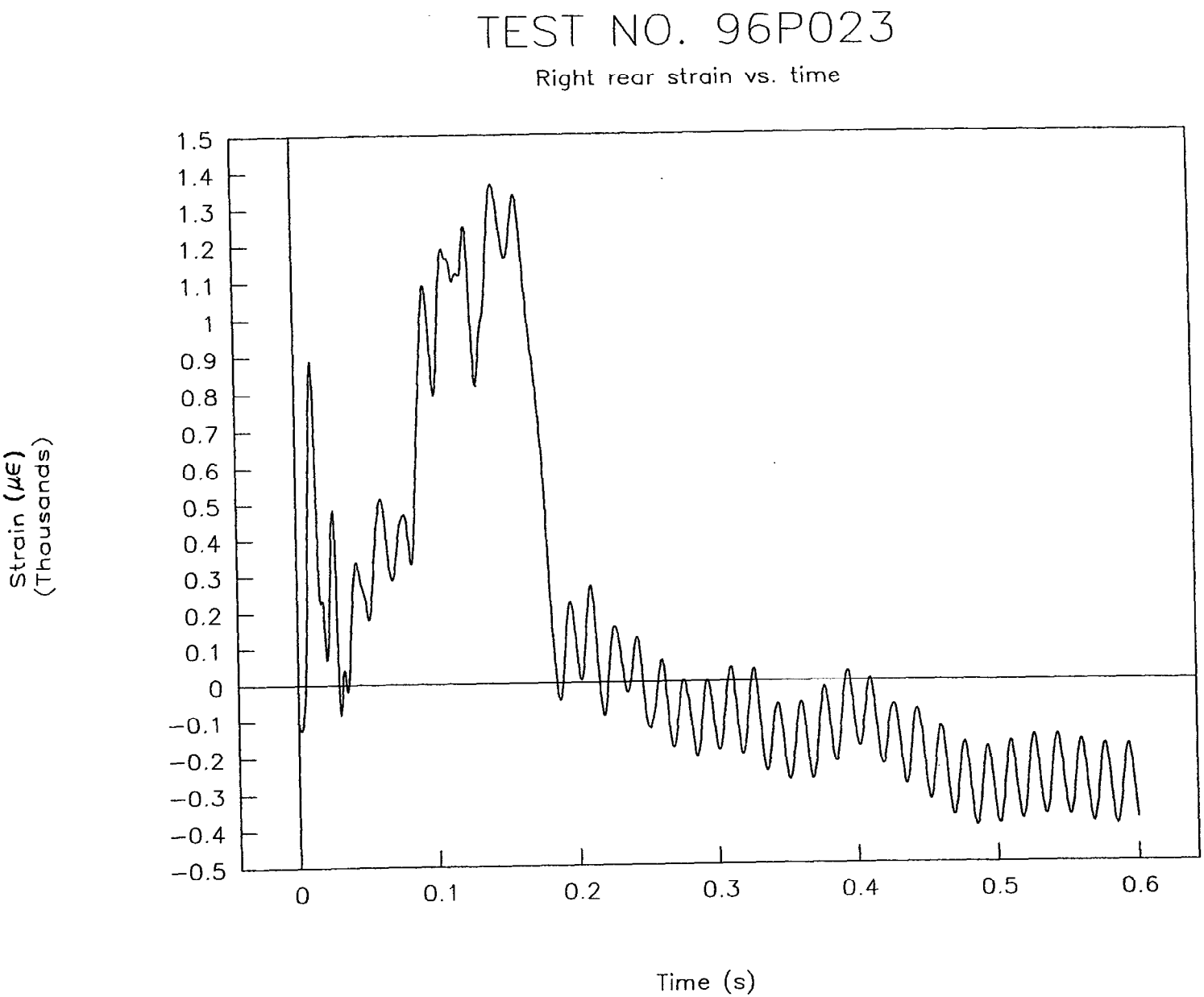

Figure 55. Strain vs. time, right rear, test 96P023.

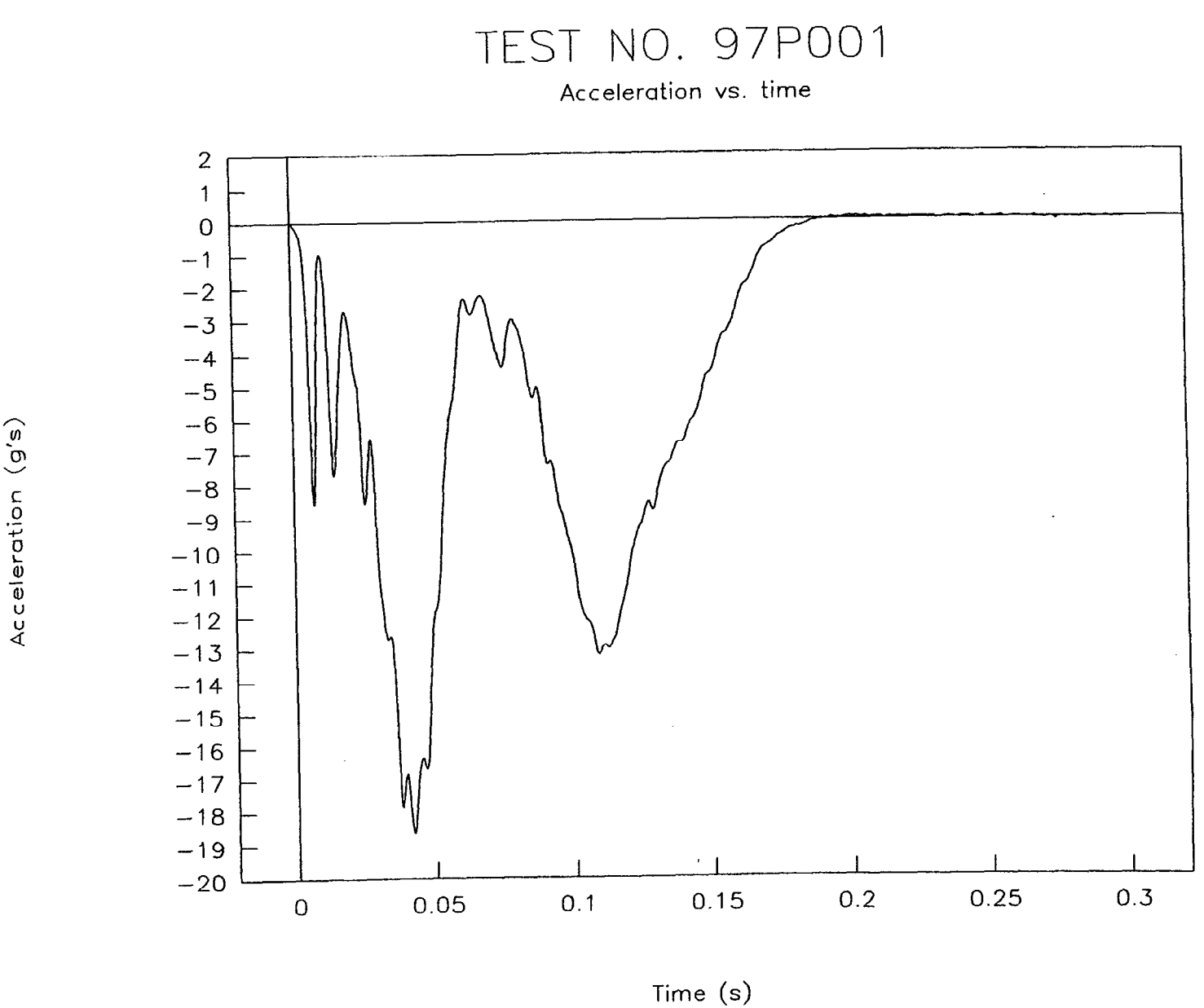

Figure 56. Acceleration vs. time, test 97P001.

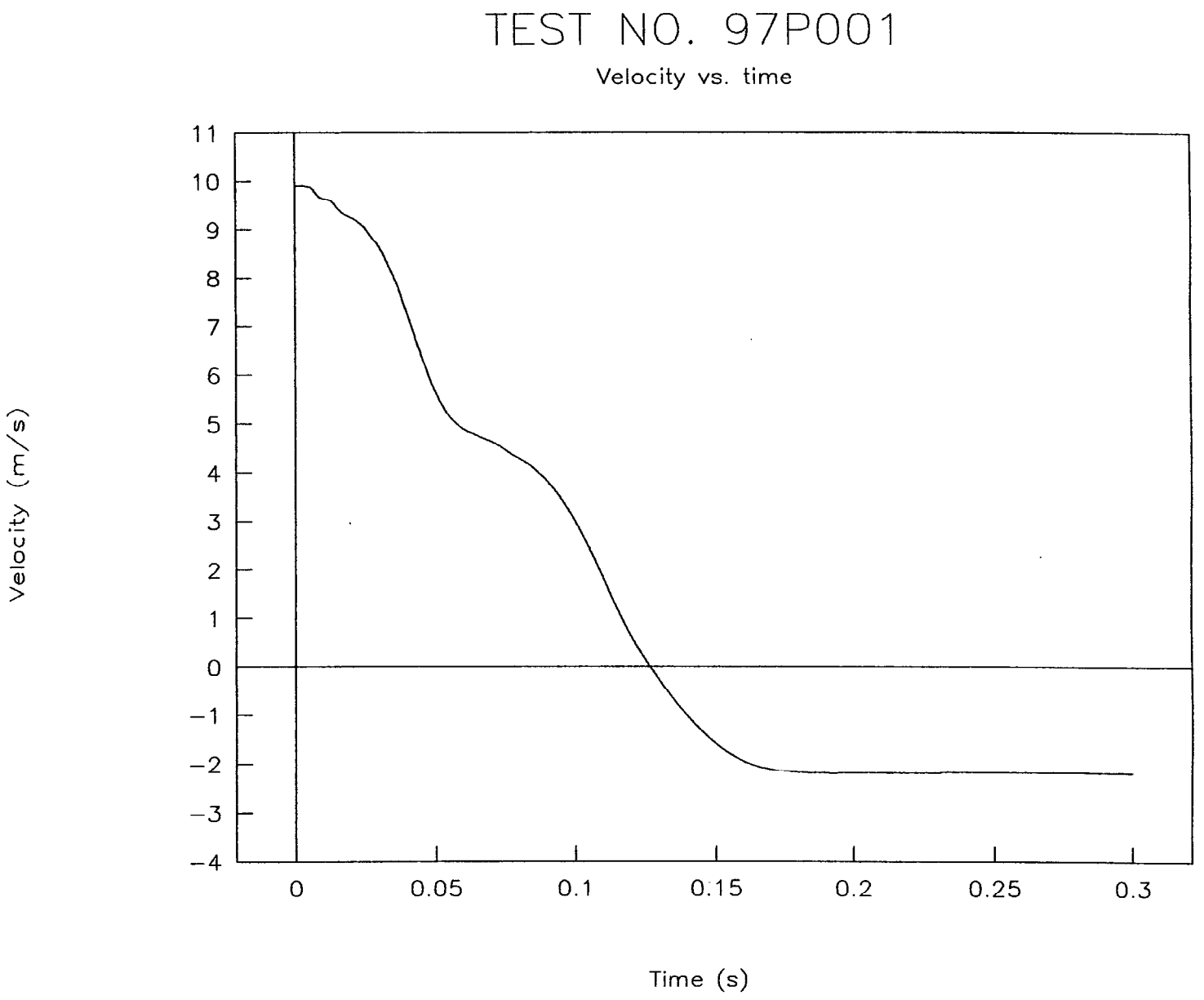

Figure 57. Velocity vs. time, test 97P001.

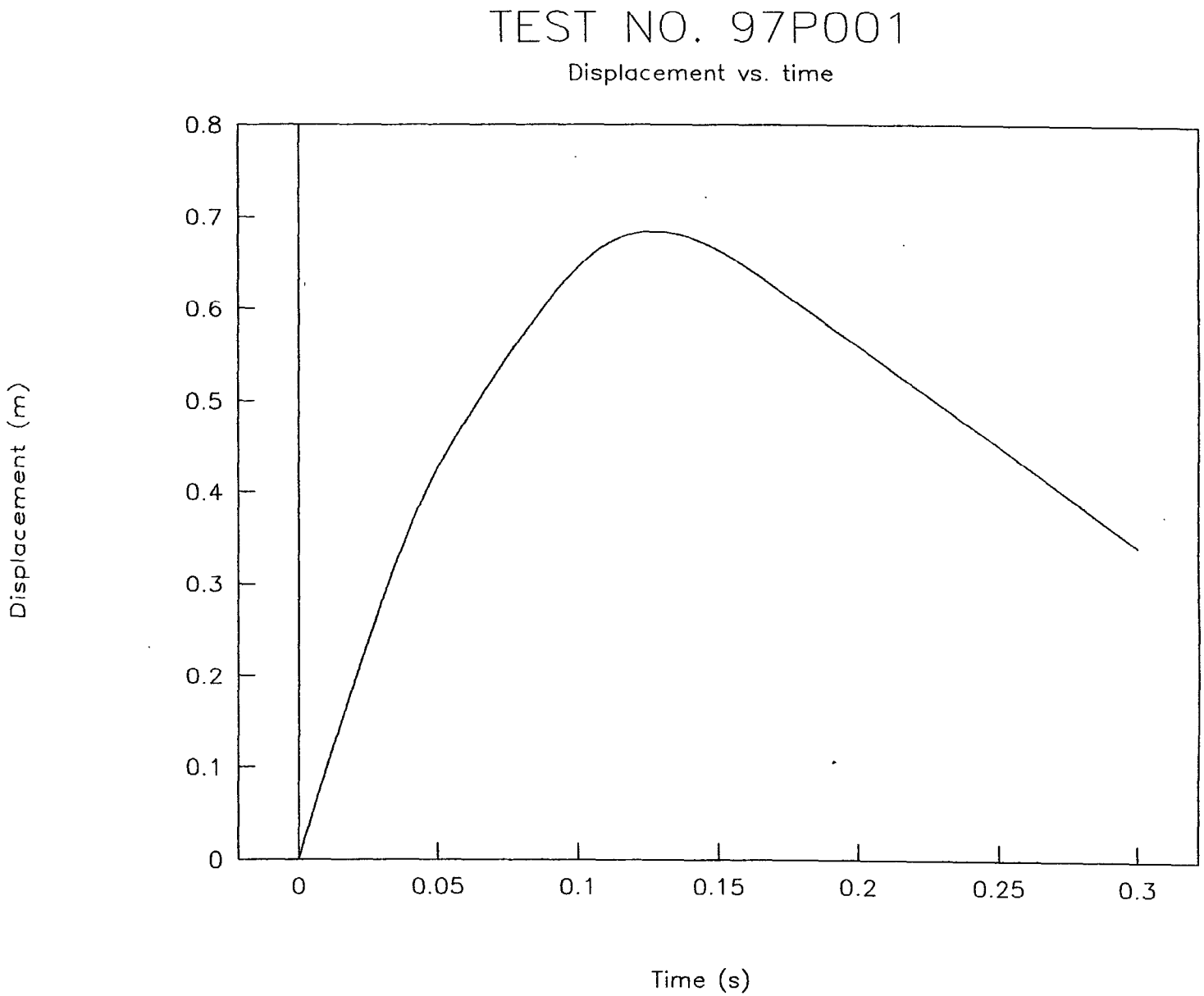

Figure 58. Displacement vs. time, test 97P001.

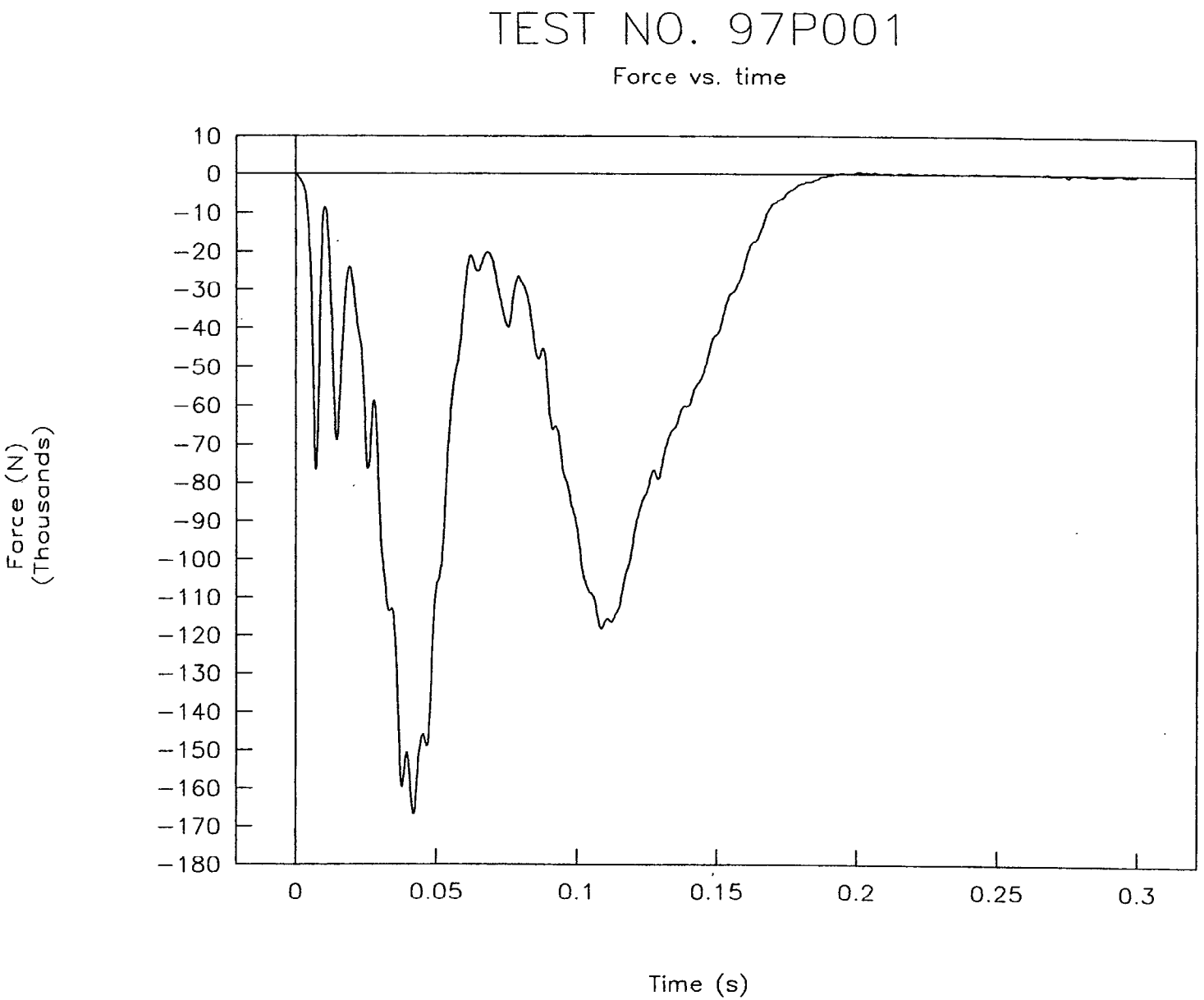

Figure 59. Force vs. time, test 97P001.

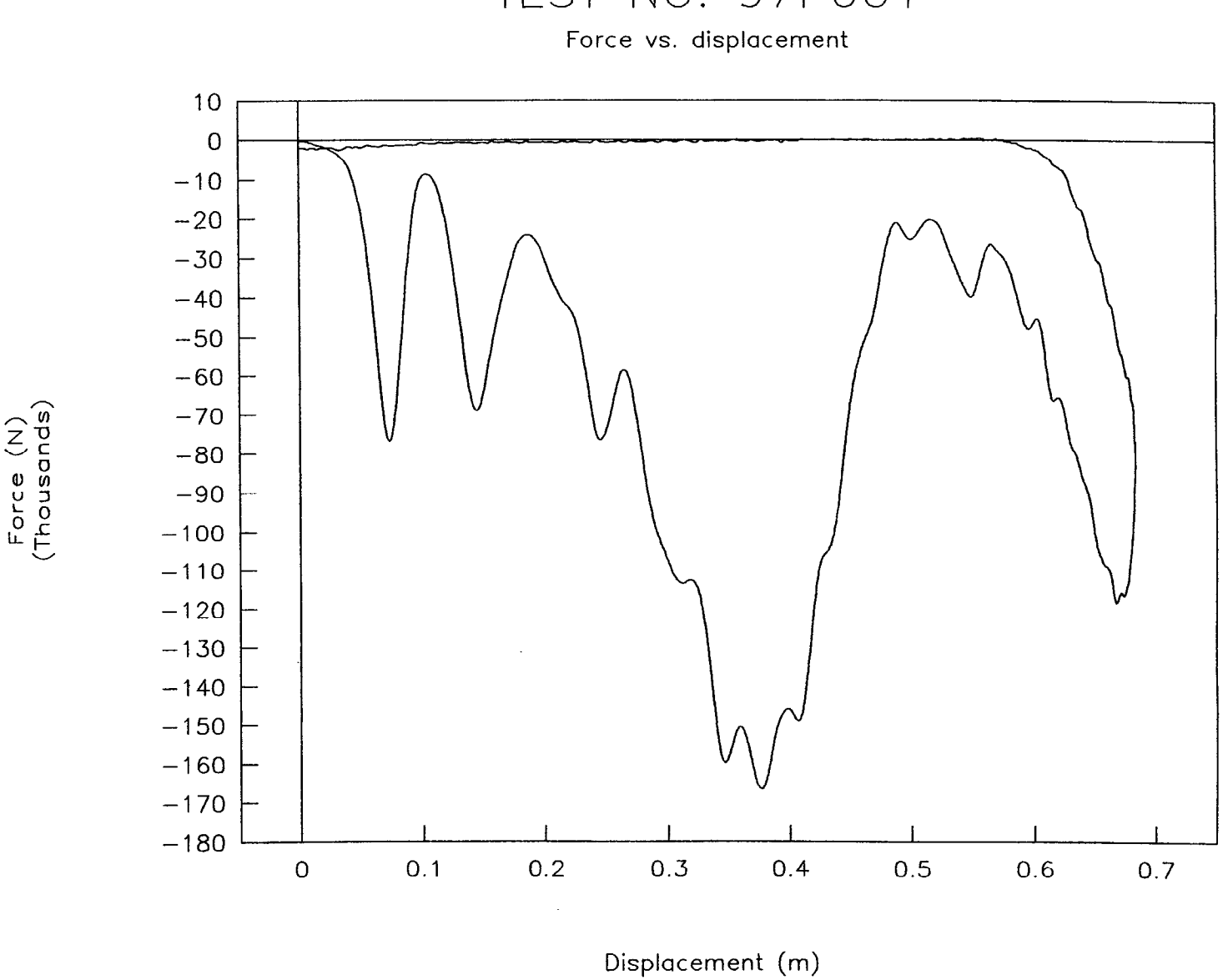

Figure 60. Force vs. displacement, test 97P001.

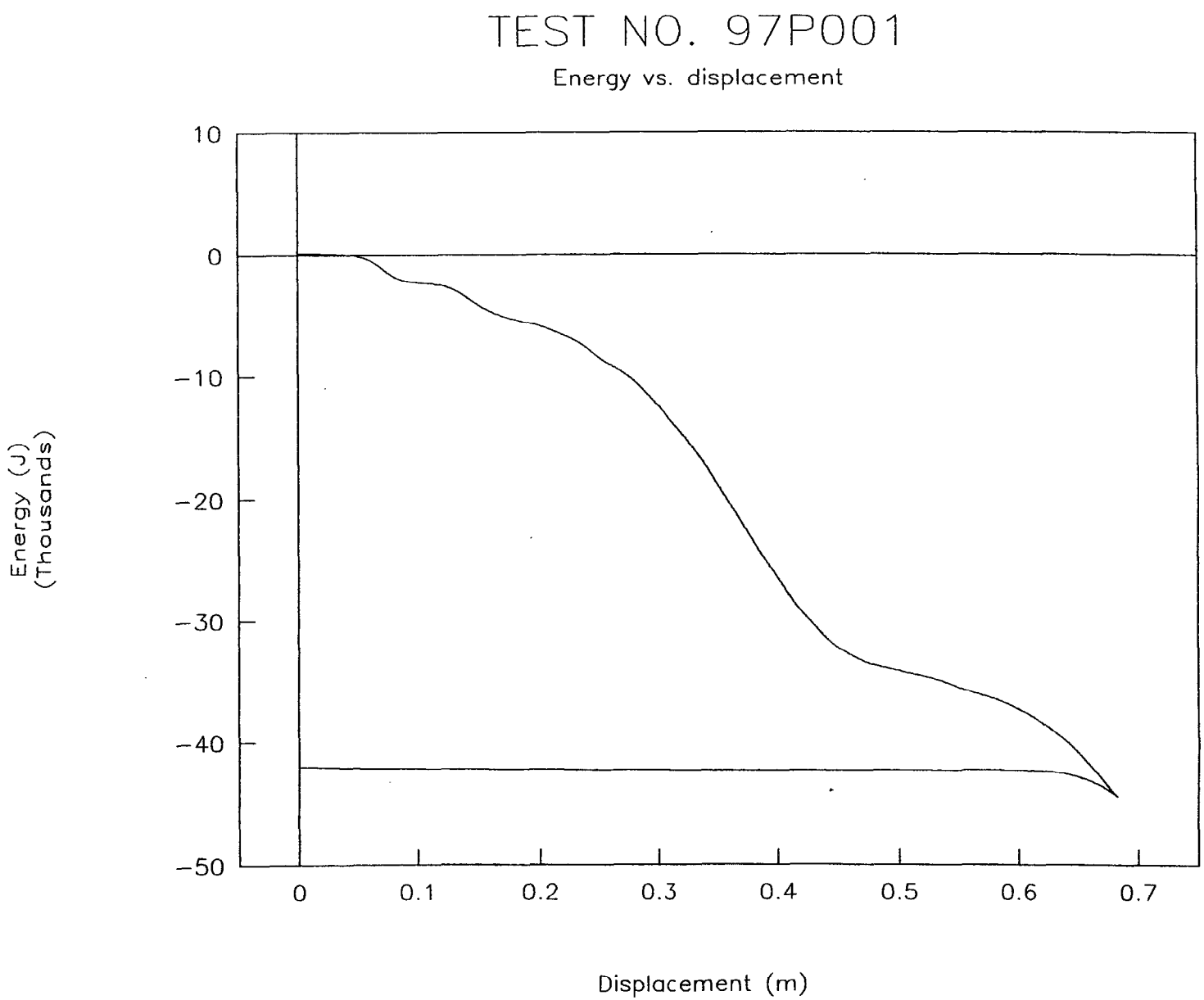

Figure 61. Energy vs. displacement, test 97P001.

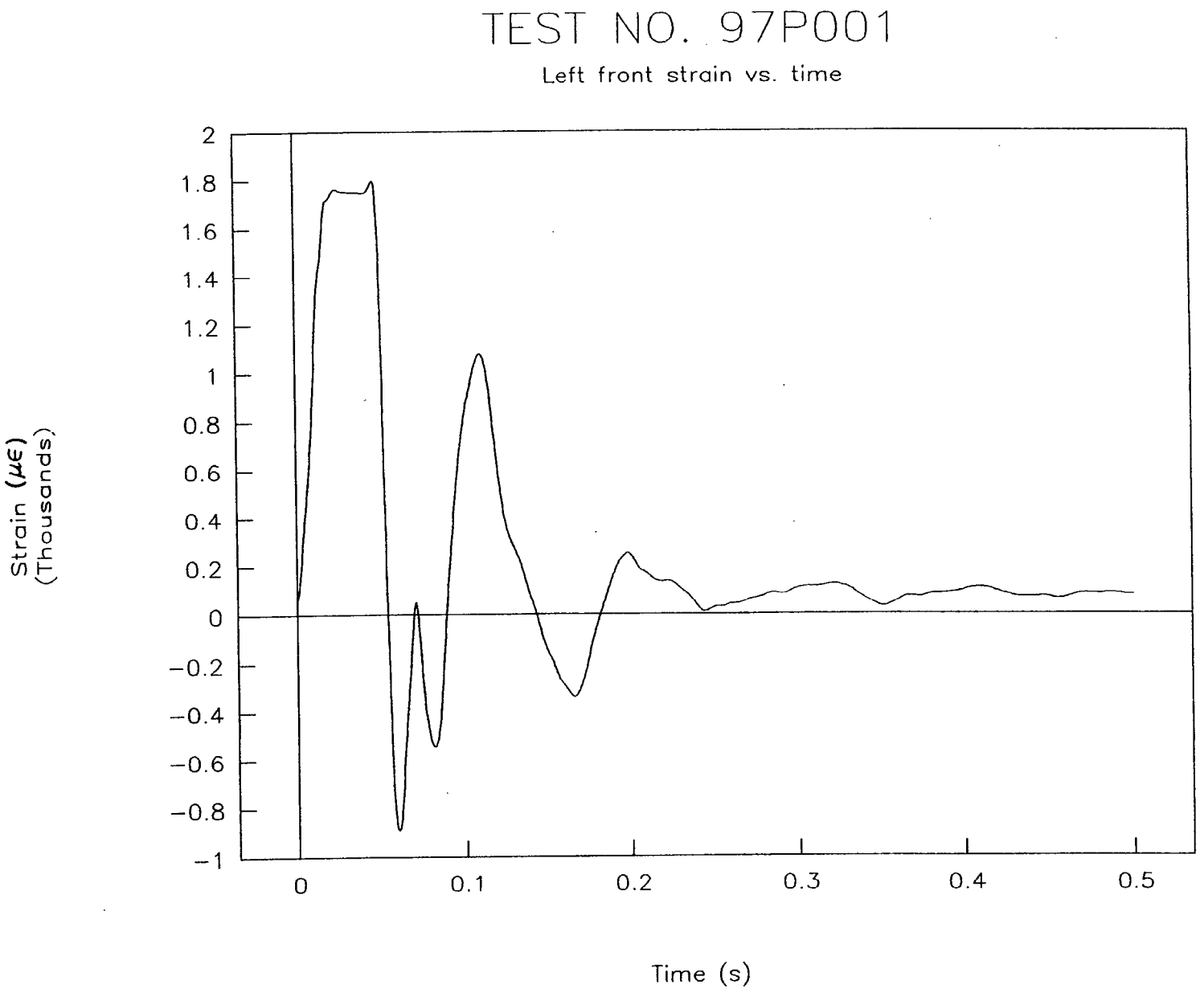

Figure 62. Strain vs. time, left front, test 97P001.

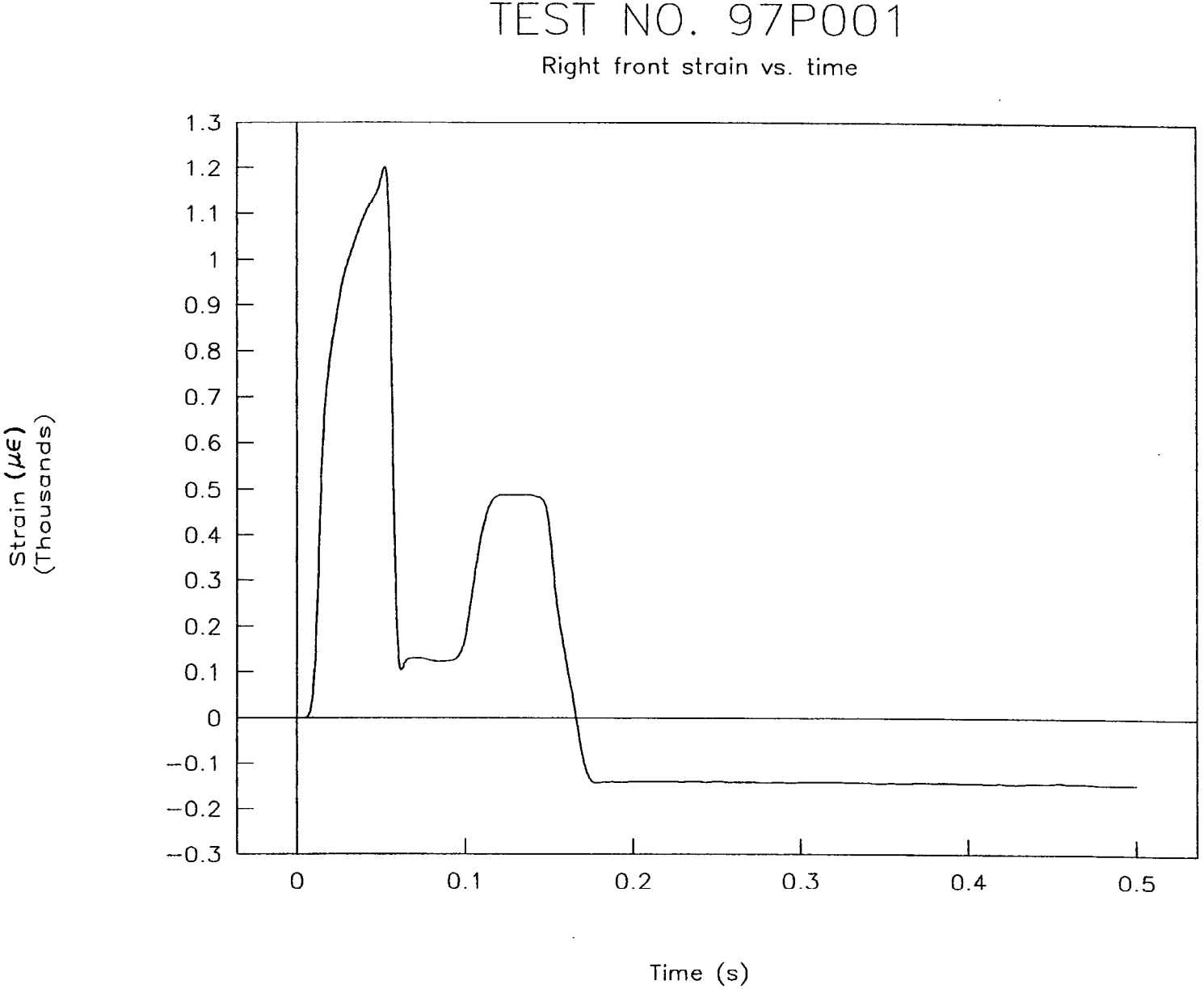

Figure 63. Strain vs. time, right front, test 97P001.

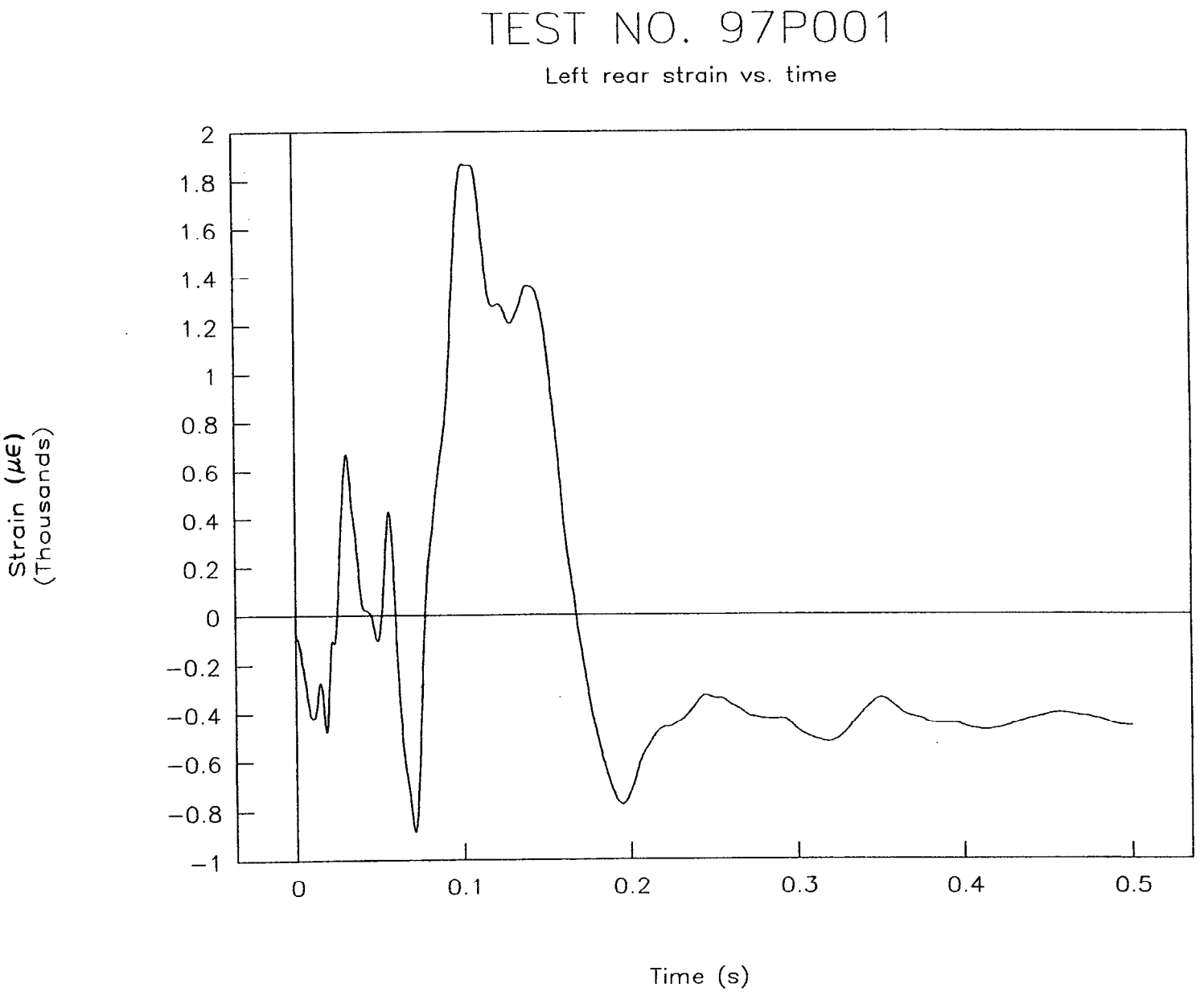

Figure 64. Strain vs. time, left rear, test 97P001.

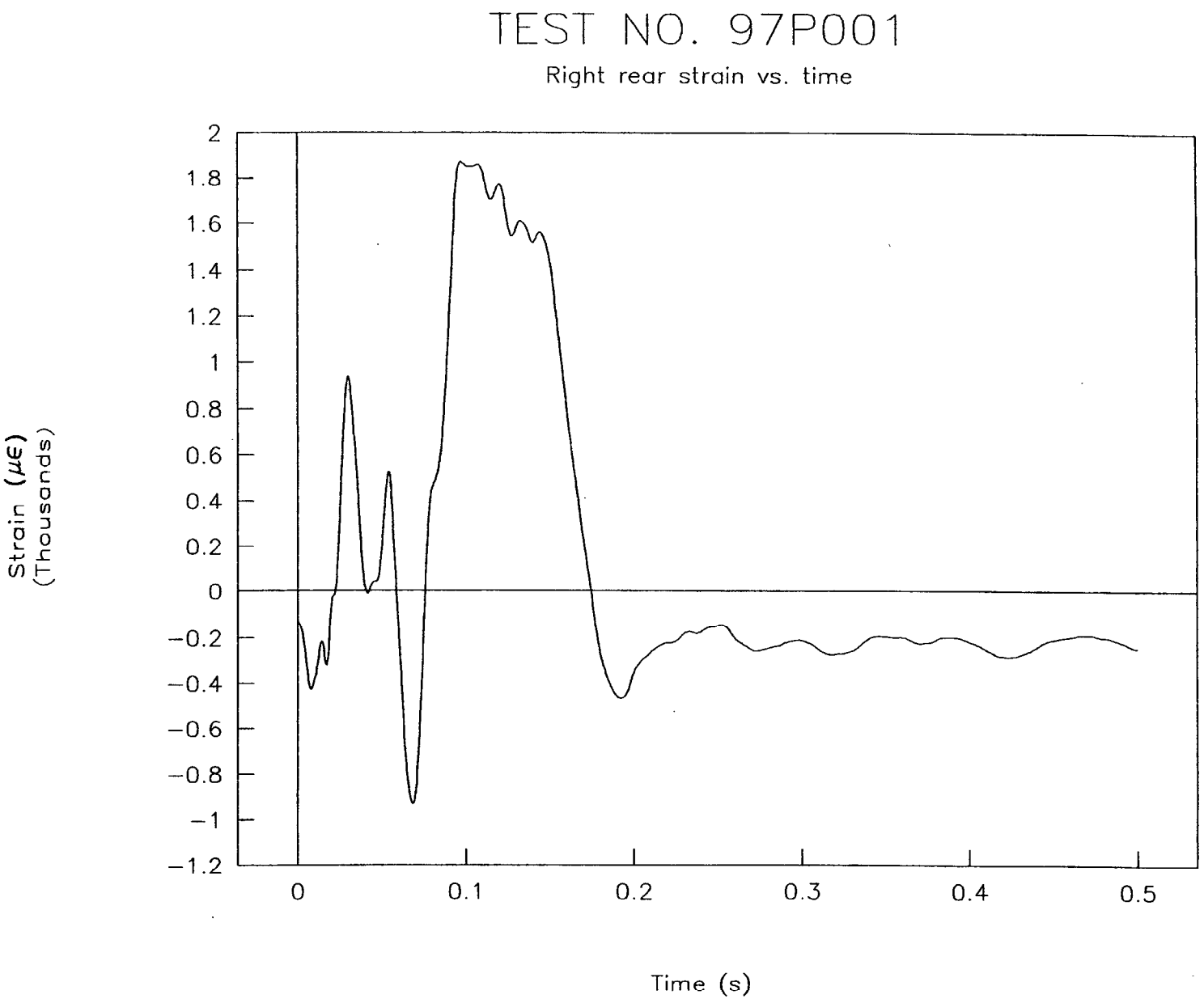

Figure 65. Strain vs. time, right rear, test 97P001.

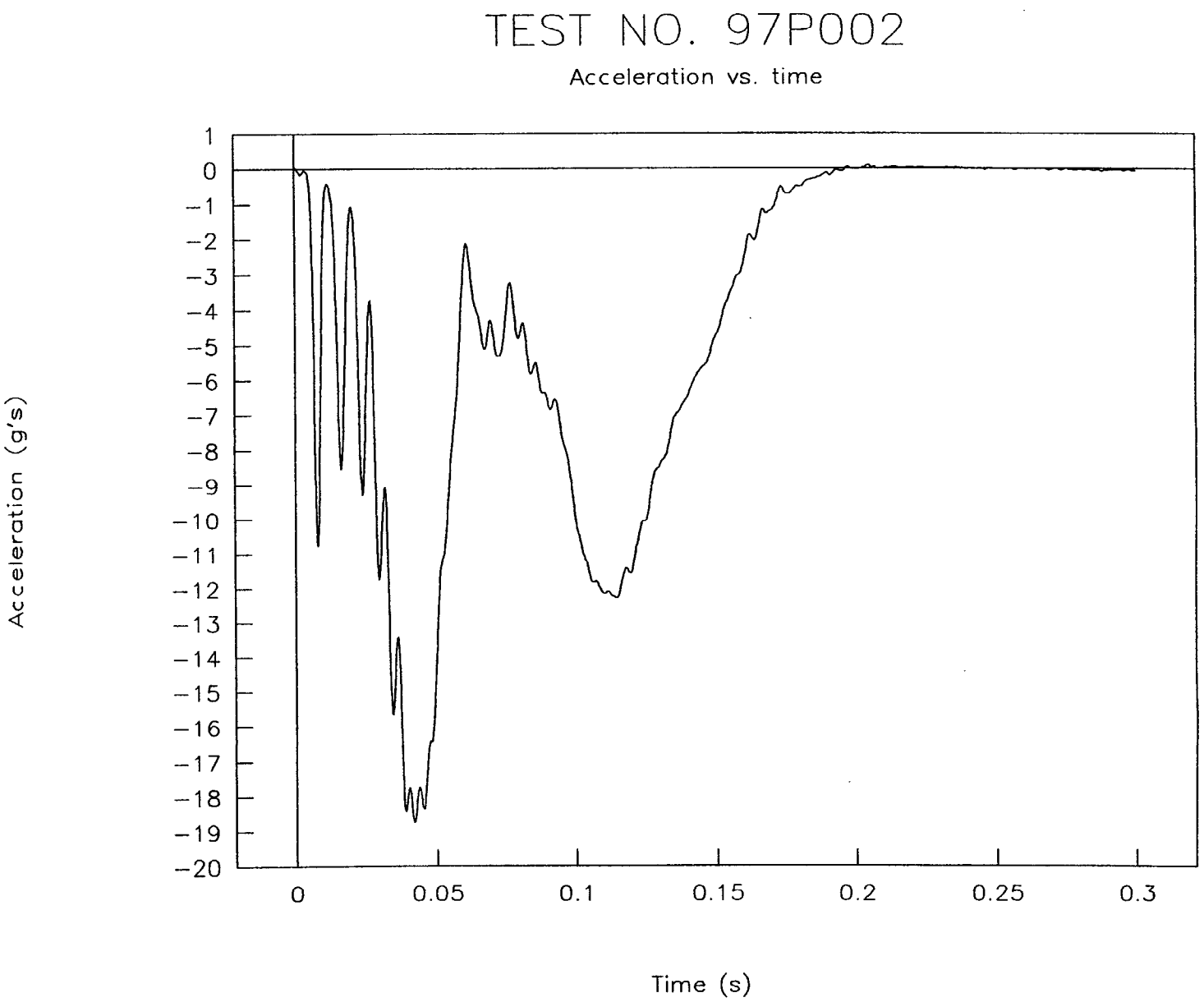

Figure 66. Acceleration vs. time, test 97P002.

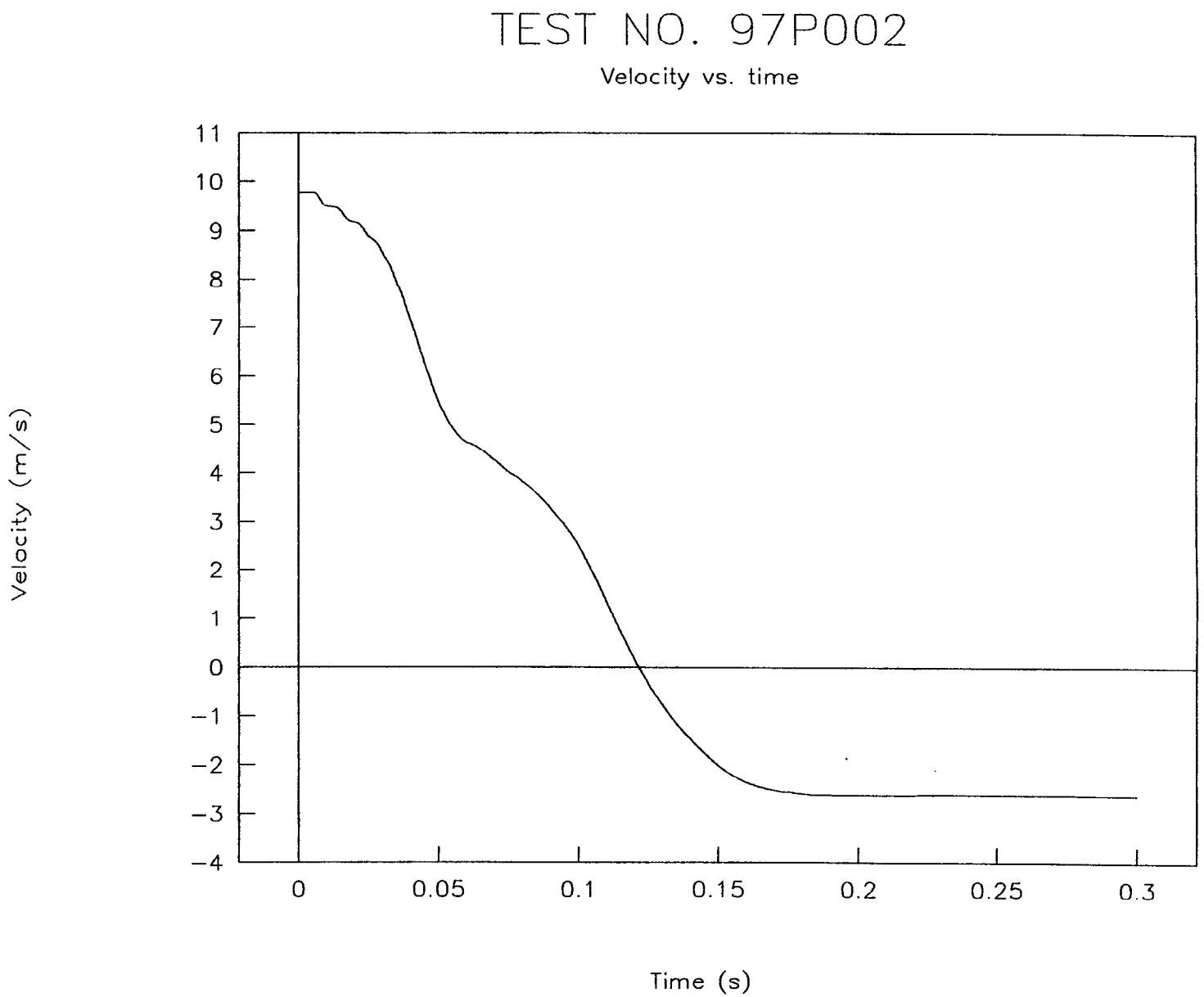

Figure 67. Velocity vs. time, test 97P002.

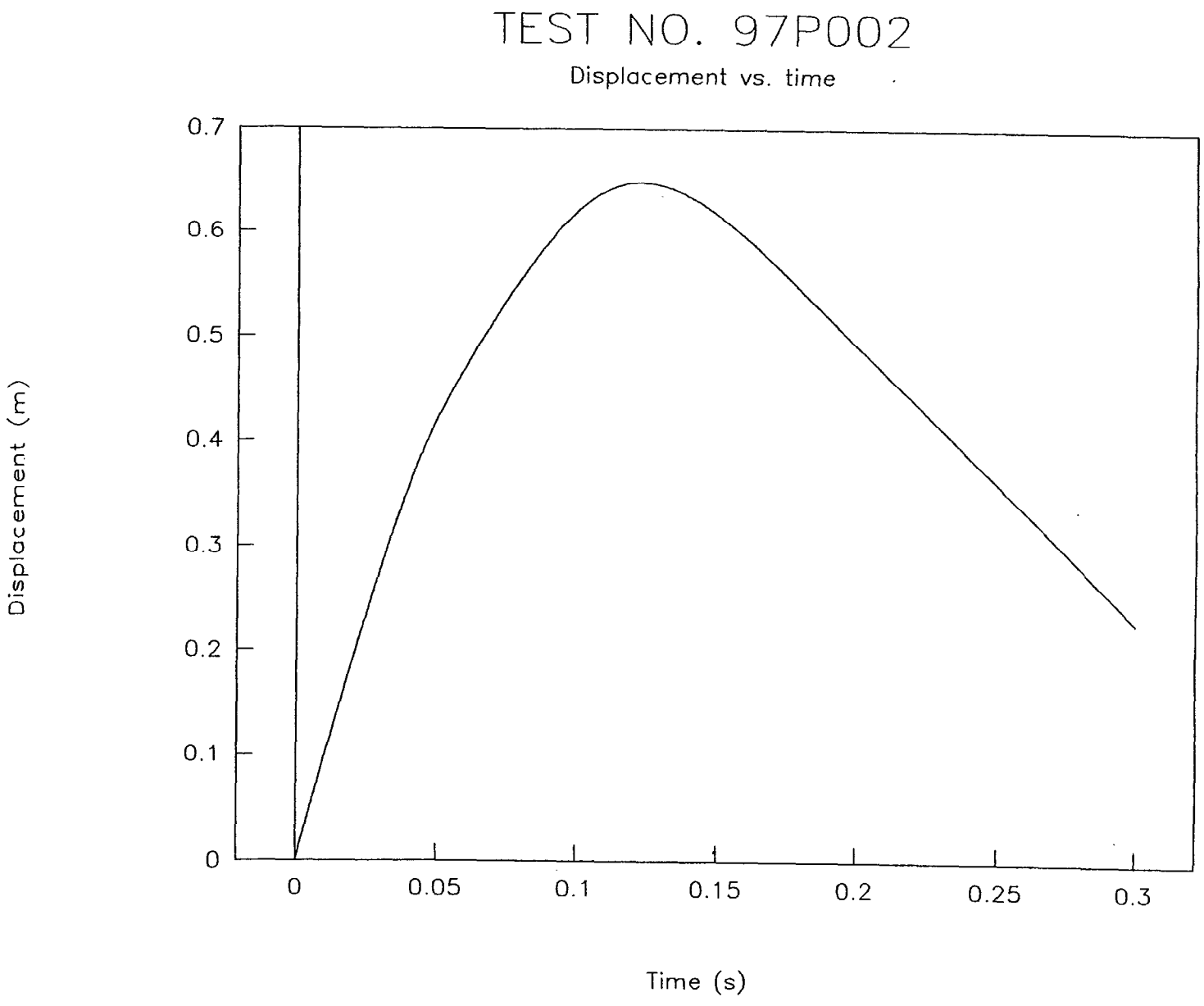

Figure 68. Displacement vs. time, test 97P002.

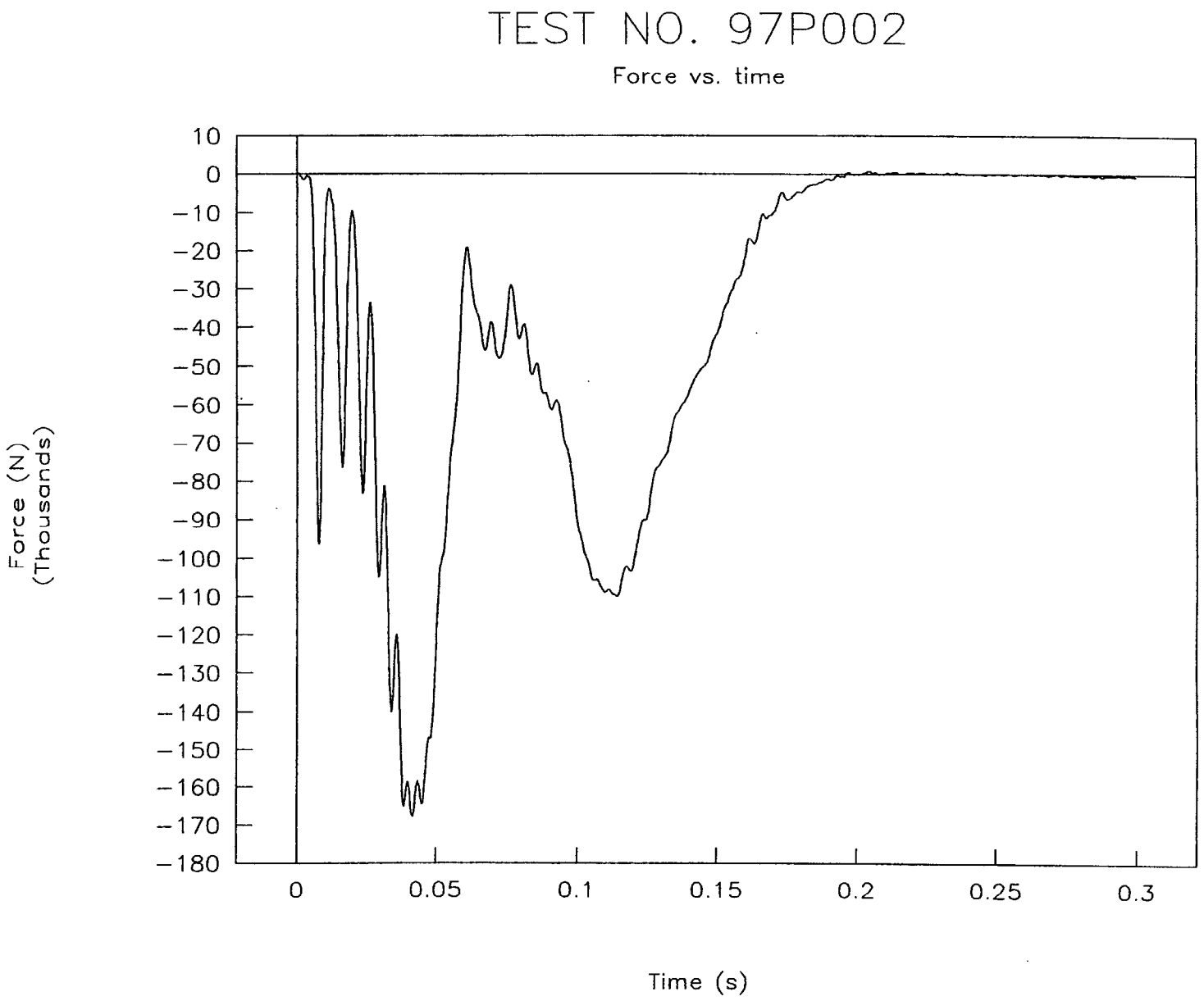

Figure 69. Force vs. time, test 97P002.

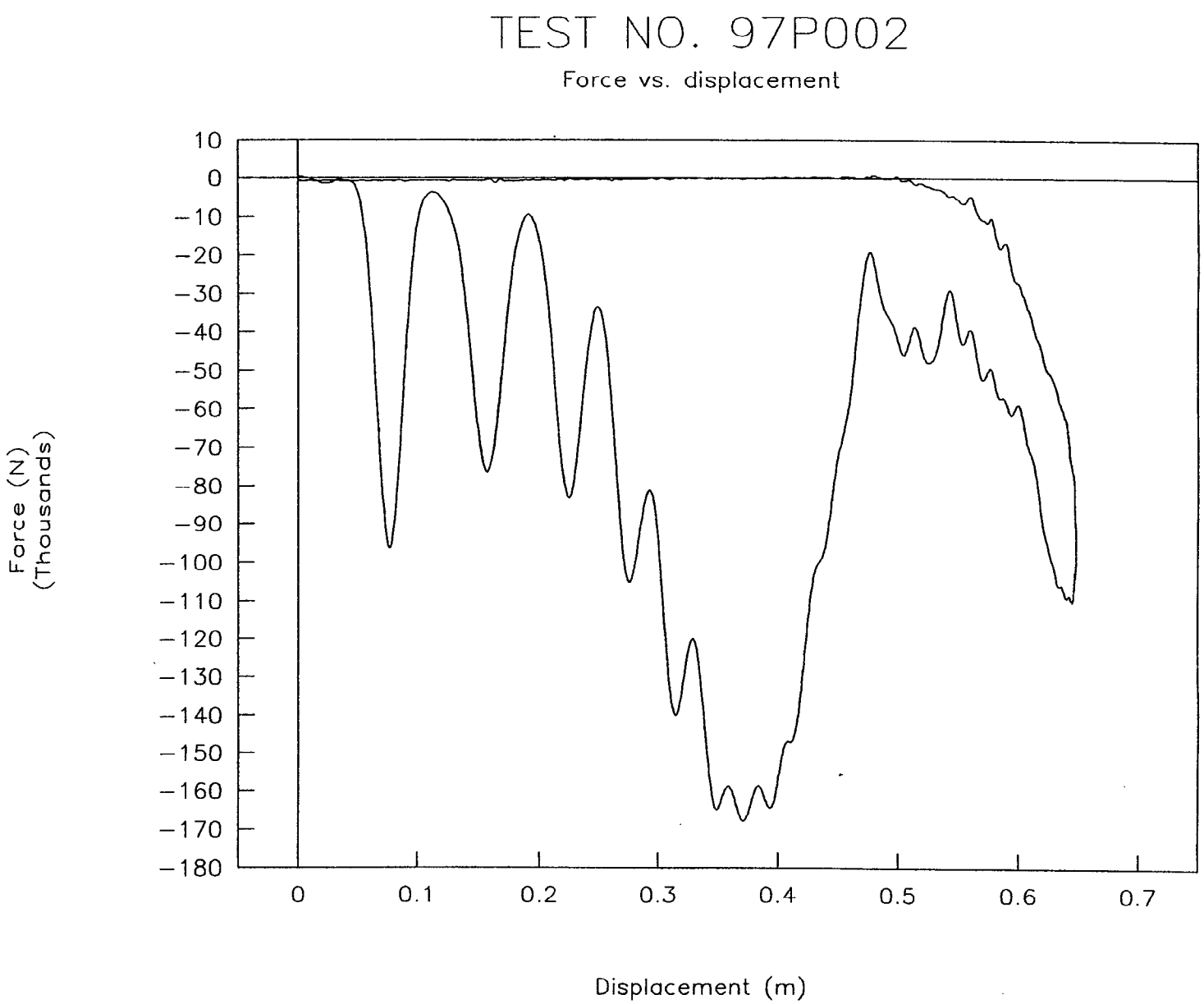

Figure 70. Force vs. displacement, test 97P002.

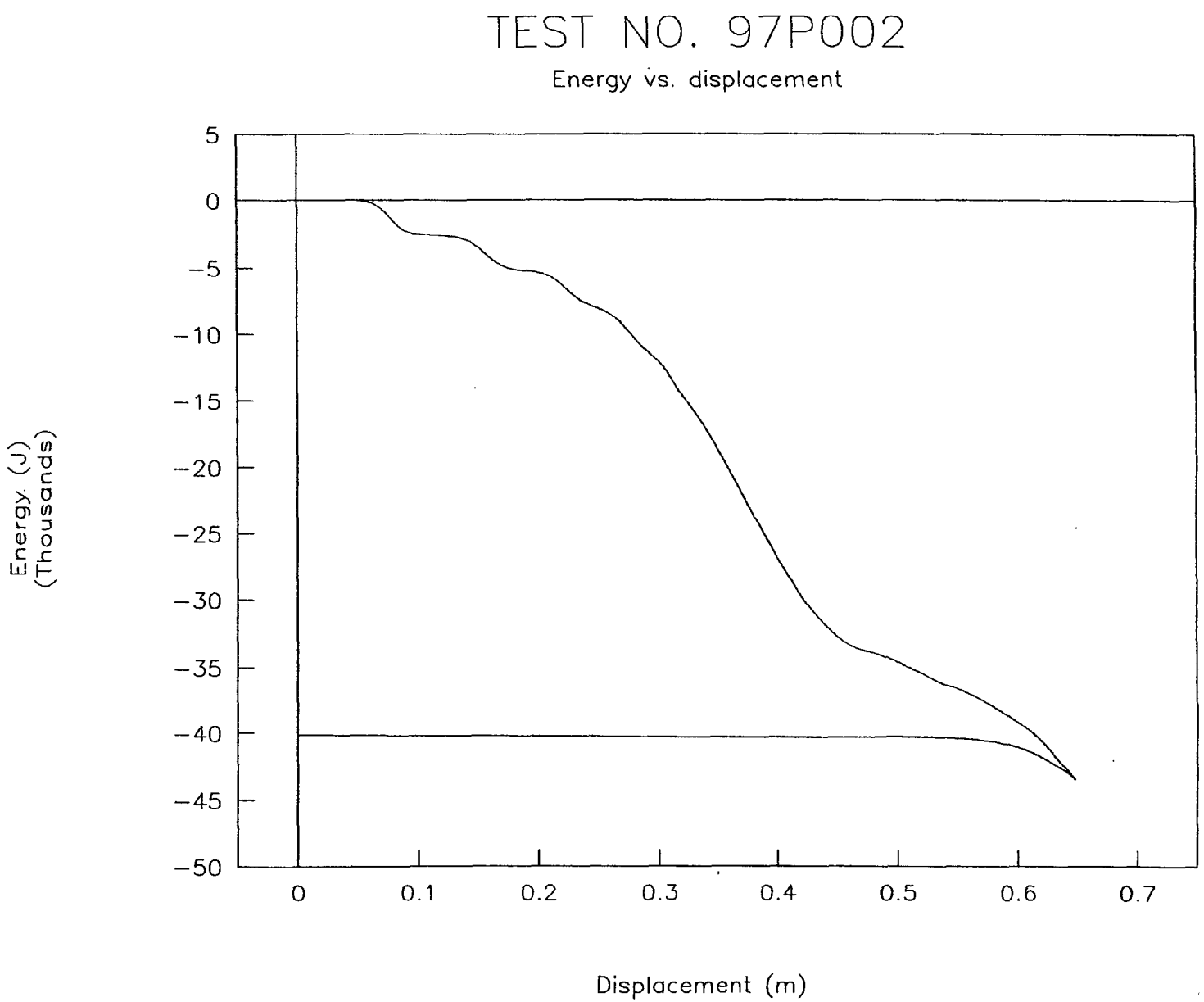

Figure 71. Energy vs. displacement, test 97P002.

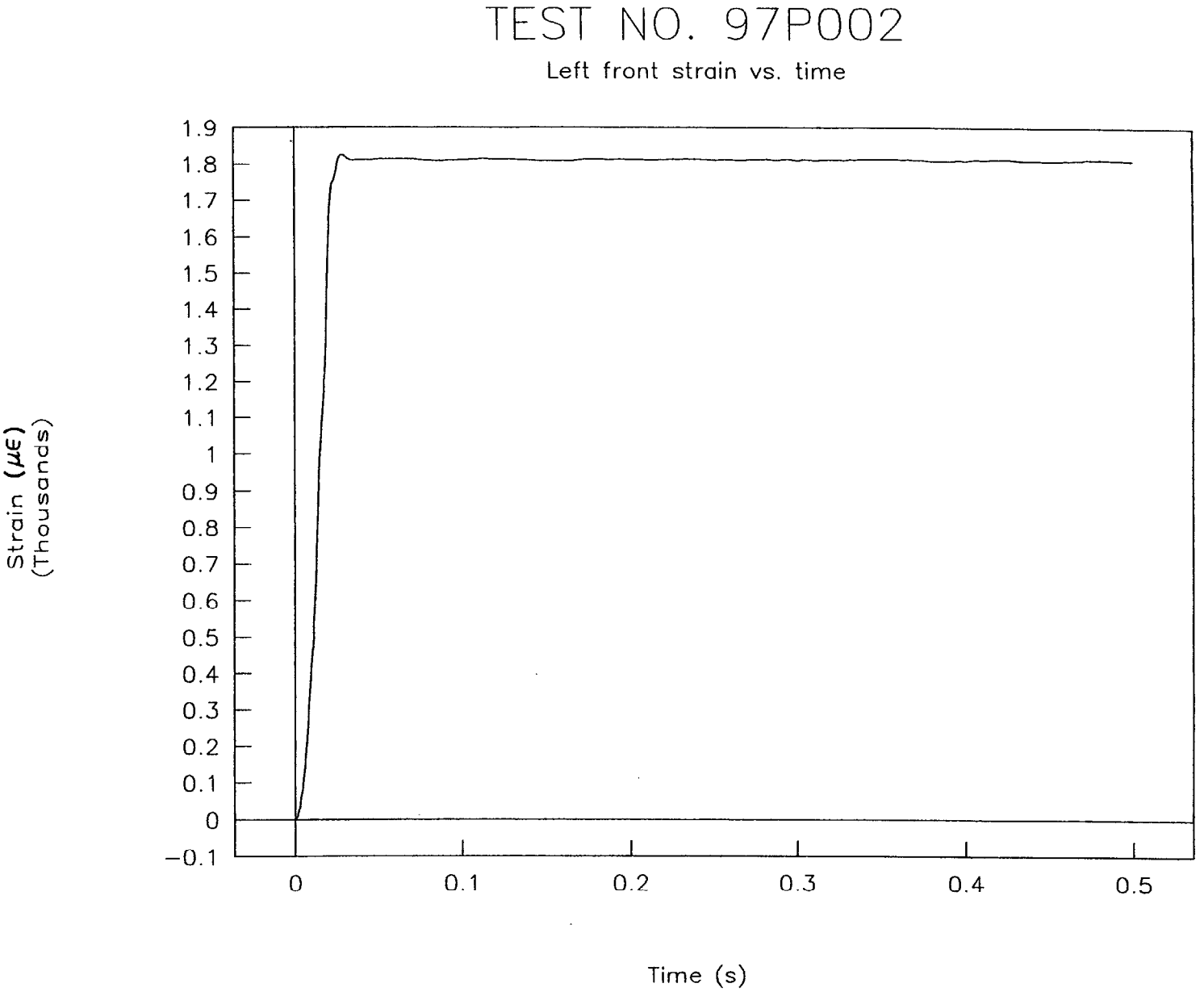

Figure 72. Strain vs. time, left front, test 97P002.

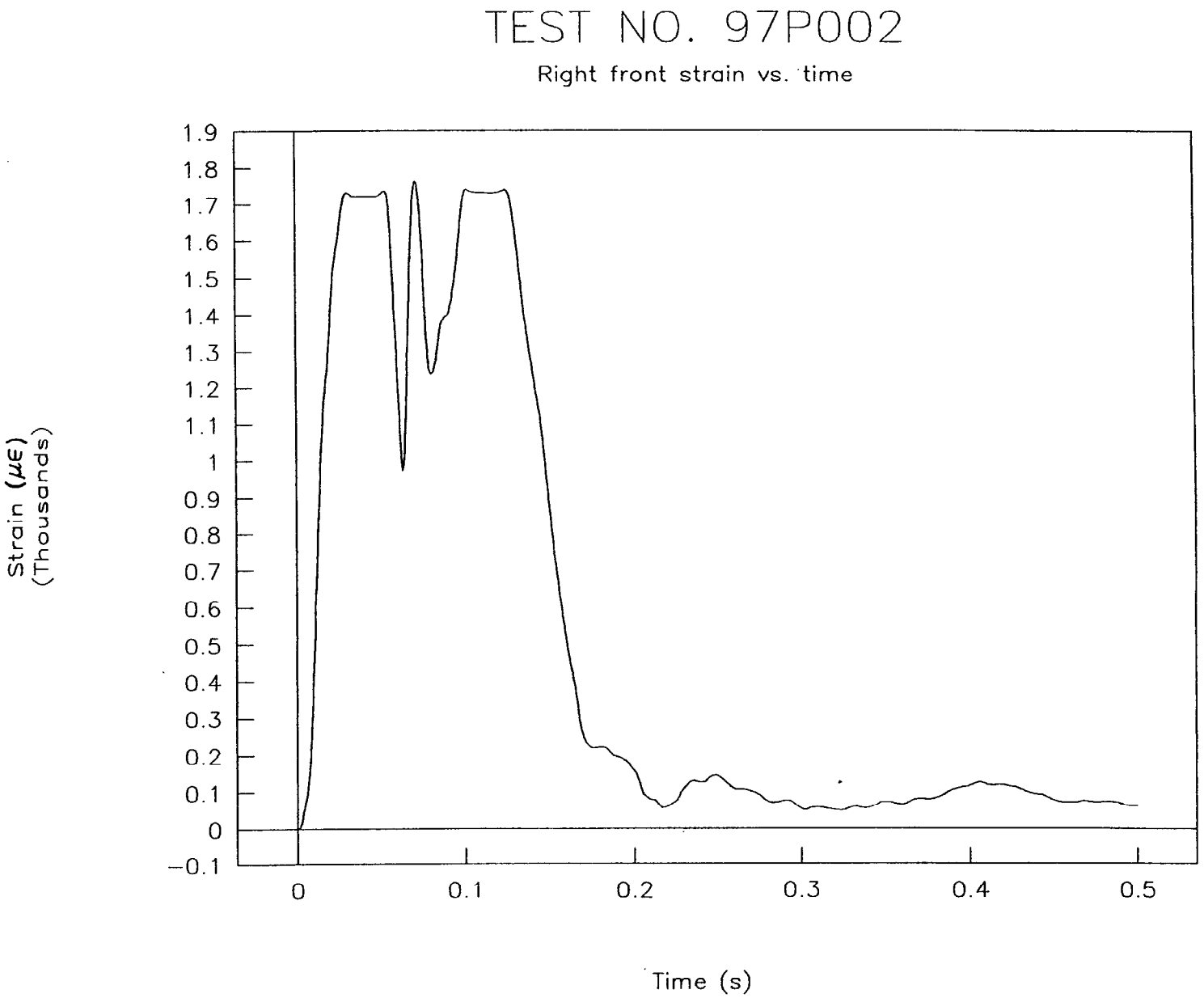

Figure 73. Strain vs. time, right front, test 97P002.

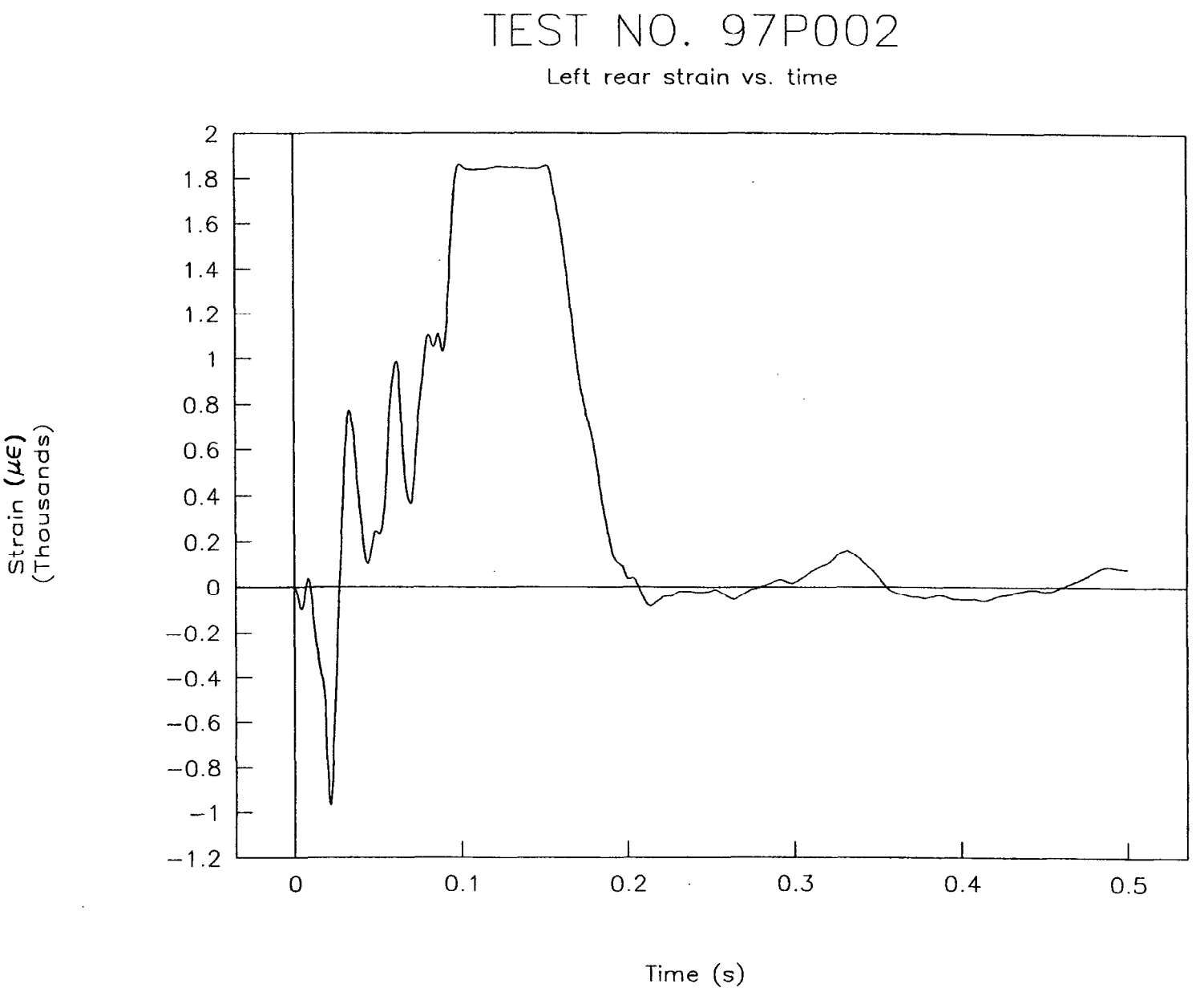

Figure 74. Strain vs. time, left rear, test 97P002.

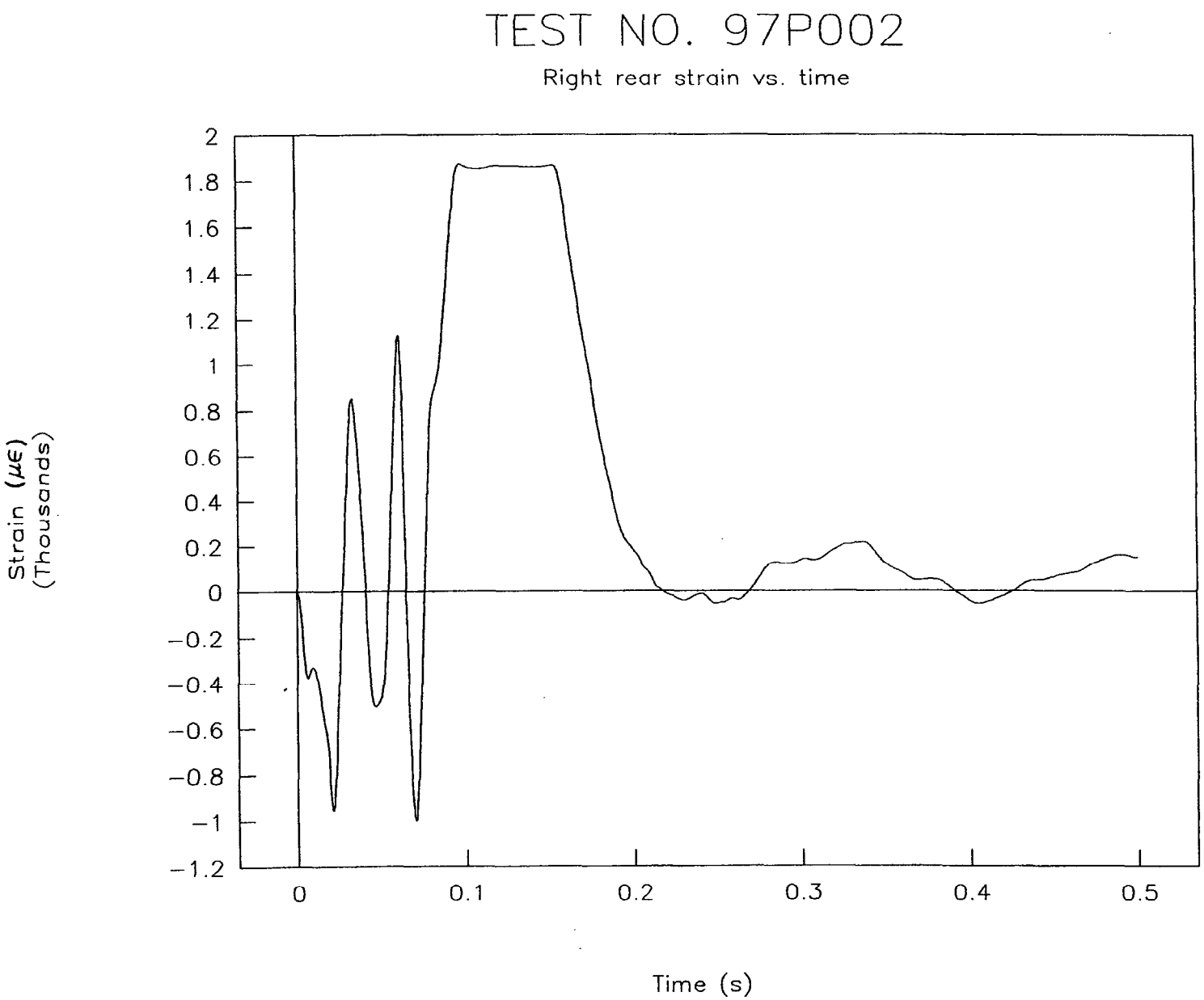

Figure 75. Strain vs. time, right rear, test 97P002.

REFERENCES

(1) Christopher M. Brown, *Pendulum Testing of Fixed-End W-Beam Guardrail: FOIL Test Numbers 96P001-96P006,* Report No. FHWA-RD-97-078, Federal Highway Administration, McLean, VA, 1997.

(2) Alrik L. Svenson and Christopher M. Brown, *Pendulum Impact Testing of Steel W-Beam Guardrail: FOIL Test Numbers 94P023-027, 94P030, and 94P031* (pending report), Federal Highway Administration, McLean, VA.

(3) H.E. Ross, Jr., D.L. Sicking, R.A. Zimmer, and J.D. Michie, *Recommended Procedures for the Safety Performance Evaluation of Highway Features, NCHRP Report 350,* National Cooperative Highway Research Program, Transportation Research Board, Washington, DC, 1993.